Contents

General Methods

Reagents were obtained from commercial suppliers and used without further purification, except DESs, lithium amides and esters **1f**, **1g**, **1m** which were prepared. DESs and *N*,*N*-di(Boc)-benzamide **6** were prepared following literature procedures.[1]

The *n*-butyllithium solution (1.6 M in hexanes) used in the synthesis of lithium amides was purchased from standard commercial sources, and concentration was established by titration of L-menthol.[2]

Hexane, THF and toluene used in the preparation of lithium amides and lithium amide solutions were dried by heating to reflux over sodium benzophenone ketyl radical under nitrogen. 2-MeTHF used in lithium amide solutions was dried by distillation from sodium. Deuterated solvents used for NMR spectroscopy were degassed (three freeze–pump–thaw cycles) and stored over 4 Å molecular sieves.

Solvents used as reaction solvent were used as supplied from commercial sources.

NMR spectra were recorded on a Bruker AVIII 400 MHz spectrometer operating at 400.1 MHz for ^{1}H, 100.6 MHz for ^{13}C{^{1}H}, 128.4 MHz for ^{19}F or 155.5 MHz for ^{7}Li for compounds **2d, 2e 2g** and **2i**. Li-amides **2a-c, 2d, 2f** and **2h** were recorded on a Bruker AVIII 300 MHz spectrometer operating at 300.1 MHz for ^{1}H, 75.5 MHz for ^{13}C{^{1}H} and 116.6 for ^{7}Li. The chemical shifts in ^{1}H NMR spectra are calibrated to the resonance of the ferrocene standard at 4.16 ppm in $CDCl_3$ when yield calculation is concerned – otherwise are calibrated to deuterated solvent signals. Stock solutions of ferrocene in $CDCl_3$ were made to be used as internal standard for yields determination. To accurately determine the amount of the internal standard present in these stock solutions, ^{1}H NMR spectra were recorded with known amounts standard solution and benzophenone.

For each ^{1}H NMR spectrum the exact amount of standard is labelled and the amount of product is corrected by this value by applying the following equation:

$$\left(\frac{a}{b \times \frac{FeCp_2\ integral}{10H}}\right) \times FeCp_2\ concentration\ = x\ mmoles\ product$$

a = integral of one distinct signal from product

b = known number of protons for signal

*$FeCp_2$ integral/10H can be cancelled and set to 1 as $FeCp_2$ is calibrated to 10H.

e.g. for **3a**

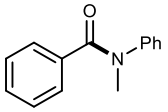

$$\left(\frac{48H\ (Me\ signal)}{3H\ \times 1}\right) \times 0.05\ M\ = 0.80\ mmoles\ product$$

Therefore, for a 1 mmol scale reaction, the yield of **3a** is 80%

GCMS measurements were performed using an Agilent Technologies 5975C GC/MS detector. High resolution mass spectrometry was carried out by University of Edinburgh Mass Spectrometry Facility.

^{1}H NMR spectra of products matched those previously reported (**3a**,[3] **3b**,[4] **3c**,[5] **3f**,[6] **3g-h**,[7] **3i-j**,[8] **3l-m**,[9] **4**,[10] **5b**,[3] **5c**,[6] **5d**,[11] **5e**,[8, 12] **5f**,[13] **5g**,[9, 14] **5h**,[15]) or where unreported were characterized by ^{1}H, ^{13}C and ^{19}F NMR spectroscopy and high-resolution mass spectrometry (**3d**, **3e**, **3k**, **5i**).

Procedure for the Synthesis of Esters

Esters **1f**, **1g**, **1m** were prepared from their corresponding acids (*p*-methoxybenzoic acid, *m*-methoxybenzoic acid and *n*-octanoic acid. Typical scale 20 mmol. Acids were dissolved in EtOH, acidified to ≤ pH 3 by addition of H_2SO_4 (conc.) and refluxed overnight. The resultant solution was neutralized with sat. $NaHCO_3$ sol. And extracted into EtOAc (3 x 20 mL). Extracts were combined, dried over $MgSO_4$ and concentrated under vacuum. The product ester did not require purification, only drying over 4 Å molecular sieves.

Reaction Set-Up

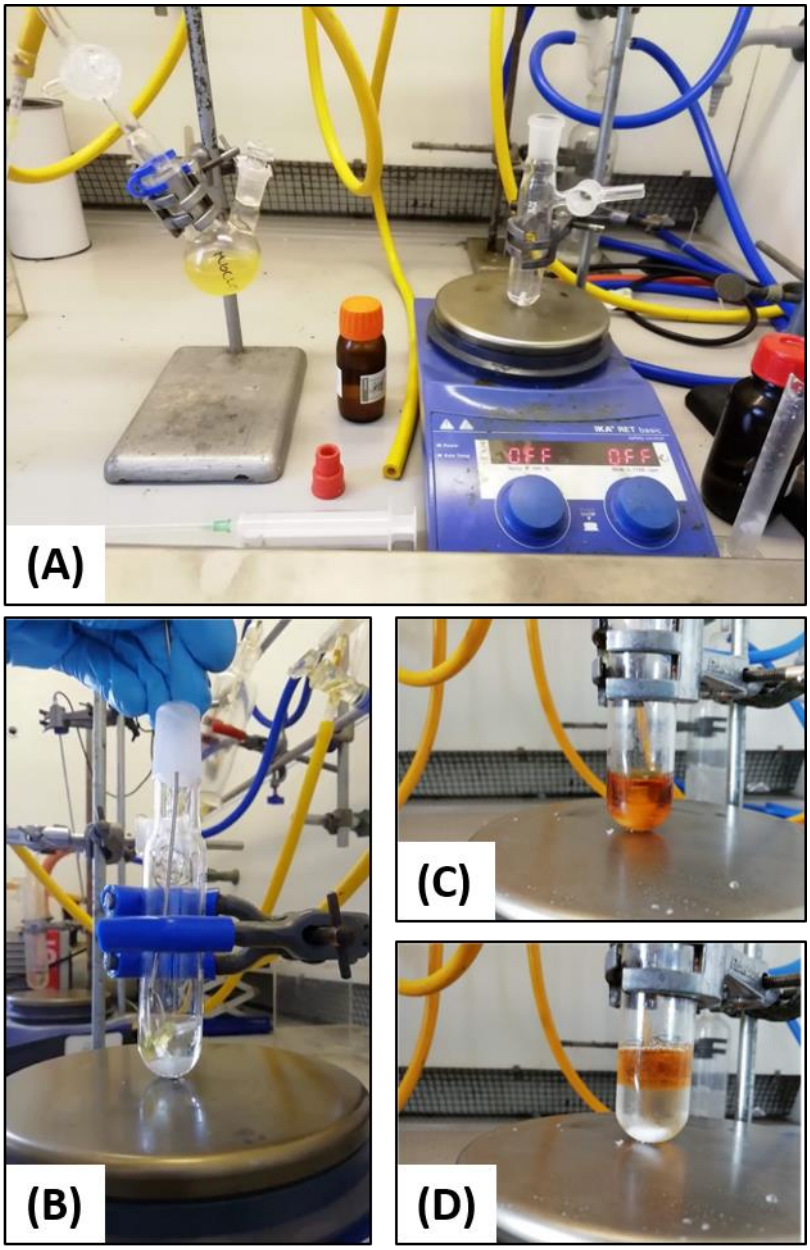

Figure 1 Reaction set up for amidation of esters using lithium amides under air. (**A**) Pre-addition (**B**) Addition of lithium amide, 1.0 M solution in 2-MeTHF. (**C**) Reaction in progress (**D**) Reaction after quench with 5 mL of Rochelle's salt

Solvent Screening – Table 1

Additions were performed under air at room temperature in an open Schlenk flask (25 mL) and 1 g of appropriate solvent. Lithium amide **2a** (1.5 mL, 1.0 M in 2-MeTHF) was added to a stirring solution of ester **1a** (1 mmol). After 20 s the reaction was quenched by the addition of saturated Rochelle's salt solution (sodium potassium tartrate tetrahydrate, 5 mL) before being extracted into 2-MeTHF (3 x 10 mL). Extracts were combined, dried over $MgSO_4$ and concentrated under vacuum.

Crude products were purified by silica column chromatography, eluted by hexane:EtOAc (10:1 – 2:1 gradient). Products were identified by GCMS and ^{1}H NMR. Yields of **3a** were obtained by ^{1}H NMR spectroscopy by integration against ferrocene as an internal standard as described in General Methods.

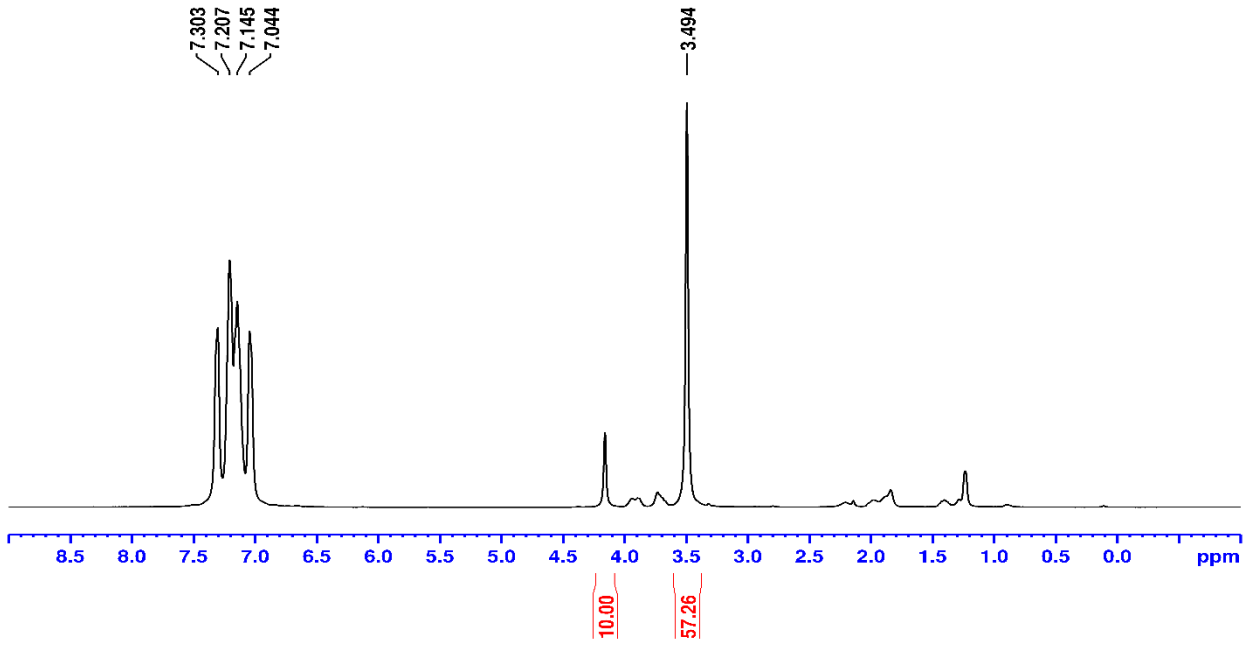

Figure 2 ^{1}H NMR spectrum (400.1 MHz, $CDCl_3$) of Table 1, Entry 1 (**3a**, THF, 93%). $FeCp_2$ (49 μmol, 4.9 mol%).

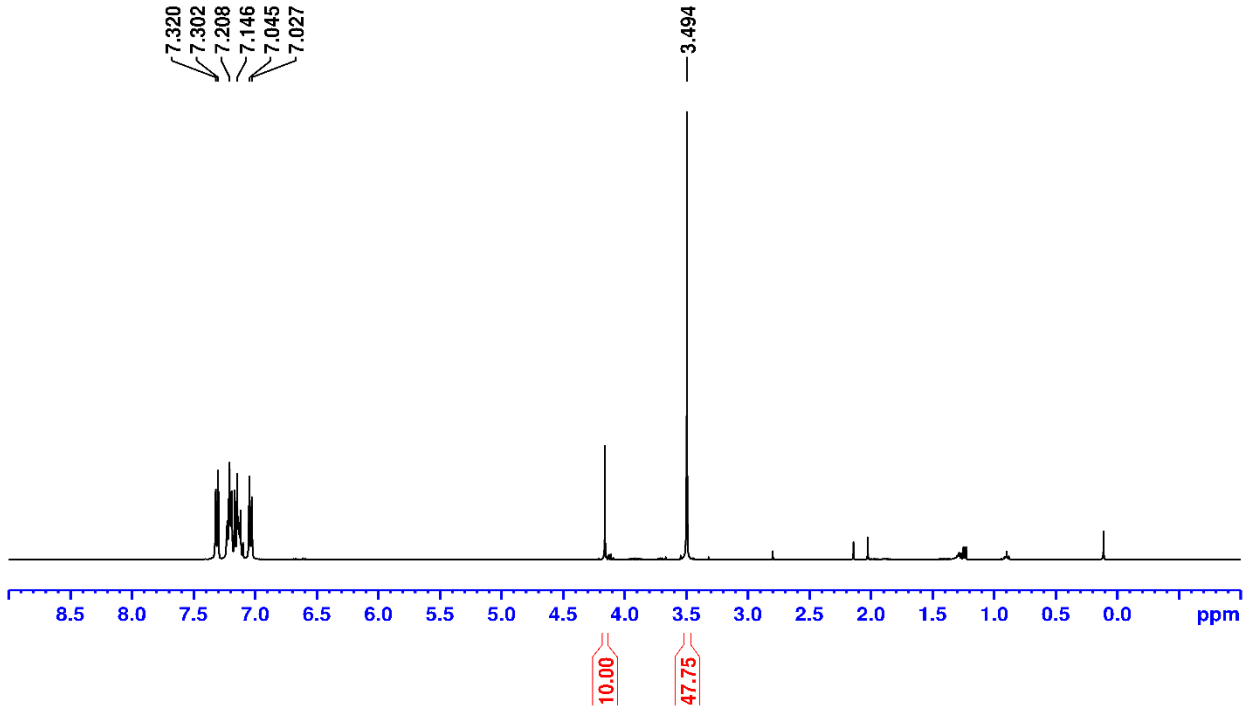

Figure 3 ^{1}H NMR spectrum (400.1 MHz, $CDCl_3$) of Table 1, Entry 2 (**3a**, 2-MeTHF 3 eq. **2a**, 80%). $FeCp_2$ (50 μmol, 5 mol%).

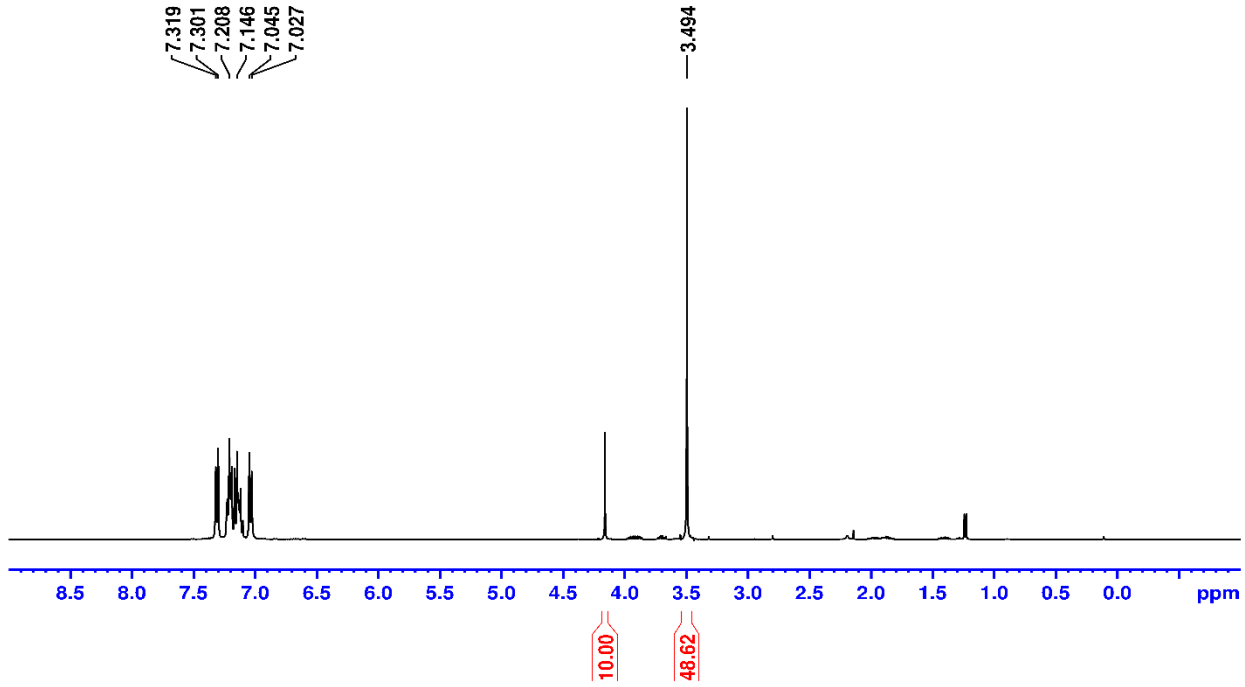

Figure 4 ^{1}H NMR spectrum (400.1 MHz, $CDCl_3$) of Table 1, Entry 3 (**3a**, 2-MeTHF 2 eq. **2a**, 81%). $FeCp_2$ (50 μmol, 5 mol%).

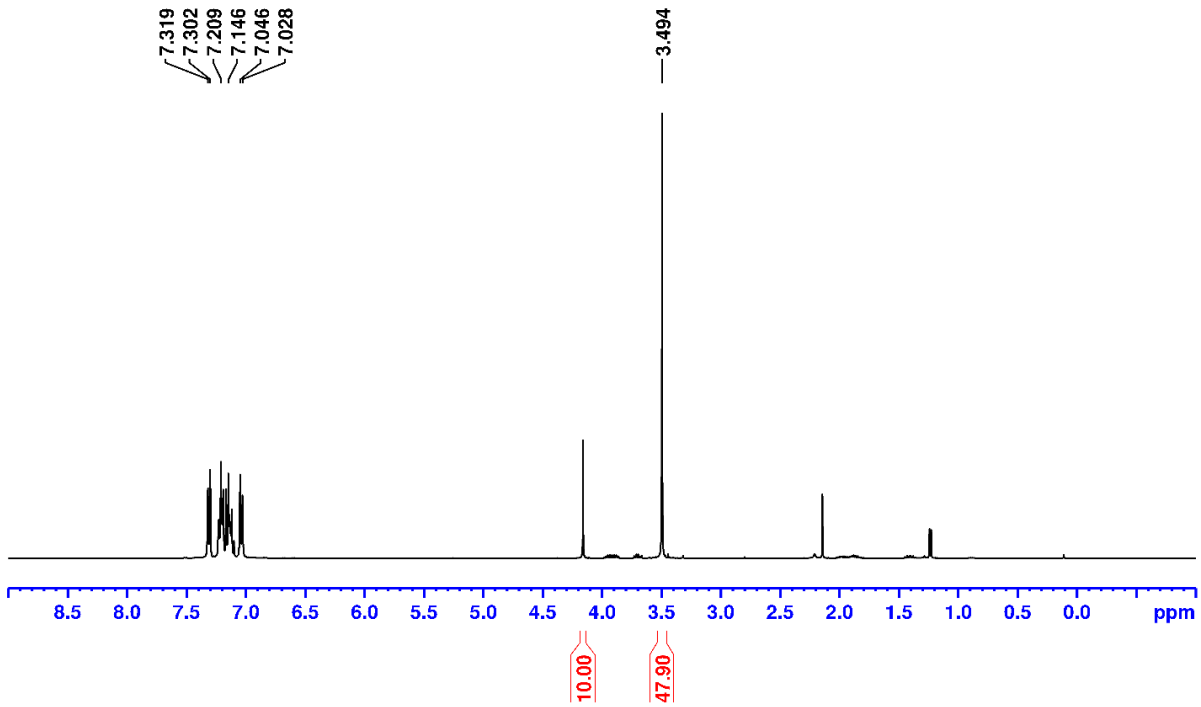

Figure 5 ^{1}H NMR spectrum (400.1 MHz, $CDCl_3$) of Table 1, Entry 4 (**3a**, 2-MeTHF 1.5 eq. **2a**, 80%). $FeCp_2$ (50 μmol, 5 mol%).

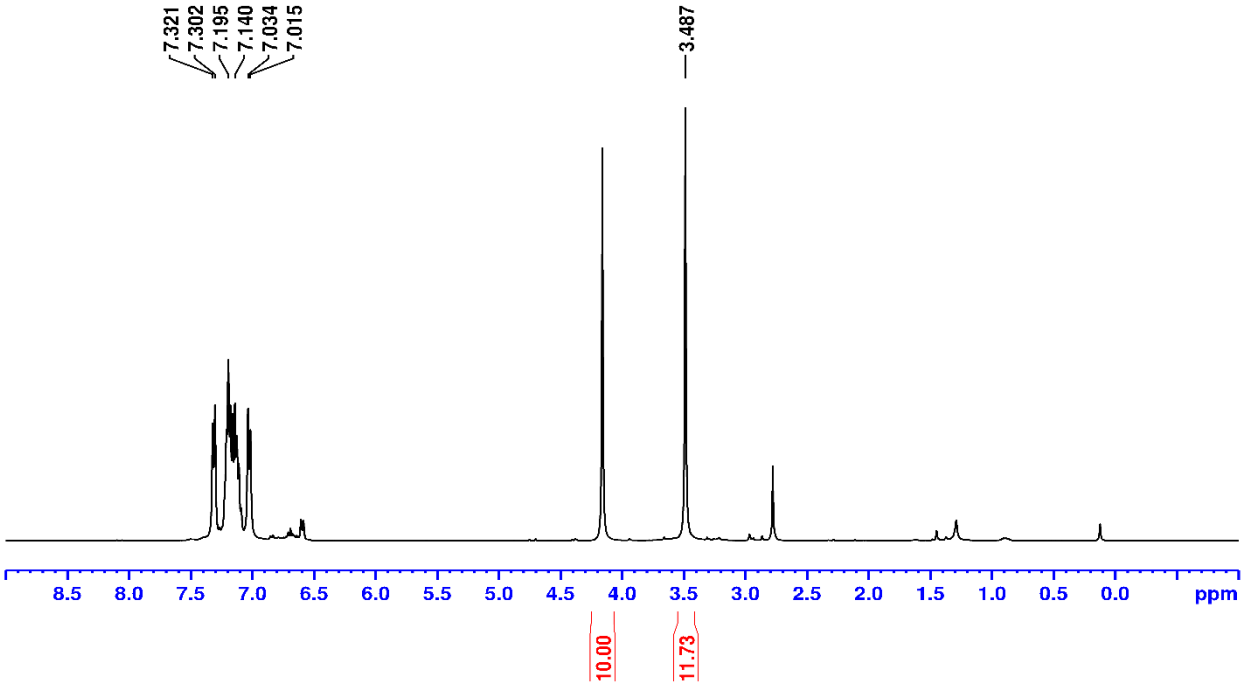

Figure 6 ^{1}H NMR spectrum (400.1 MHz, $CDCl_3$) of Table 1, Entry 5 (**3a**, 2-MeTHF 1 eq. **2a**, 78%). $FeCp_2$ (200 μmol, 20 mol%).

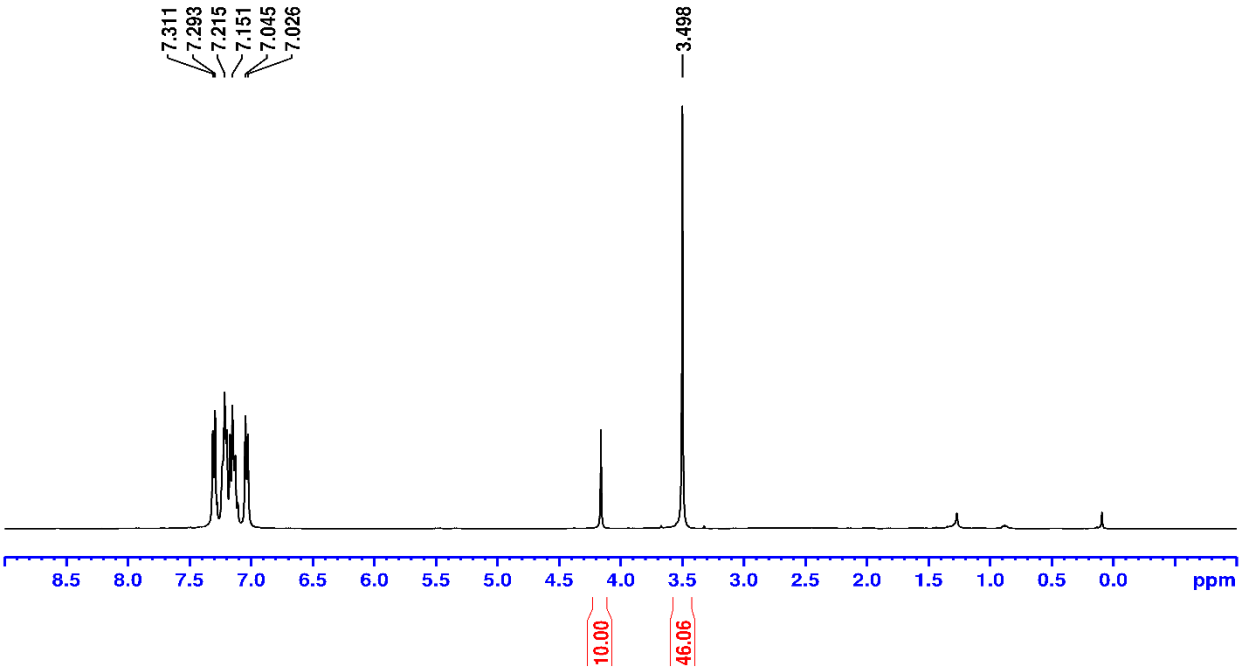

Figure 7 ^{1}H NMR spectrum (400.1 MHz, $CDCl_3$) of Table 1, Entry 6 (**3a**, ChCl/2Gly, 3 eq. **2a**, 83%). $FeCp_2$ (54 μmol, 5.4 mol%).

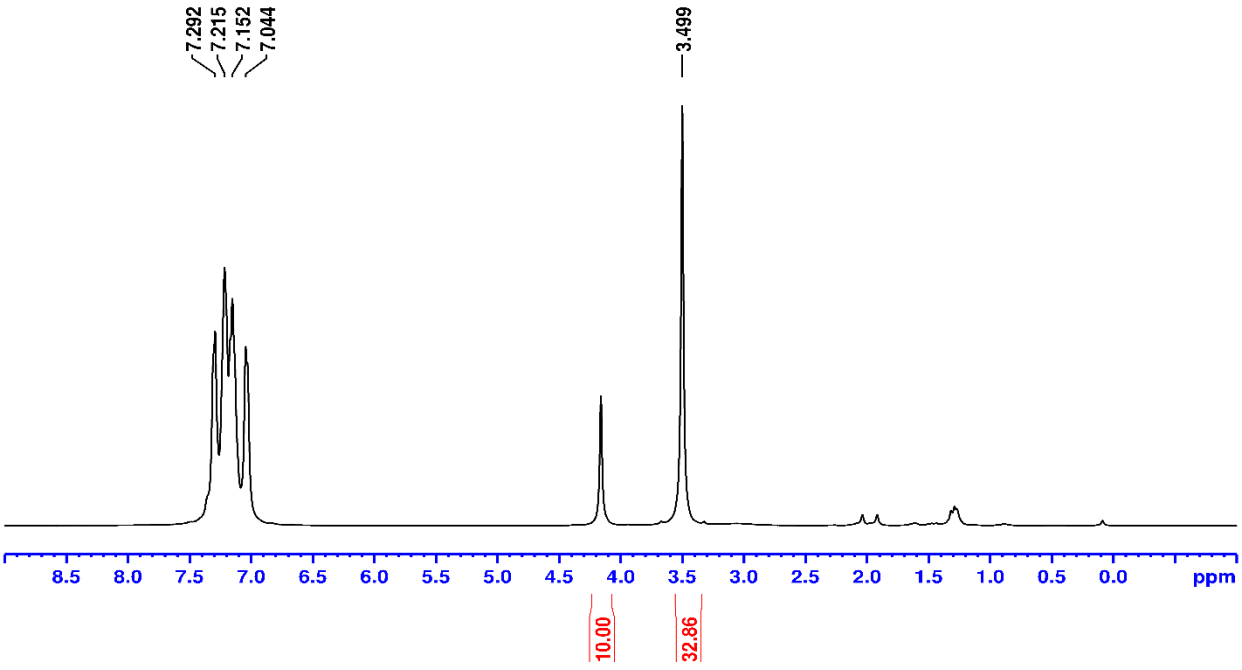

Figure 8 ^{1}H NMR spectrum (400.1 MHz, $CDCl_3$) of Table 1, Entry 7 (**3a**, ChCl/2EG, 3 eq. **2a**, 59%). $FeCp_2$ (54 μmol, 5.4 mol%).

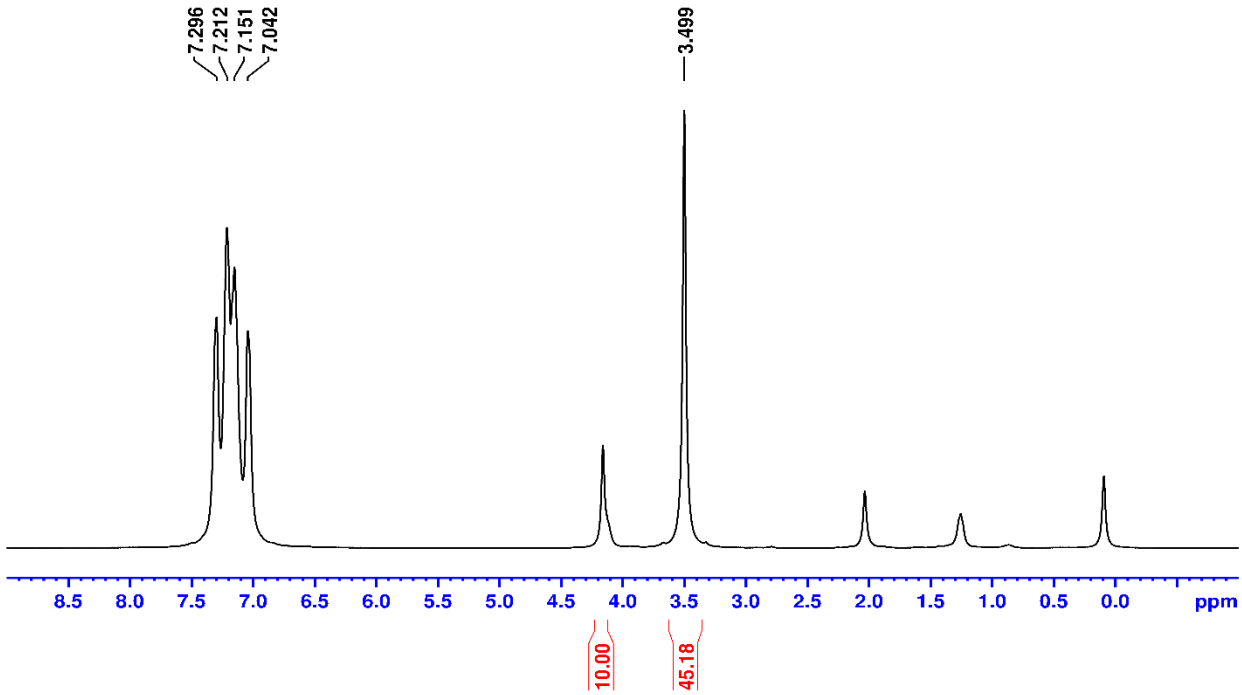

Figure 9 ^{1}H spectrum (400.1 MHz, $CDCl_3$) of Table 1, Entry 8 (**3a**, ChCl/2H2O, 3 eqs. **2a**, 81%). $FeCp_2$ (54 μmol, 5.4 mol%).

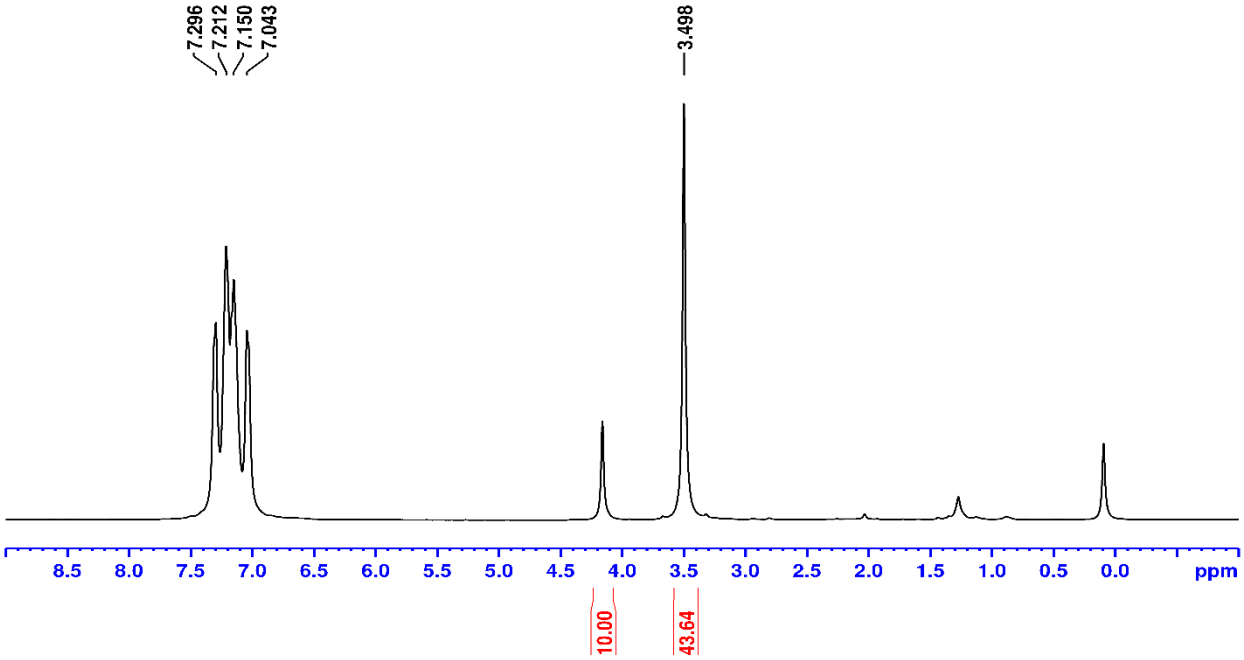

Figure 10 ^{1}H NMR spectrum (400.1 MHz, $CDCl_3$) of Table 1, Entry 9 (**3a**, LiCl/2H_2O, 3 eq. **2a**, 53 °C, 79%). $FeCp_2$ (54 μmol, 5.4 mol%).

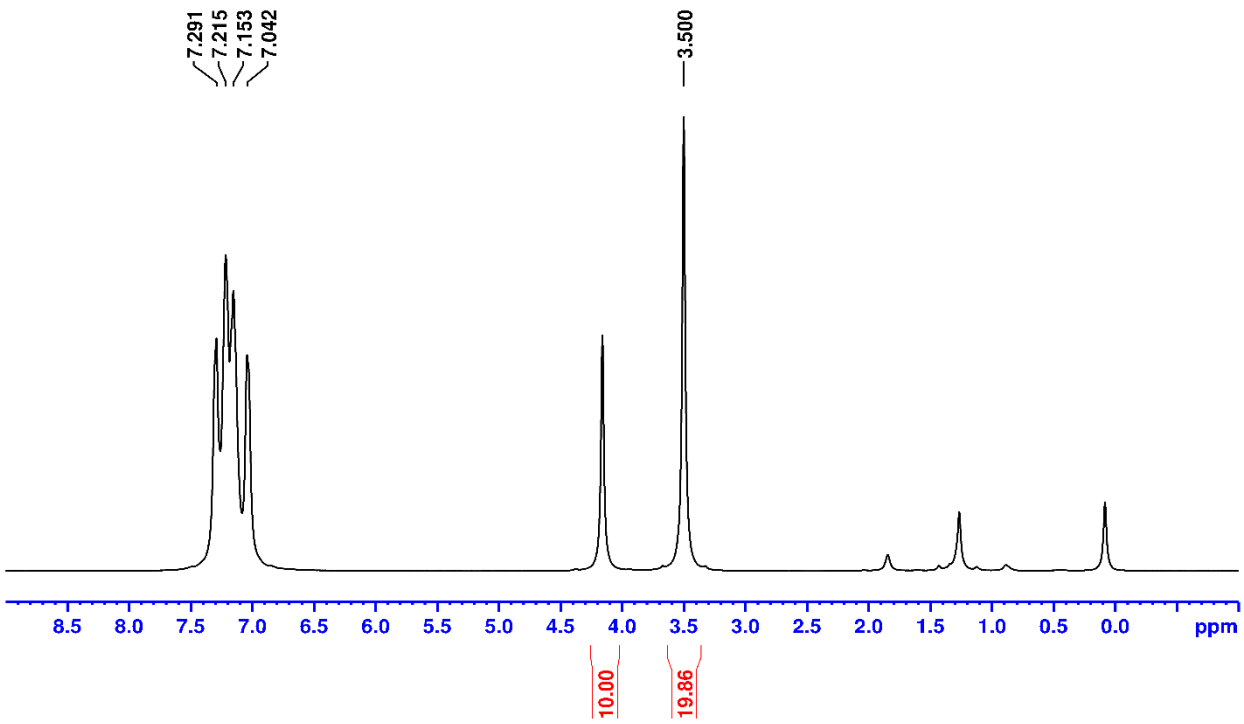

Figure 11 ^{1}H NMR spectrum (400.1 MHz, $CDCl_3$) of Table 1, Entry 10 (**3a**, H_2O, 3 eq. **2a**, 36%). $FeCp_2$ (54 μmol, 5.4 mol%).

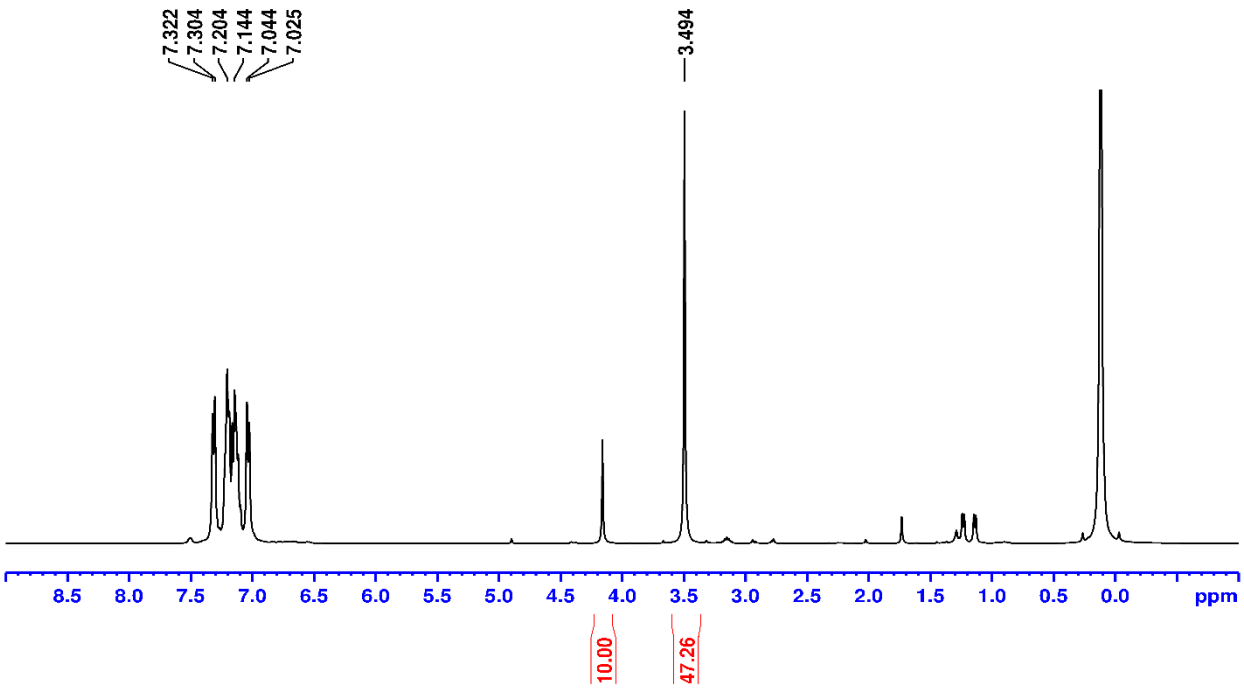

Figure 12 ^{1}H NMR spectrum (400.1 MHz, $CDCl_3$) of Table 1, Entry 11 (**3a**, Gly, 3 eq. **2a**, 85%). $FeCp_2$ (54 μmol, 5.4 mol%).

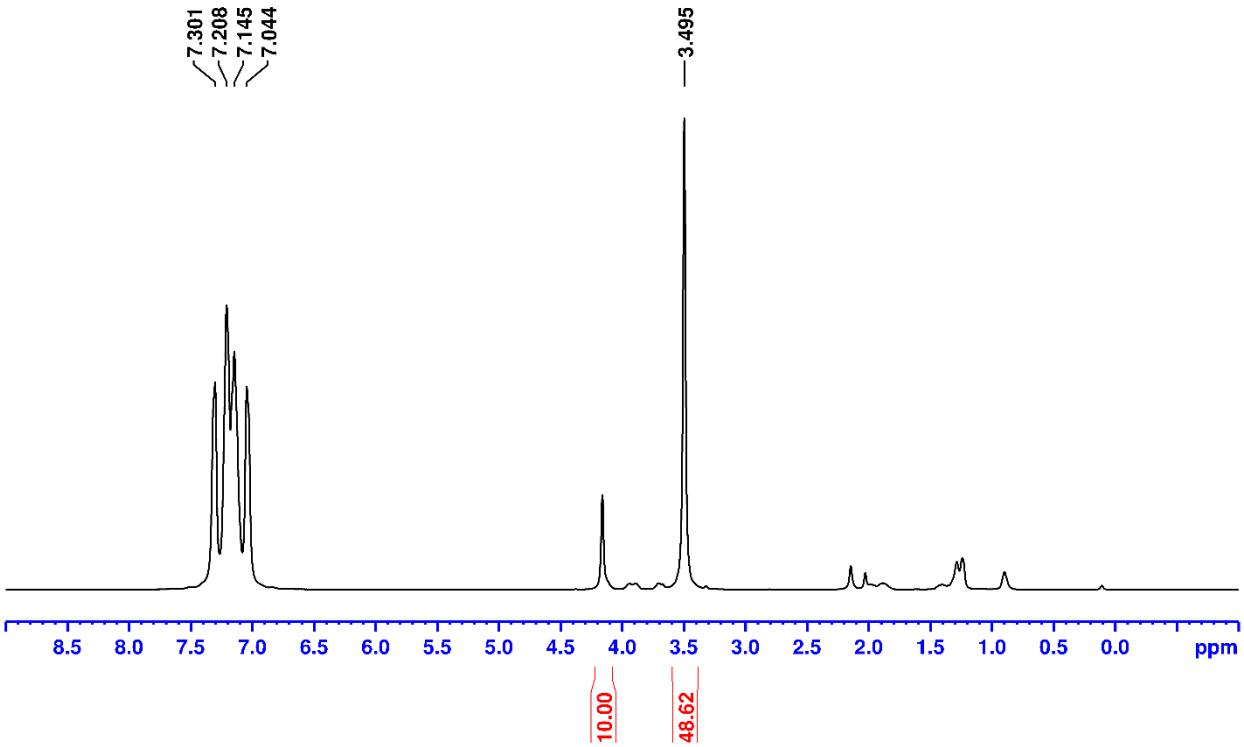

Figure 13 ^{1}H NMR spectrum (400.1 MHz, $CDCl_3$) of Table 1, Entry 12 (**3a**, Gly, 1.5 eq. **2a**, 79%). $FeCp_2$ (49 μmol, 4.9 mol%).

Procedure for the Lifetime Study of Lithium *N*-Methylanilide in Glycerol and 2-MeTHF – Table 2

Additions were performed under air at room temperature in an open Schlenk flask (25 mL) using 1 g of solvent. Lithium *N*-methylanilide solution (1.5 mL, 1.0 M in 2-MeTHF) was added to and after a set time interval, ethyl benzoate (144 µL, 1 mmol) was added. After 20 s the reaction was quenched by the addition of saturated Rochelle's salt solution (sodium potassium tartrate tetrahydrate, 5 mL) before being extracted into 2-MeTHF (3 x 10 mL). Extractions were combined, dried over $MgSO_4$ and concentrated under vacuum.

Crude products were purified by silica column chromatography eluted by hexane:EtOAc (10:1 – 2:1 gradient). Products were identified by GCMS and ^{1}H spectroscopy. Yields of **3a** were obtained by ^{1}H NMR spectroscopy by integration against ferrocene as an internal standard as described in General Methods.

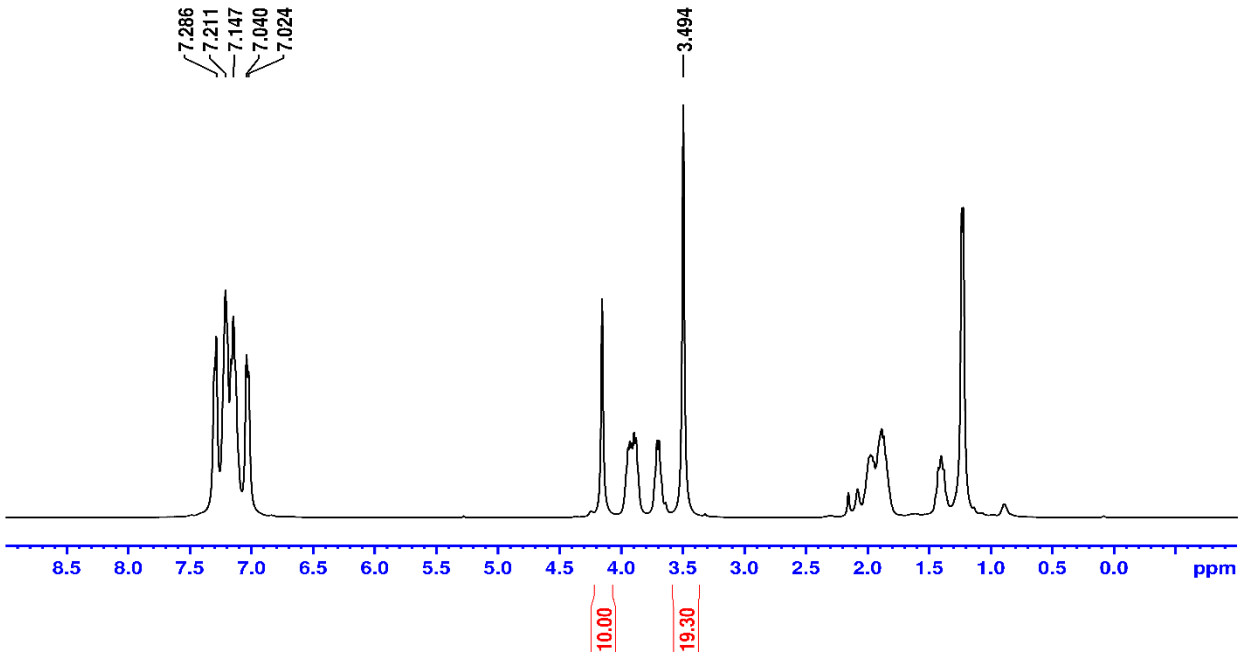

Figure 14 ^{1}H NMR spectrum (400.1 MHz, $CDCl_3$) of Table 2, Entry 1 (**3a**, Gly, 10 s stirring with **2a** before addition of **1a**, 32%). FeCp2 (50 µmol, 5 mol%).

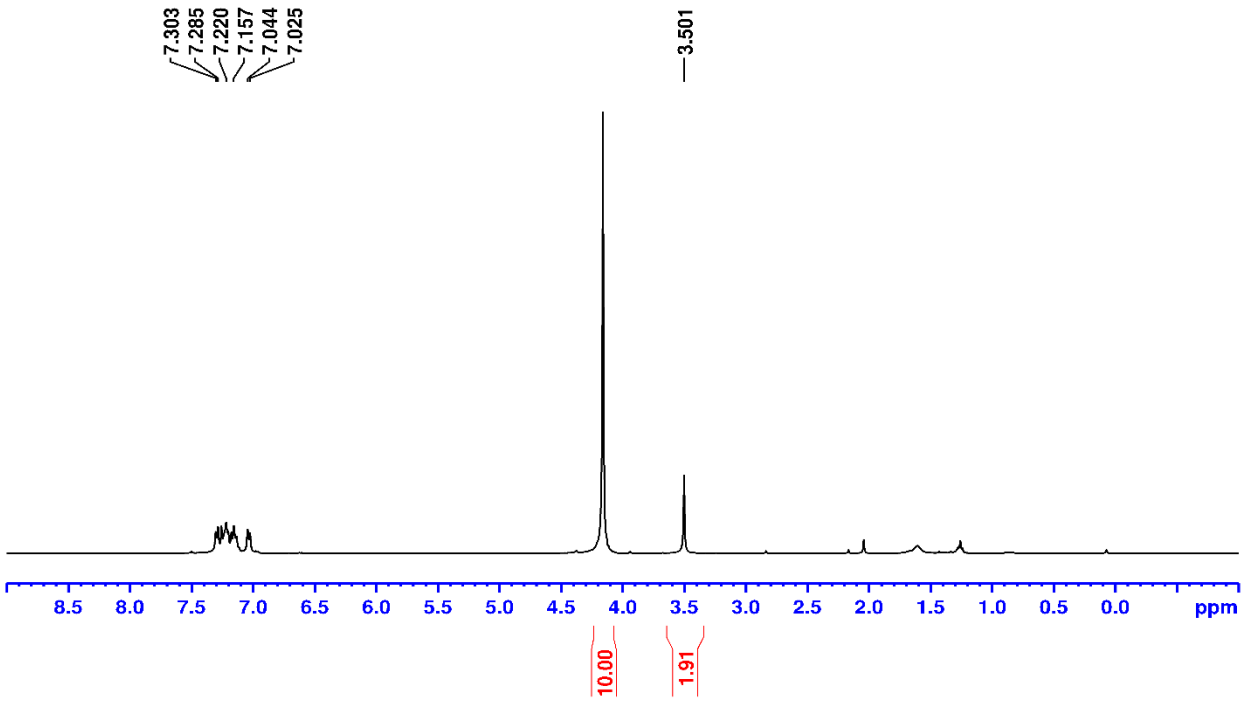

Figure 15 ^{1}H NMR spectrum (400.1 MHz, $CDCl_3$) of Table 2, Entry 2 (**3a**, Gly 30 s stirring with **2a** before addition of **1a**, 3%). $FeCp_2$ (50 μmol, 5 mol%).

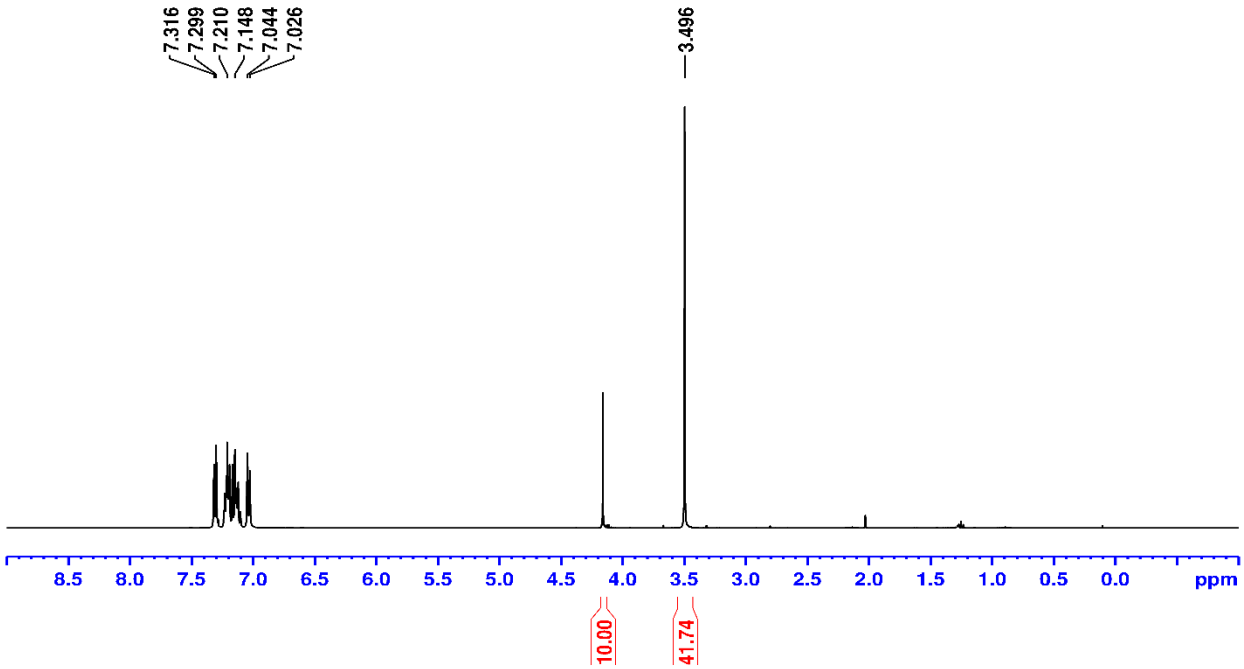

Figure 16 ^{1}H NMR spectrum (400.1 MHz, $CDCl_3$) of Table 2, Entry 3 (**3a**, 2-MeTHF 1 min stirring with **2a** before addition of **1a**, 70%). $FeCp_2$ (50 μmol, 5 mol%).

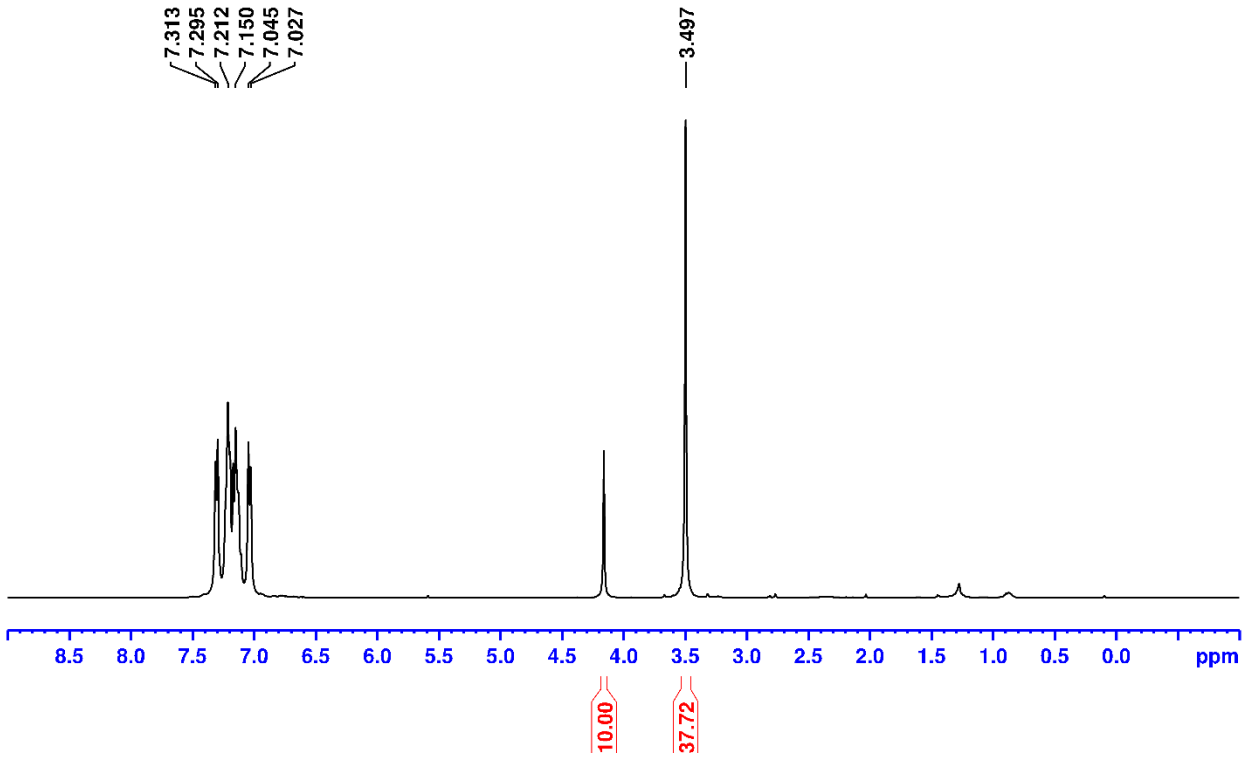

Figure 17 ^{1}H NMR spectrum (400.1 MHz, $CDCl_3$) of Table 2, Entry 4 (**3a**, 2-MeTHF 2 min stirring with **2a** before addition of **1a**, 62%). $FeCp_2$ (49 μmol, 4.9 mol%).

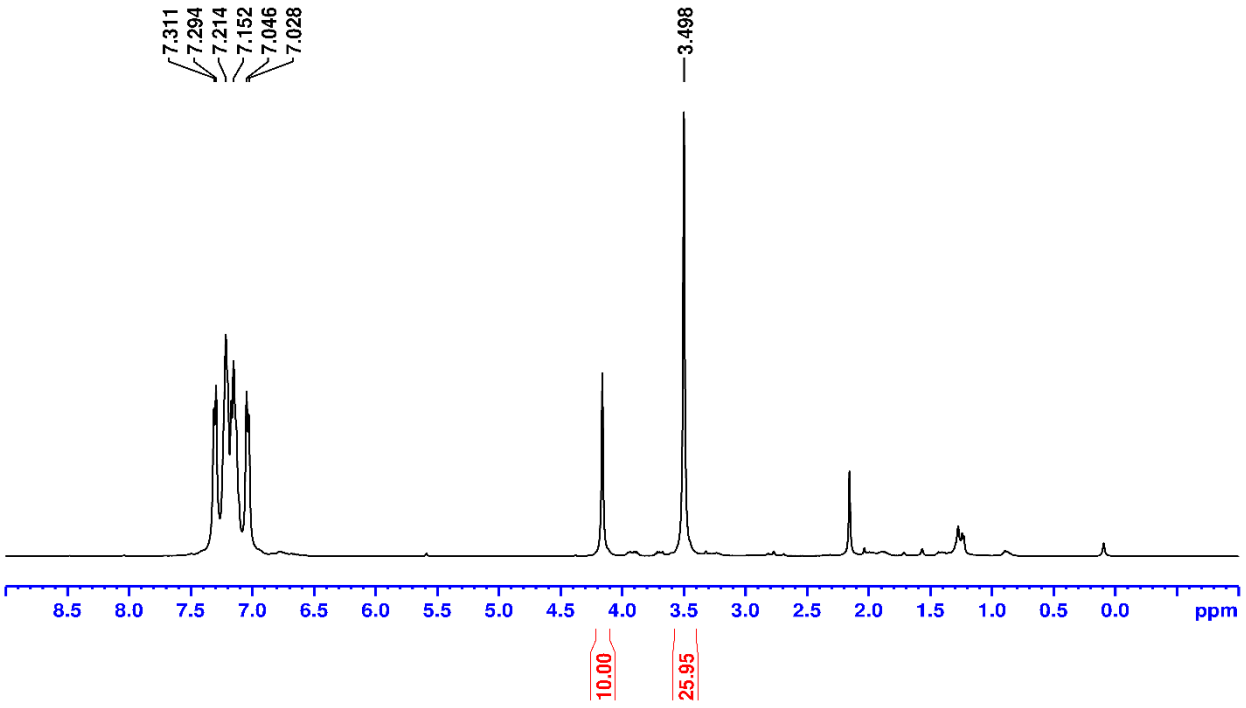

Figure 18 ^{1}H spectrum (400.1 MHz, $CDCl_3$) of Table 2, Entry 5 (**3a**, 2-MeTHF 5 min stirring with **2a** before addition of **1a**, 42%). $FeCp_2$ (49 μmol, 4.9 mol%).

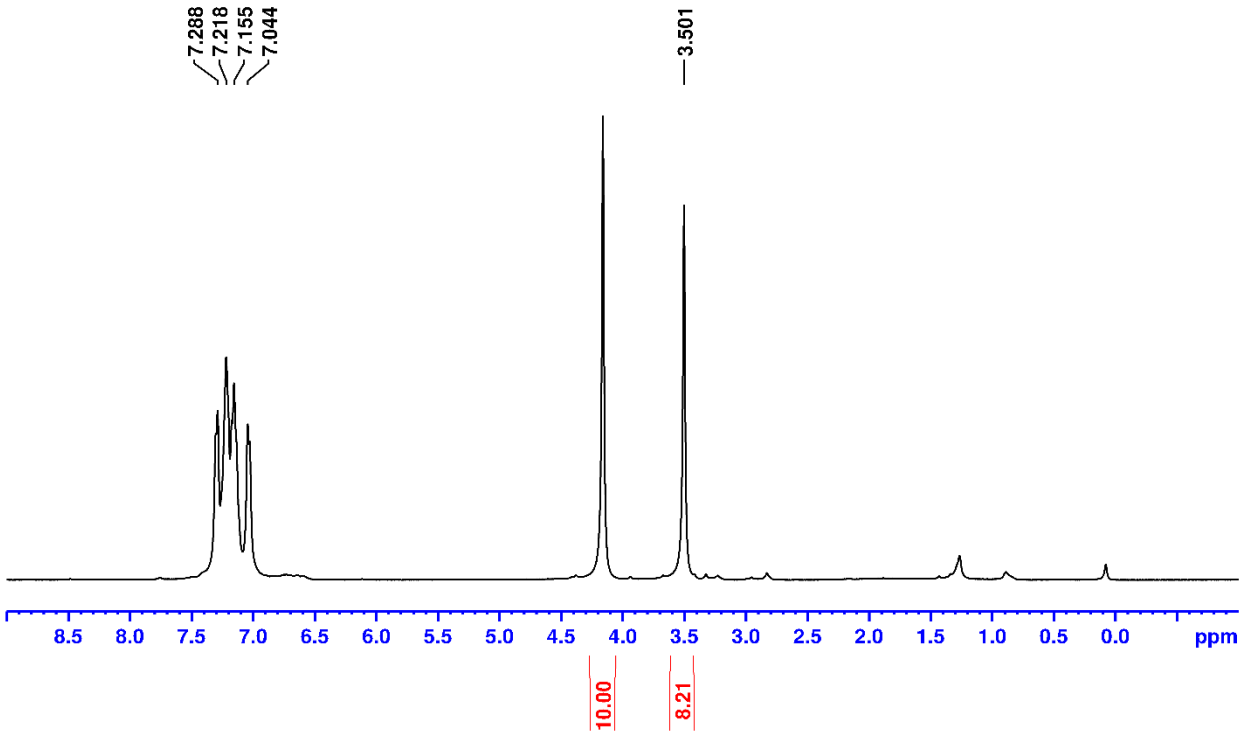

Figure 19 ^{1}H NMR spectrum (400.1 MHz, $CDCl_3$) of Table 2, Entry 6 (**3a**, 2-MeTHF 10 min stirring with **2a** before addition of **1a**, 13%). $FeCp_2$ (49 μmol, 4.9 mol%).

Procedure for Addition of Solid Li-N(Me)Ph (**2a**) – Scheme 2

Additions were performed under air at room temperature in an open Schlenk flask (25 mL) with 1 g of Gly or 2-MeTHF. Lithium amide **2a** (170 mg, 1.5 mmoles) was added to a stirring solution of ester **1a** (144 μL, 1 mmol). After 20 s the reaction was quenched by the addition of saturated Rochelle's salt solution (sodium potassium tartrate tetrahydrate, 5 mL) before being extracted into 2-MeTHF (3 x 10 mL). Extracts were combined, dried over $MgSO_4$ and concentrated under vacuum.

Crude products were purified by silica column chromatography, eluted by hexane:EtOAc (10:1 – 2:1 gradient). Products were identified by GCMS and ^{1}H NMR. The yields of **3a** were obtained by ^{1}H NMR spectroscopy by integration against ferrocene as an internal standard as described in General Methods.

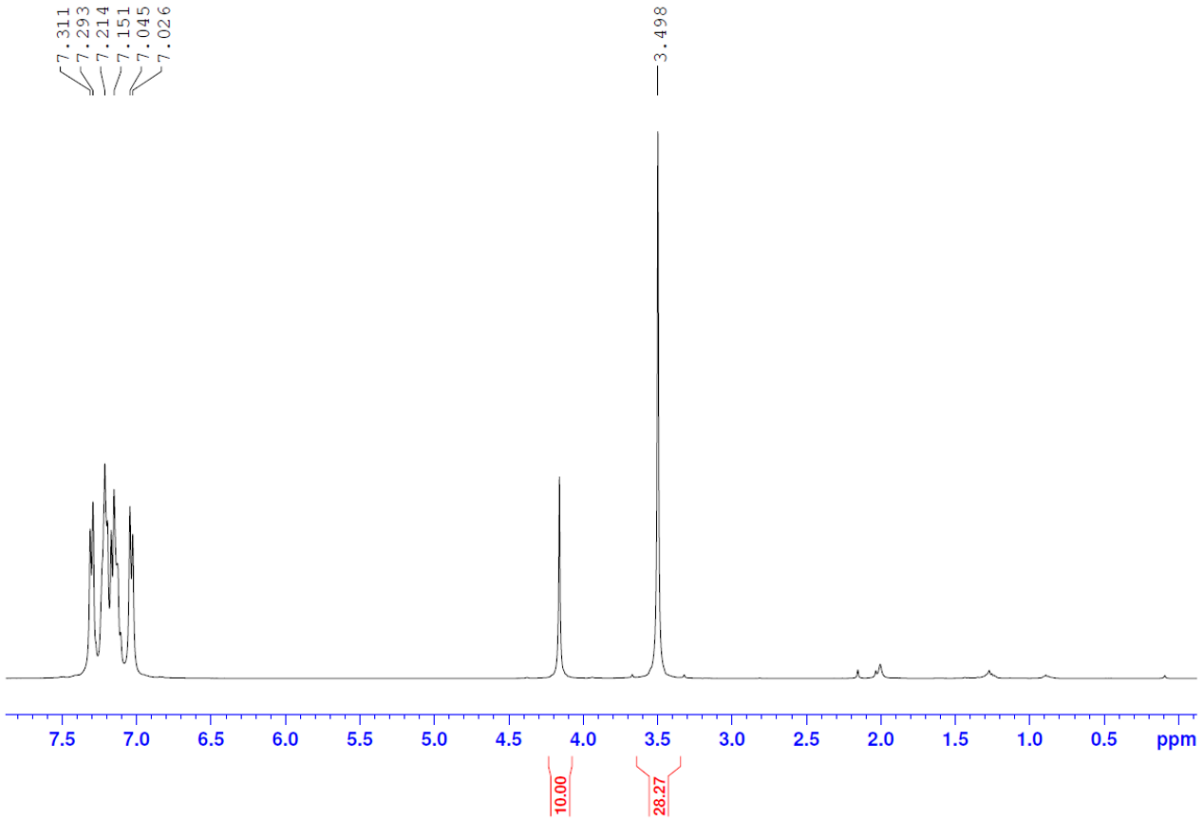

Figure 20 ^{1}H NMR spectrum (400.1 MHz, $CDCl_3$) of **3a** synthesized via addition of solid Li-N(Me)Ph (**2a**) in Gly. **3a** obtained in 47% yield against $FeCp_2$ (50 μmol, 5.0 mol%).

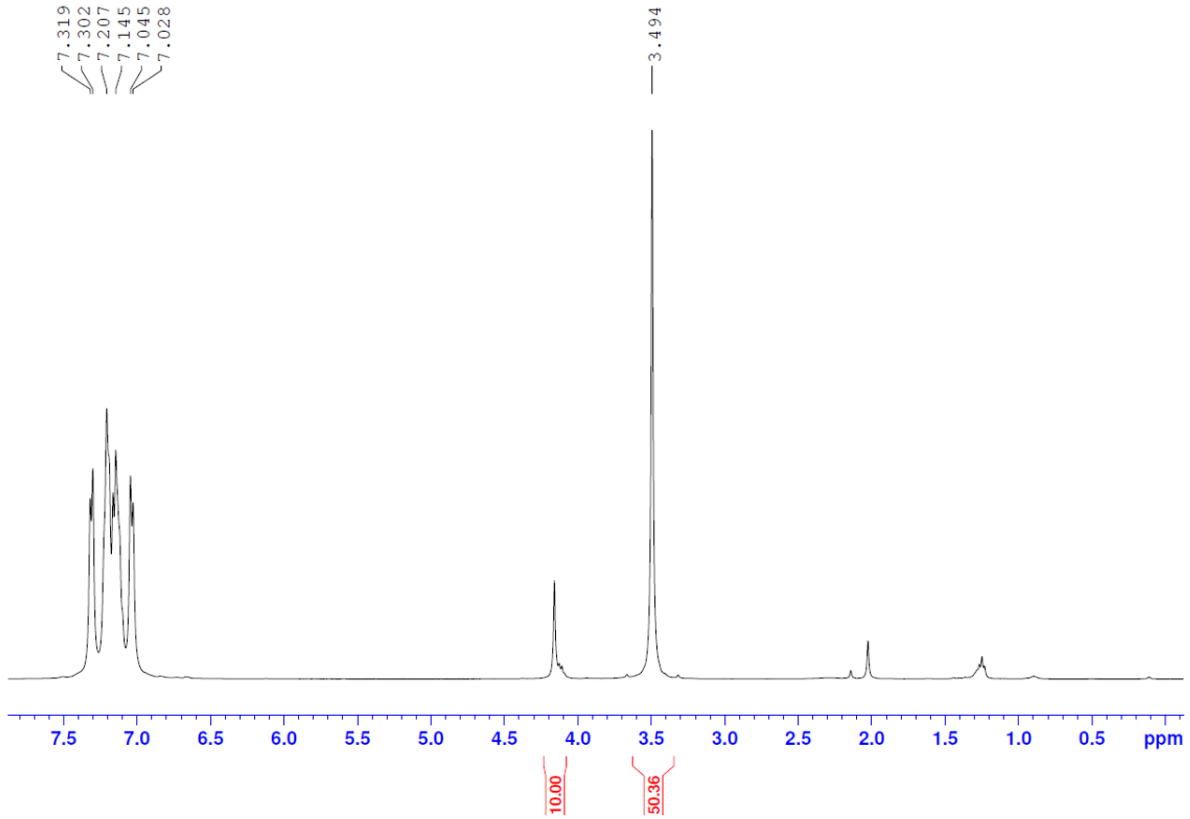

Figure 21 ^{1}H NMR spectrum (400.1 MHz, $CDCl_3$) of **3a** synthesized via addition of solid Li-N(Me)Ph (**2a**) in 2-MeTHF. **3a** obtained in 82% yield against $FeCp_2$ (49 μmol, 4.9 mol%).

Procedure for Reaction Scale-Up

In an open Schlenk flask (25 mL) and 2 mL of 2-MeTHF was added alongside 10 mmol (1.44 mL) of ethylbenzoate (**1a)** and stirred at room temperature. To this, 1.5 equivalents (4.06 mL, 3.7 M solution in 2-MeTHF) of **2a** (Li-N(Me)Ph) was added – 6 mL of 2-MeTHF in total giving concentration of 2.5 M of Li-N(Me)Ph. After 20 s the reaction was quenched by the addition of saturated Rochelle's salt solution (sodium potassium tartrate tetrahydrate, 5 mL) before being extracted into 2-MeTHF (3 x 10 mL). Extracts were combined, dried over $MgSO_4$ and concentrated under vacuum.

Product **3a** was purified by silica column chromatography, eluted by hexane:EtOAc (10:1 – 2:1 gradient). The yield was obtained by ^{1}H NMR spectroscopy by integration against ferrocene as an internal standard as described in General Methods, and calculated to be 89%.

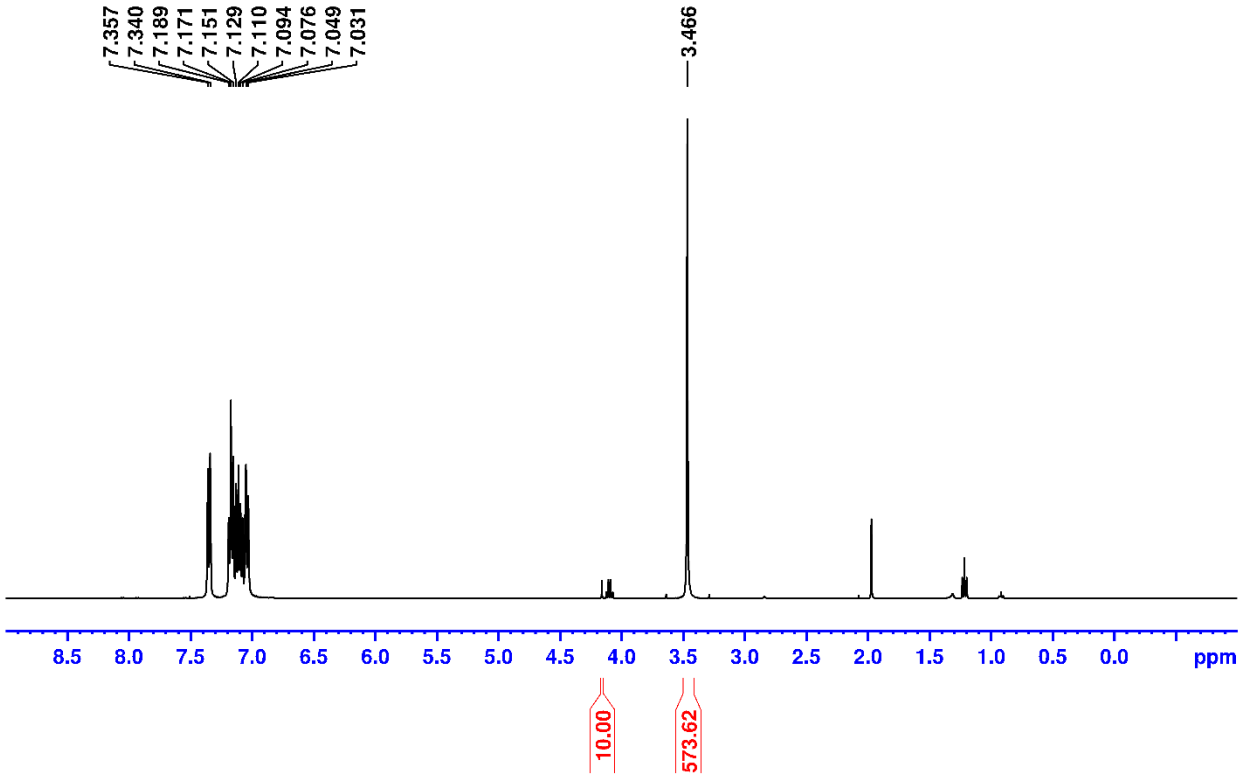

Figure 22 ^{1}H NMR spectrum (400.1 MHz, $CDCl_3$) of **3a** synthesized at 10 mmol scale in 6 mL total of 2 MeTHF. **3a** obtained in 89% yield against $FeCp_2$ (46 μmol, 4.6 mol%).

Procedure for the *in-situ* Amidation of Ethylbenzoate – Scheme 3

Additions were performed under air at room temperature in an open Schlenk flask (25 mL) and 1 g/1.16 mL of 2-MeTHF. *n*-BuLi (1.5 mmol, 0.94 mL, 1.6 M solution in hexane) was added to a stirring solution of ethyl benzoate (144 µL, 1 mmol) and 1.5 mmol (162 µL) of HN(Me)Ph. After 20 s the reaction was quenched by the addition of saturated Rochelle's salt solution (sodium potassium tartrate tetrahydrate, 5 mL) before being extracted into 2-MeTHF (3 x 10 mL). Extractions were combined, dried over $MgSO_4$ and concentrated under vacuum.

The crude yields were obtained by ^{1}H NMR spectroscopy by integration against ferrocene as an internal standard as described in General Methods – full conversion of starting materials into products is observed. Calculations showed a 26% yield of **4** (compound identified by GCMS analysis and with reference to literature-reported NMR spectra)[10] and a 79% crude yield of **3a** (slight overlap with N-H of *N*-methylaniline gives overall conversion of 105%). Comparison with conversion by GC shows 26:74 yield of **4**:**3a** which is almost identical to the yield observed by NMR against ferrocene as an internal standard.

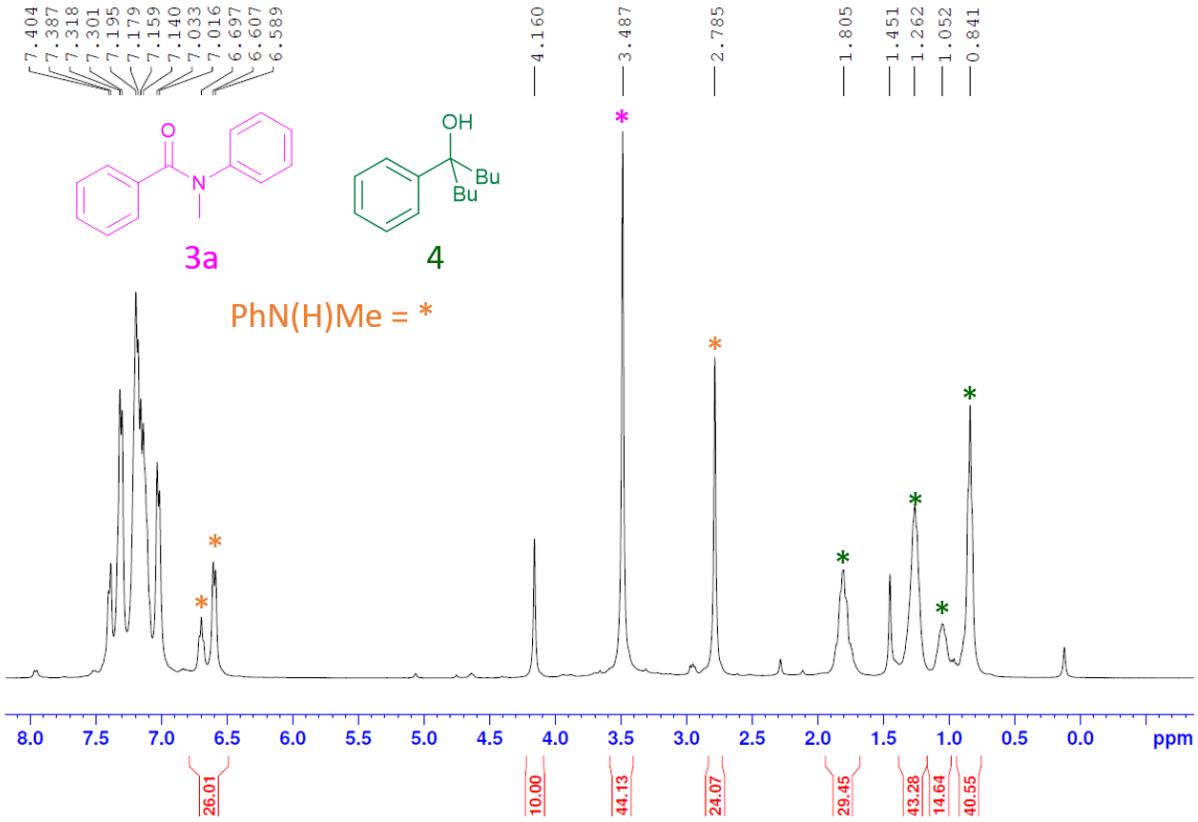

Figure 23 ^{1}H NMR spectrum (400.1 MHz, $CDCl_3$) of Scheme 3. $FeCp_2$ (54 µmol, 5.4 mol%)

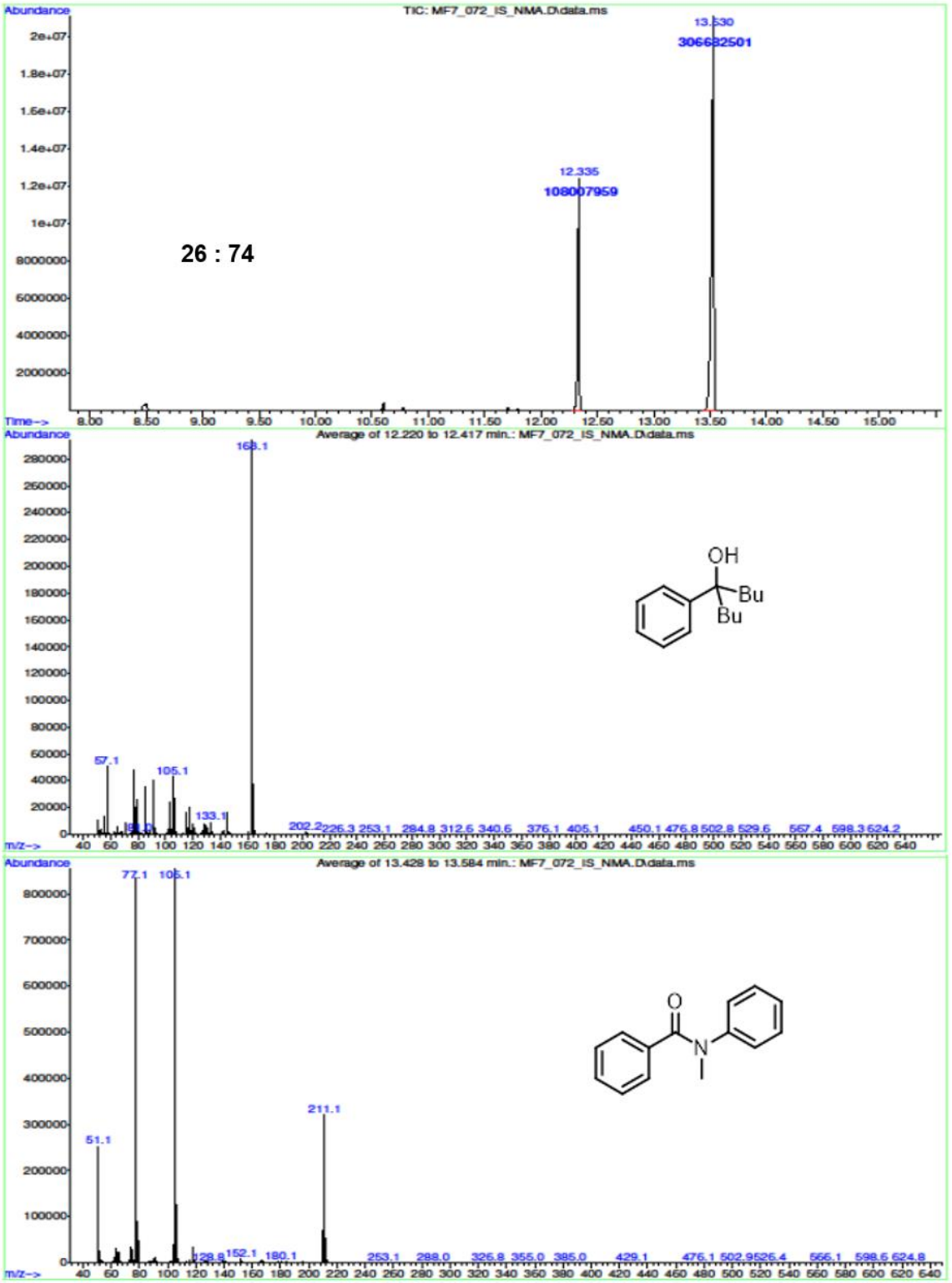

Figure 24 GC/EI-MS spectrum of the reaction shown in Scheme 3 (**3a** and **4** detected in 74:26 ratio)

Transamidation of Esters and Amides (**3a-3m**) – Table 3

Additions were performed under air at room temperature in an open Schlenk flask (25 mL) and 1 g of 2-MeTHF. Lithium amide **2a** (1.5 mL, 1.0 M in 2-MeTHF) was added to a stirring solution of ester **1a-1m** (1 mmol). After 20 s the reaction was quenched by the addition of saturated Rochelle's salt solution (sodium potassium tartrate tetrahydrate, 5 mL) before being extracted into 2-MeTHF (3 x 10 mL). Extracts were combined, dried over $MgSO_4$ and concentrated under vacuum.

Crude products were purified by silica column chromatography, eluted by hexane:EtOAc (10:1 – 2:1 gradient). Products were identified by GCMS and ^{1}H NMR. Yields were obtained by ^{1}H NMR spectroscopy by integration against ferrocene as an internal standard as described in General Methods.

N-Methyl-*N*-phenylbenzamide **3a**. Spectral data were in accord with published data.[3]

^{1}H NMR (400.1 MHz, $CDCl_3$): δ / ppm 7.34–7.28 (2H, m, Ar), 7.24–7.09 (6H, m, Ar), 7.06–7.01 (2H, m, Ar), 3.49 (3H, s, C*H*$_3$).

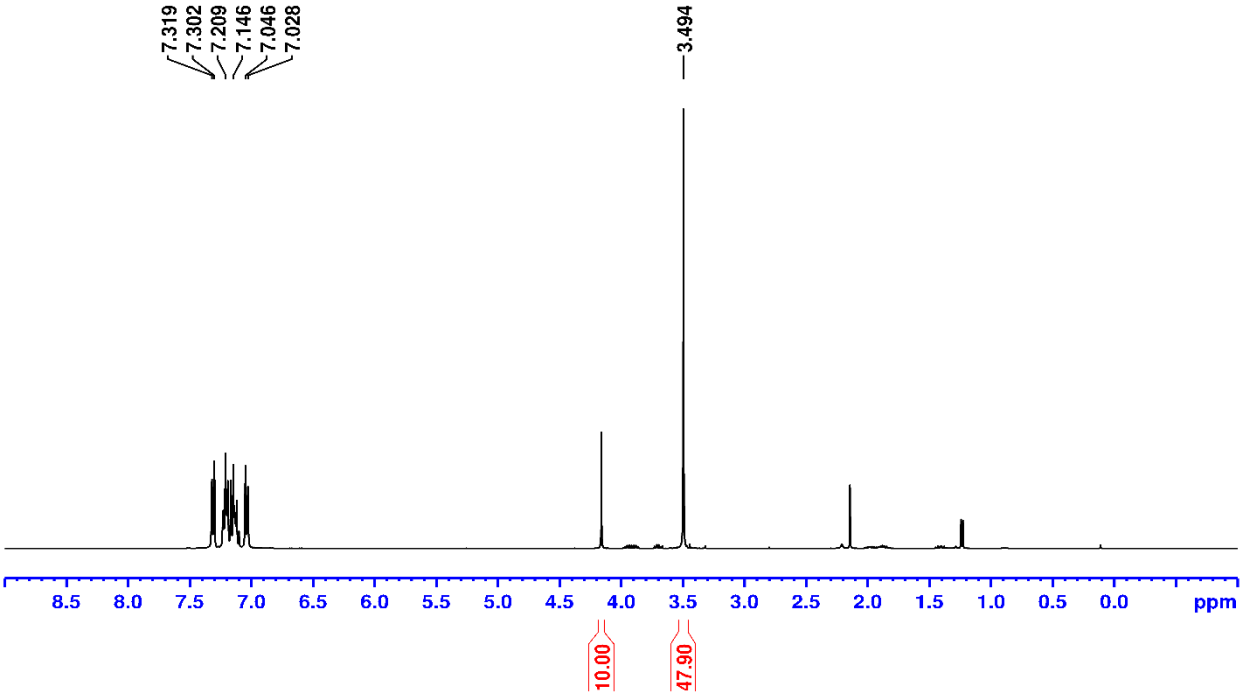

Figure 25 ^{1}H NMR spectrum (400.1 MHz, $CDCl_3$) of Table 3, Entry **3a**, 80%. $FeCp_2$ (50 μmol, 5 mol%).

4-Chloro-*N*-methyl-*N*-phenylbenzamide **3b**. Spectral data were in accord with published data.[4]

^{1}H NMR (400.1 MHz, $CDCl_3$): δ / ppm 7.31–7.19 (4H, m, Ar), 7.19–7.09 (3H, m, Ar), 7.09–6.98 (2H, m, Ar), 3.49 (3H, s, CH_3).

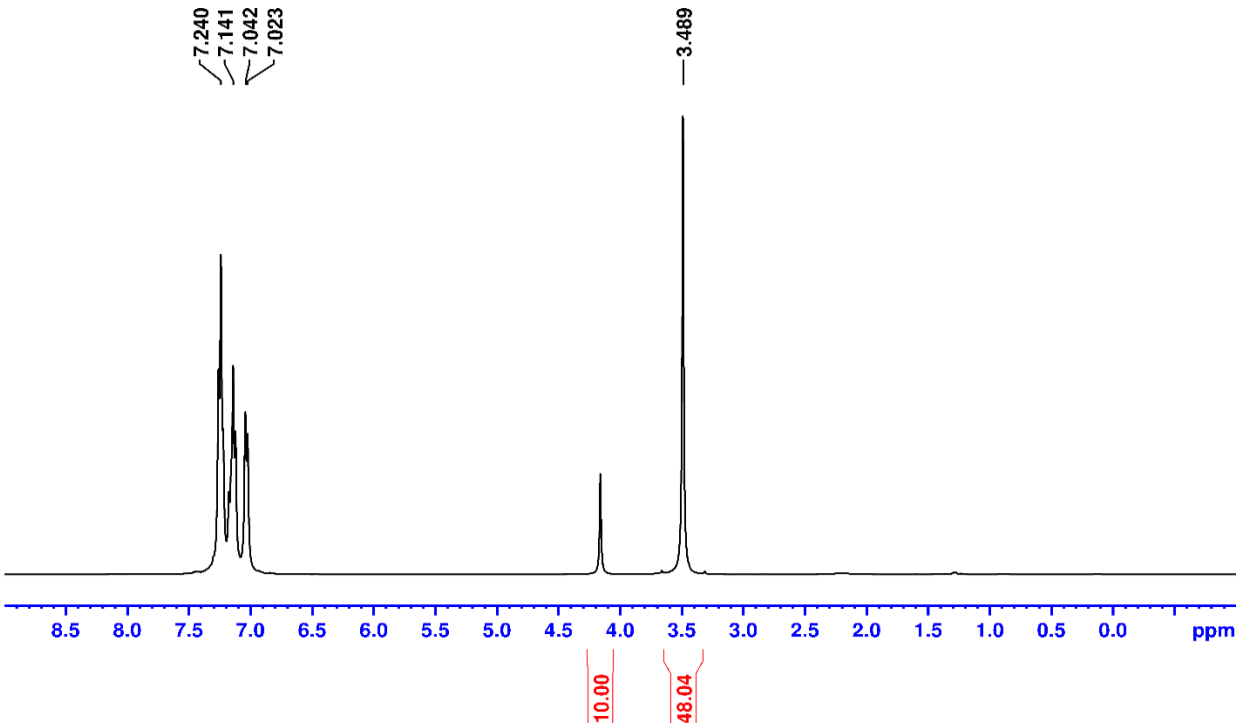

Figure 26 ^{1}H NMR spectrum (400.1 MHz, $CDCl_3$) of Table 3, Entry **3b**, 85%. $FeCp_2$ (53 μmol, 5.3 mol%).

4-Fluoro-*N*-methyl-*N*-phenylbenzamide **3c**. Spectral data were in accord with published data.[5]

^{1}H NMR (400.1 MHz, $CDCl_3$): δ / ppm 7.33–7.27 (2H, m, Ar), 7.26–7.20 (2H, m, Ar), 7.17–7.11 (1H, m, Ar), 7.06–7.00 (2H, m, Ar), 6.86–6.79 (2H, m, Ar), 3.48 (3H, s, CH_3)

^{19}F NMR (376.4 MHz, $CDCl_3$): δ / ppm −110.12 (1F, s, Ar*F*).

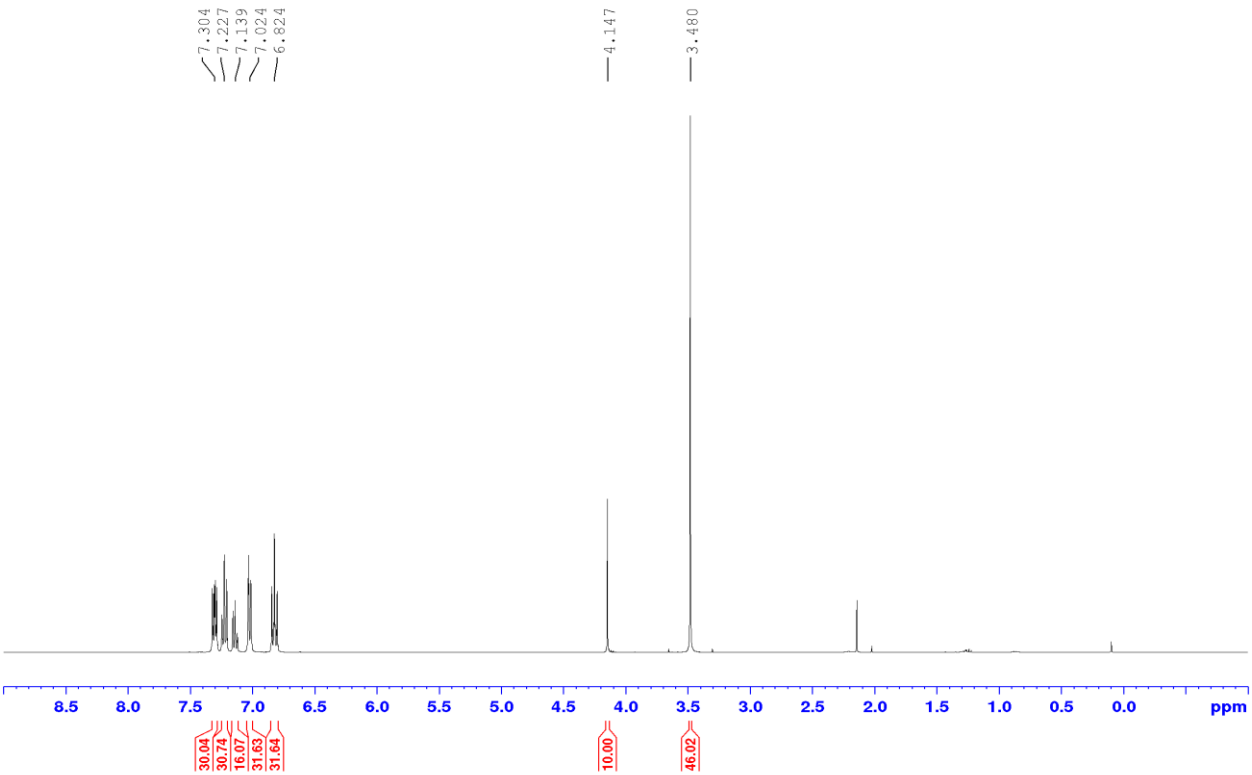

Figure 27 ^{1}H spectrum (400.1 MHz, $CDCl_3$) of Table 3, Entry **3c**, 77%. $FeCp_2$ (50 μmol, 5 mol%).

3-Fluoro-*N*-methyl-*N*-phenylbenzamide **3d**.

^{1}H NMR (400.1 MHz, $CDCl_3$): δ / ppm 7.26 (3H, m, Ar), 7.14 (6H, m, Ar), 6.95 (1H, m, Ar), 3.52 (3H, s, CH_3)

^{13}C{^{1}H} NMR (100.6 MHz, $CDCl_3$): δ / ppm 168.6 (*C*O), 162.7 (Ar), 160.3 (Ar), 144.0 (1C, s, Ar), 137.6 (d, *J* = 7 Hz, Ar), 128.9 (Ar), 128.8 (Ar), 126.3 (Ar), 123.9 (1C, d, *J* = 3 Hz, Ar), 116.1 (d, *J* = 21 Hz, Ar), 115.3 (d, *J* = 23 Hz, Ar), 38 (*C*H_3)

^{19}F NMR (128.4 MHz, $CDCl_3$): δ / ppm -112.8 (3F, s, Ar*F*)

HR-MS found: 229.08991; calculated for [M^+] ($C_{14}H_{12}ONF^+$): 229.08974 (error 0.17 ppm).

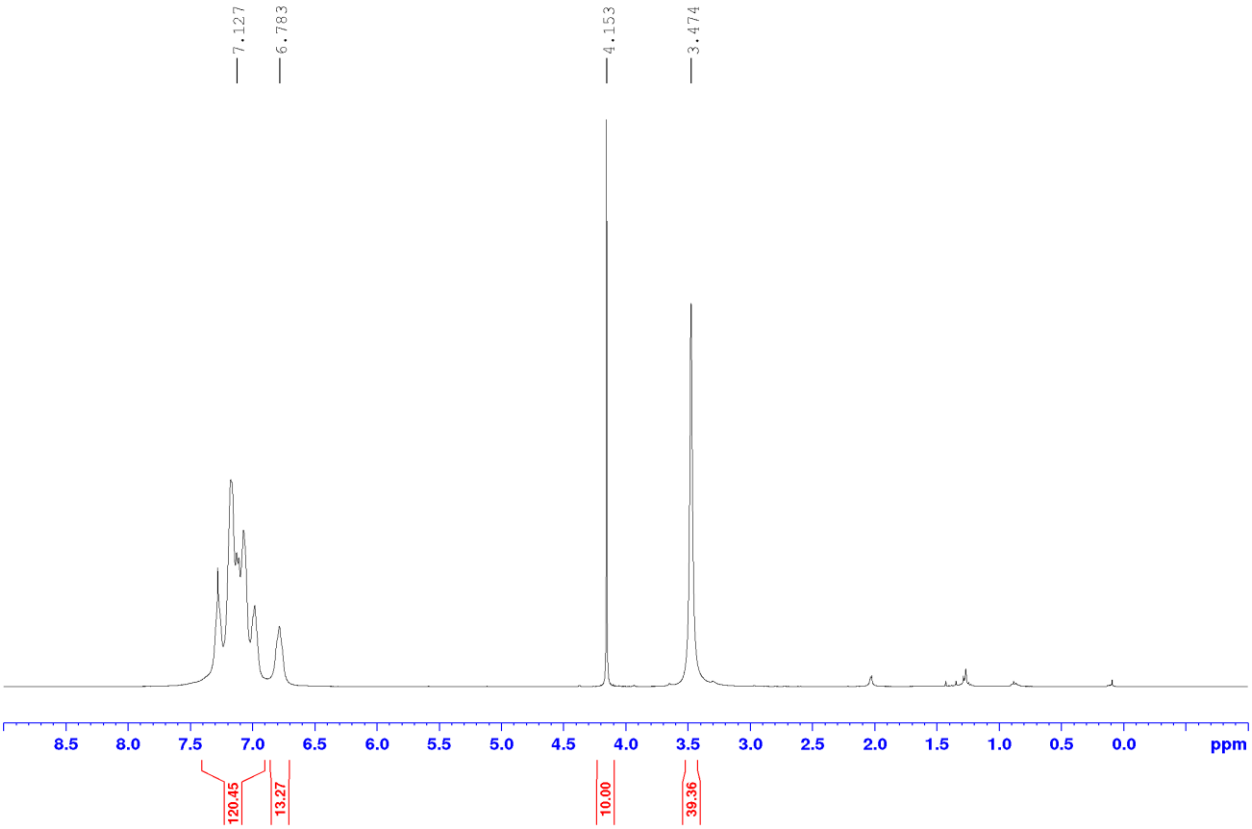

Figure 28 ^{1}H NMR spectrum (400.1 MHz, $CDCl_3$) of Table 3, Entry **3d**, 70%. $FeCp_2$ (53 μmol, 5.3 mol%).

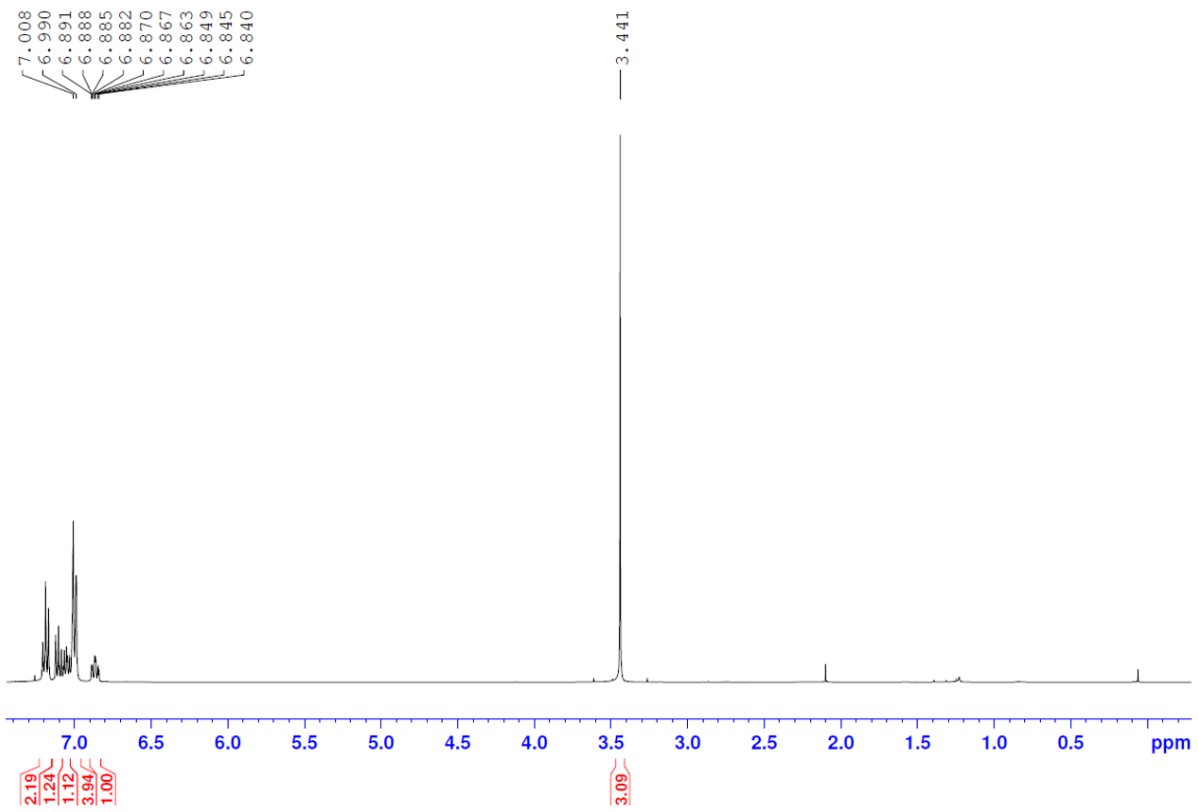

Figure 29 ^{1}H NMR spectrum of **3d** in $CDCl_3$

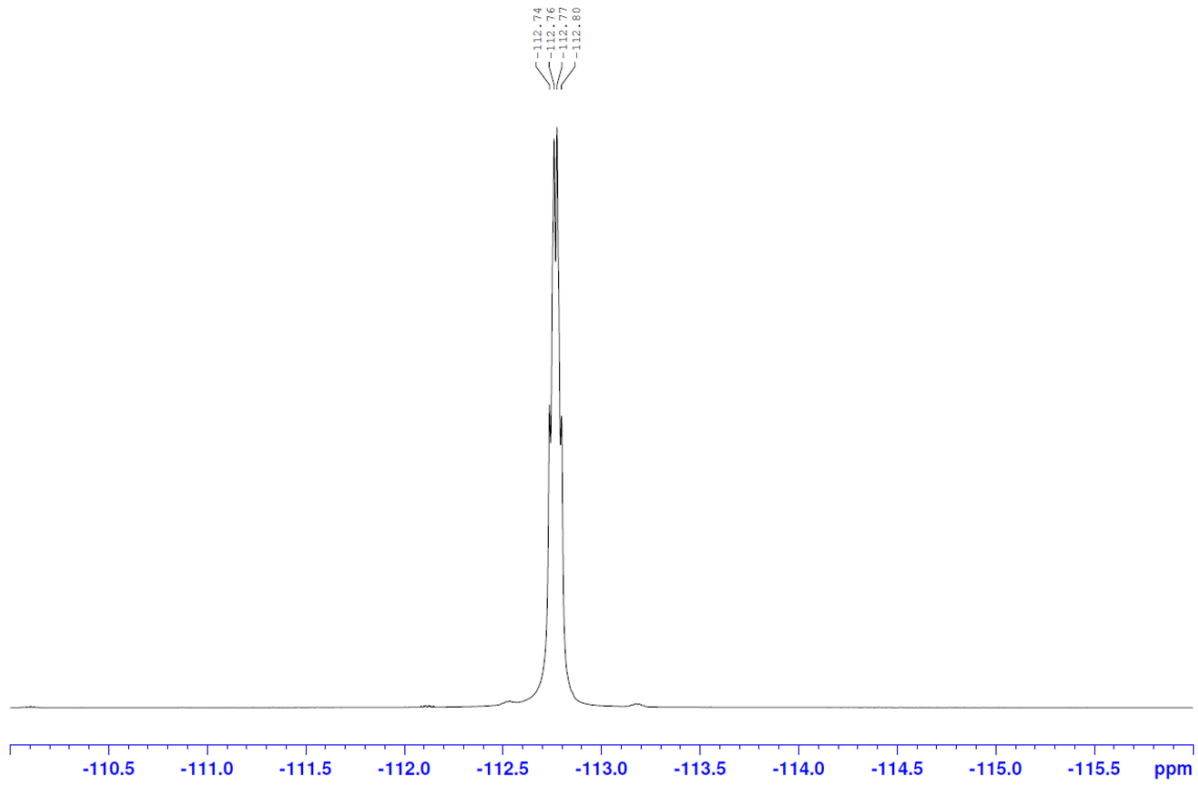

Figure 30 ^{19}F NMR spectrum of **3d** in $CDCl_3$

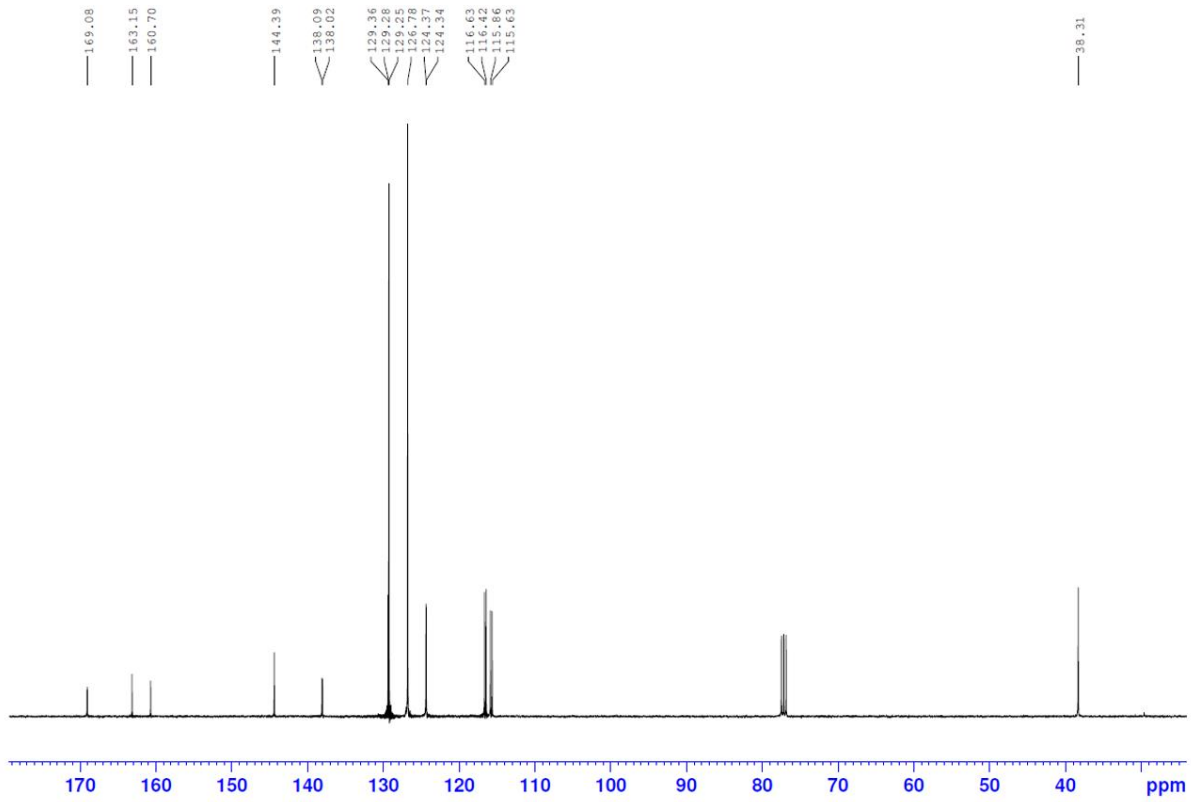

Figure 31 $^{13}C\{^{1}H\}$ NMR spectrum of **3d** in $CDCl_3$

2-Fluoro-*N*-methyl-*N*-phenylbenzamide **3e**.

^{1}H NMR (400.1 MHz, $CDCl_3$): δ / ppm 7.19 (8H, m, Ar), 6.78 (1H, s, Ar), 3.47 (3H, s, C*H*$_3$)

^{13}C{^{1}H} NMR (100.6 MHz, $CDCl_3$): δ / ppm 166.6 (*C*O), 159.2 (Ar), 156.8 (Ar), 143.4 (Ar), 131.1 (d, *J* = 8 Hz, Ar), 129.3 (d, *J* = 3 Hz, Ar), 127.0 (Ar), 126.8 (Ar), 125.3 (1C, d, *J* = 17 Hz, Ar), 123.9 (Ar), 115.5 (d, *J* = 22 Hz, Ar), 37.4 (*C*H$_3$)

^{19}F NMR (128.4 MHz, $CDCl_3$): δ / ppm 113.1 (1F, s, Ar*F*)

HR-MS found: 229.08959; calculated for [M$^+$] ($C_{14}H_{12}ONF^+$): 229.08974 (error -0.15 ppm).

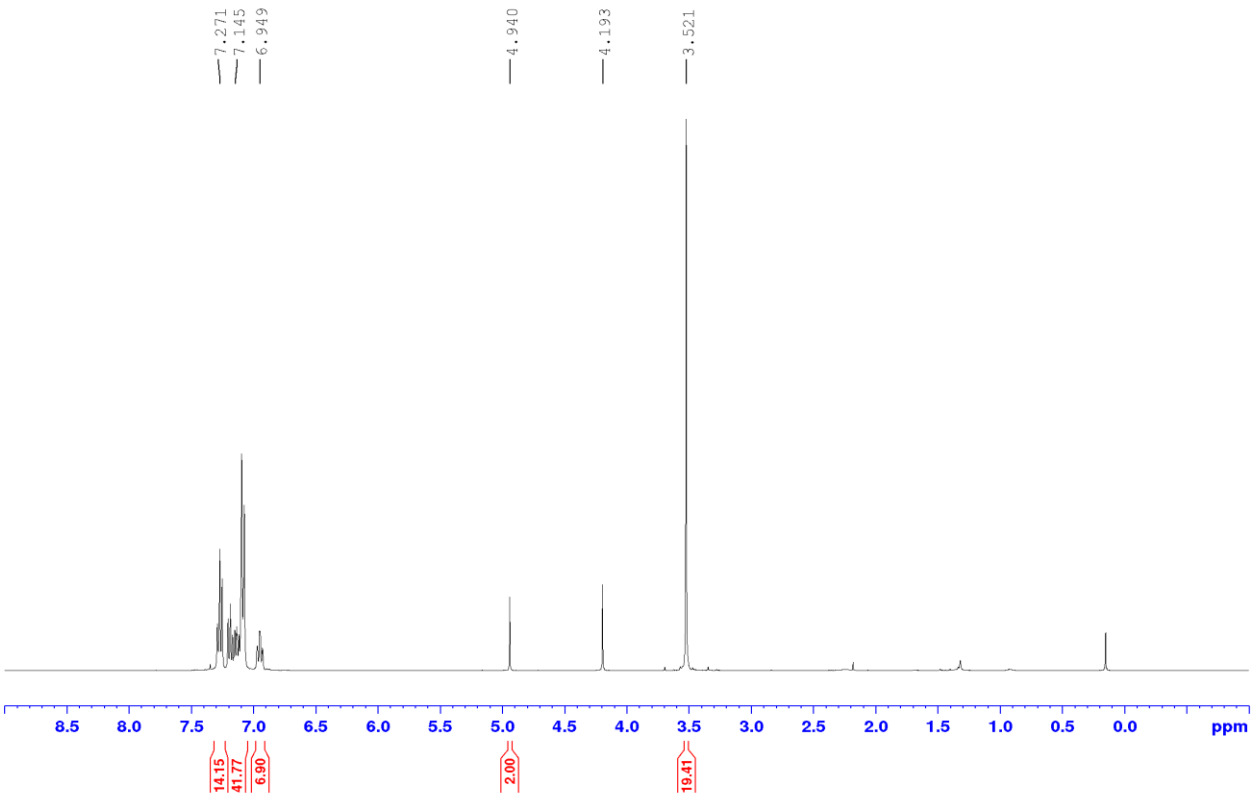

Figure 32 ^{1}H spectrum (400.1 MHz, $CDCl_3$) of Table 3, Entry **3e**, 67%. $FeCp_2$ (50 µmol, 5 mol%).

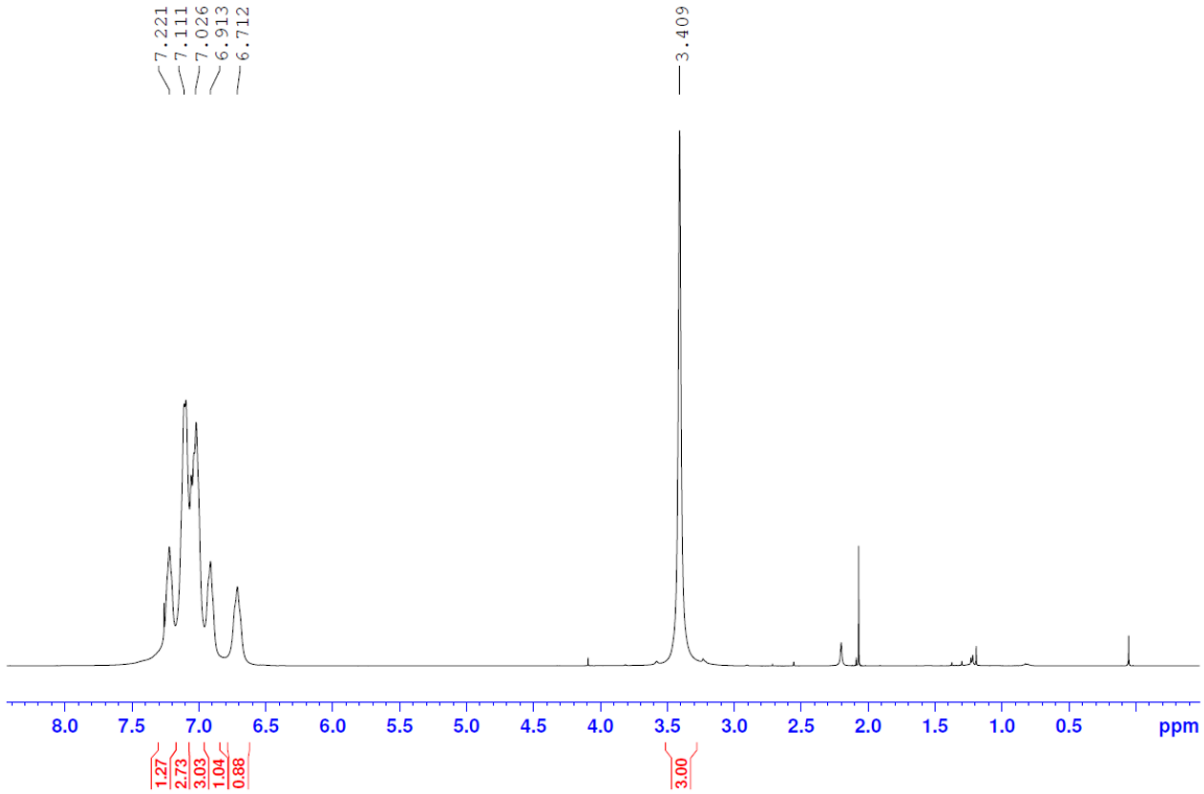

Figure 33 ^{1}H NMR spectrum of **3e** in $CDCl_3$

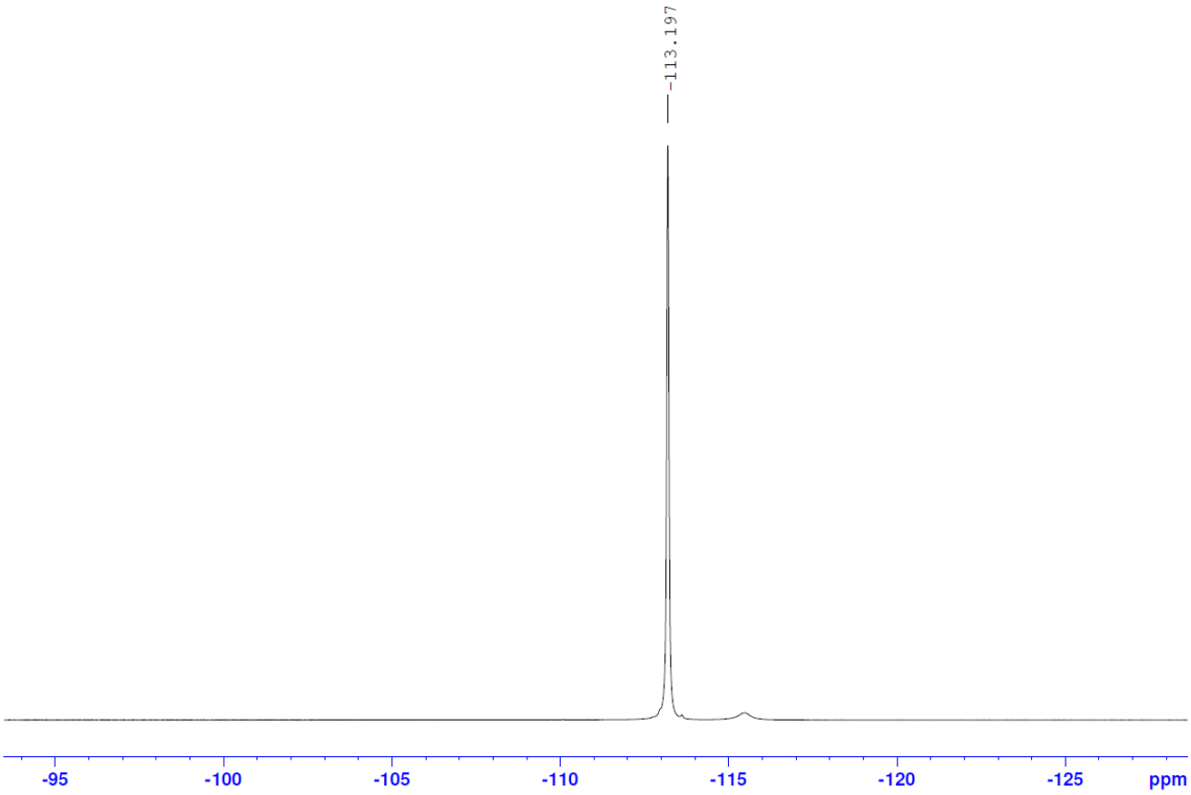

Figure 34 ^{19}F NMR spectrum of **3e** in $CDCl_3$

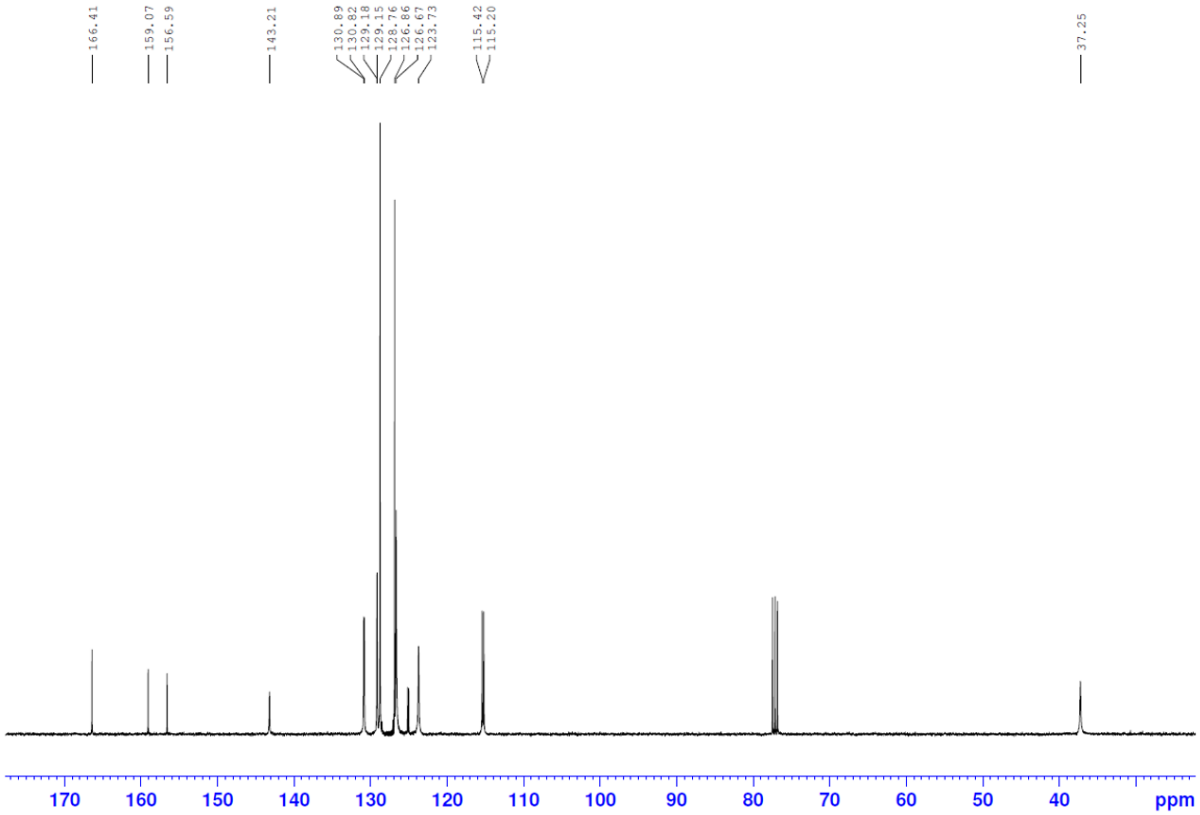

Figure 35 $^{13}C\{^{1}H\}$ NMR spectrum of **3e** in $CDCl_3$

4-Methoxy-*N*-methyl-*N*-phenylbenzamide **3f**. Spectral data were in accord with published data.[6]

^{1}H NMR (400.1 MHz, $CDCl_3$): δ / ppm 7.28 (2H, d, *J* = 8.6 Hz, Ar), 7.23 (2H, t, *J* = 7.4 Hz, Ar), 7.14 (1H, t, *J* = 7.4 Hz, Ar), 7.05 (2H, d, *J* = 7.4 Hz, Ar), 6.66 (2H, d, *J* = 8.6 Hz, Ar), 3.49 (3H, s, CH_3).

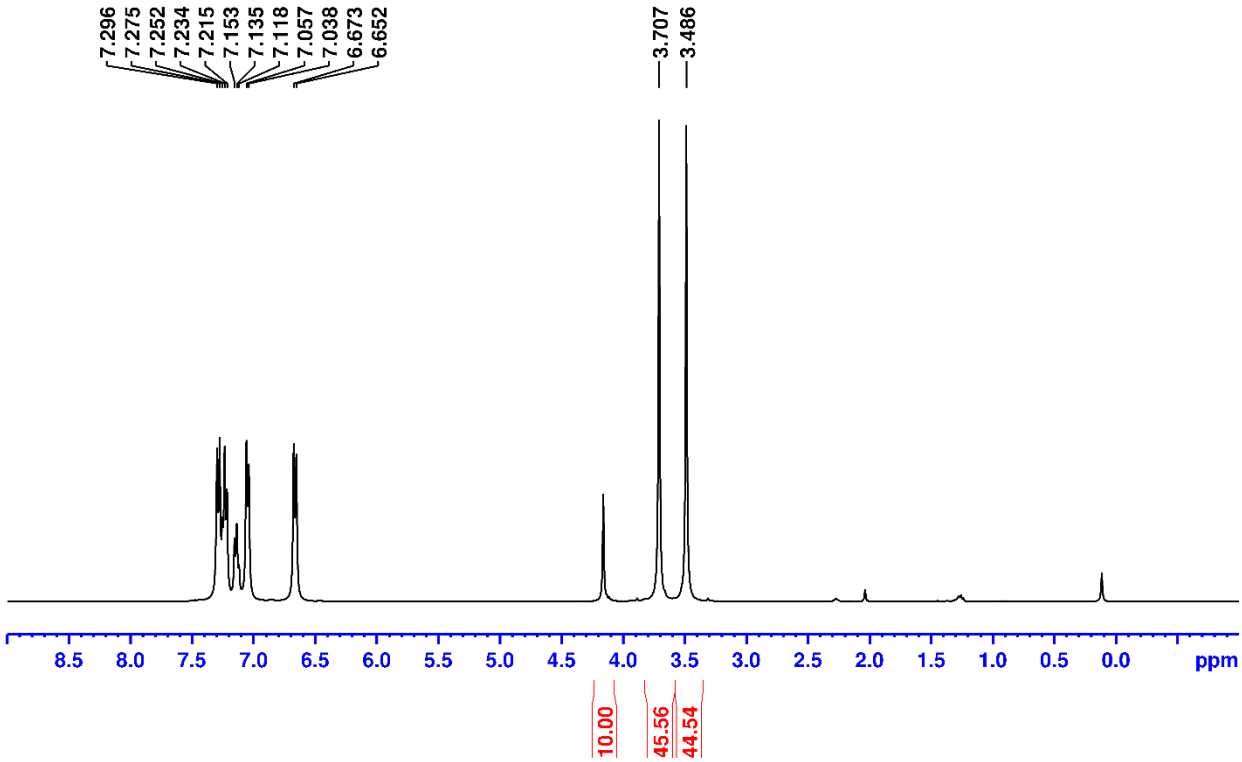

Figure 36 ^{1}H NMR spectrum (400.1 MHz, $CDCl_3$) of Table 3, Entry **3f**, 74%. $FeCp_2$ (50 µmol, 5 mol%).

3-Methoxy-*N*-methyl-*N*-phenylbenzamide **3g**. Spectral data were in accord with published data.[7]

^{1}H NMR (400.1 MHz, $CDCl_3$): δ / ppm 7.27–7.18 (2H, m, Ar), 7.18–7.10 (1H, m, Ar), 7.10–6.98 (3H, m, Ar), 6.92–6.83 (2H, m, Ar), 6.82–6.72 (1H, m, Ar), 3.63 (3H, s, CH_3), 3.49 (3H, s, CH_3).

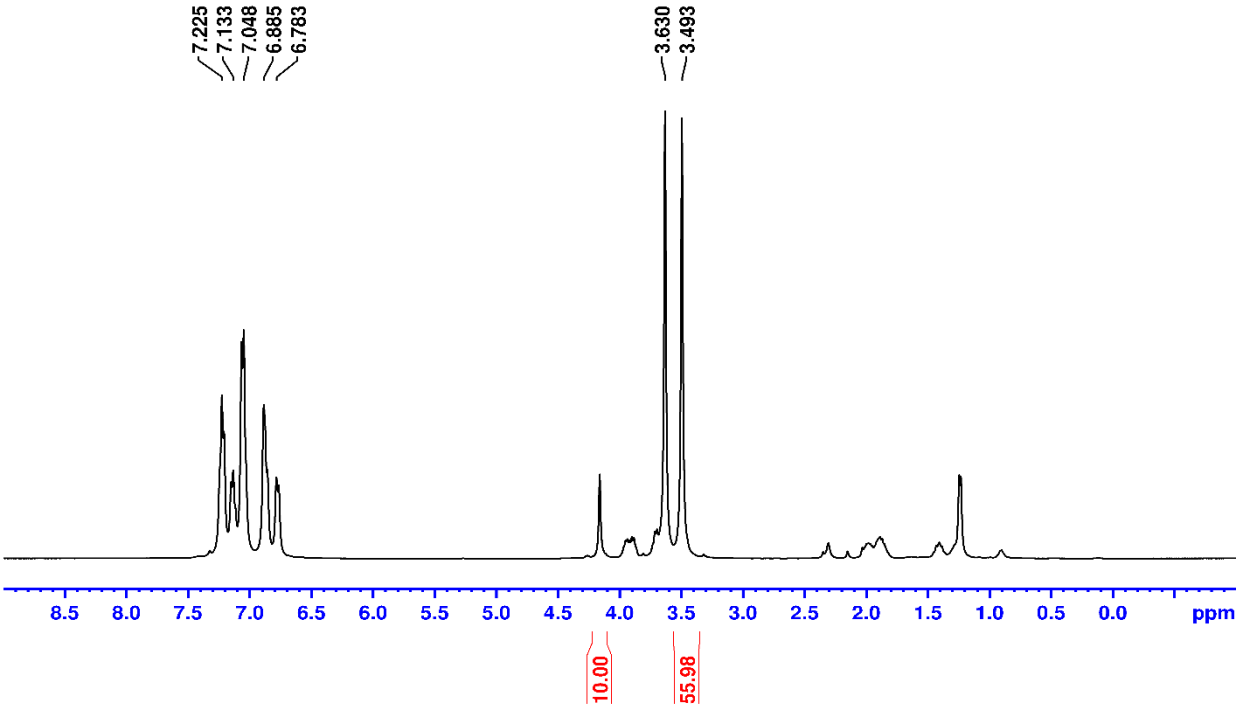

Figure 37 ^{1}H NMR spectrum (400.1 MHz, $CDCl_3$) of Table 3, Entry **3g**, 89%. $FeCp_2$ (4 μmol, 4.8 mol%).

2-Methoxy-*N*-methyl-*N*-phenylbenzamide **3h**. Spectral data were in accord with published data.[7]

^{1}H NMR (400.1 MHz, $CDCl_3$): δ / ppm 7.24–6.99 (7H, m, Ar), 6.85–6.71 (1H, m, Ar), 6.69–6.52 (1H, m, Ar), 3.60 (3H, s, CH_3), 3.48 (3H, s, CH_3).

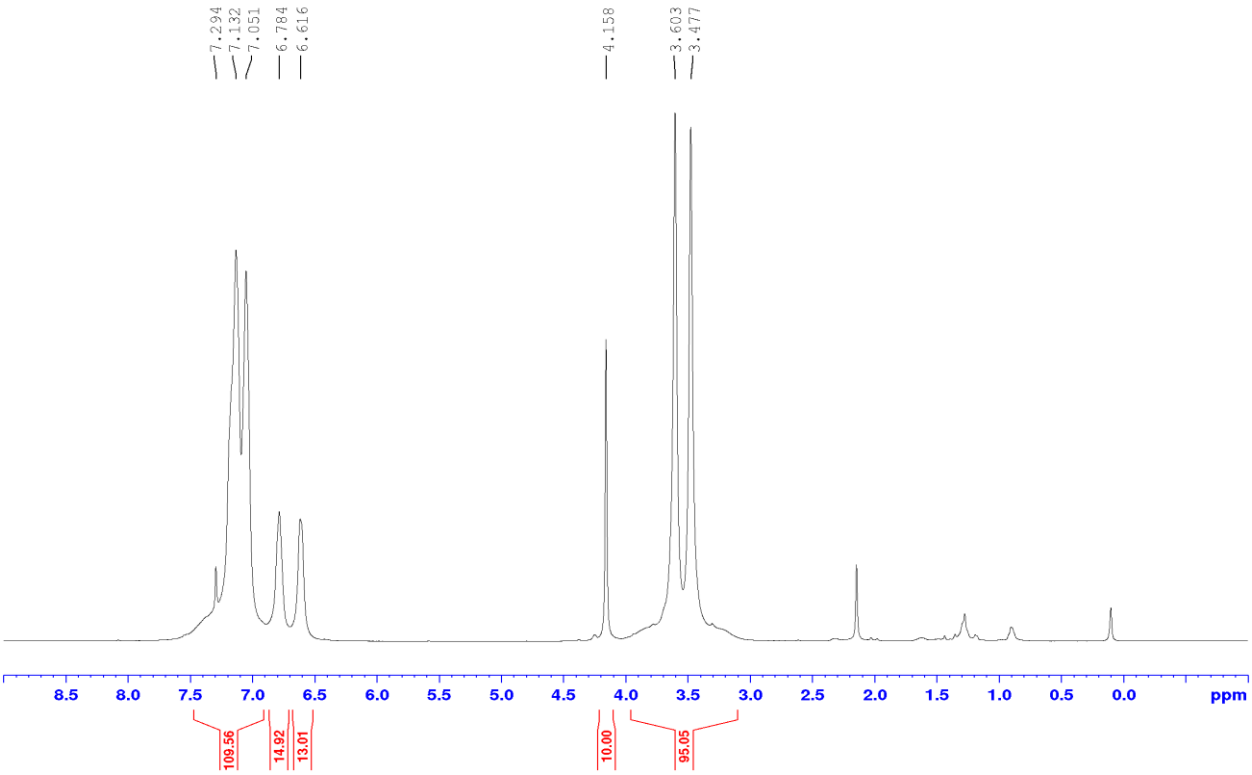

Figure 38 ^{1}H NMR spectrum (400.1 MHz, $CDCl_3$) of Table 3, Entry **3h**, 63%. $FeCp_2$ (40 µmol, 4 mol%).

2-Methyl-*N*-methyl-*N*-phenylbenzamide **3i**. Spectral data were in accord with published data.[8]

^{1}H NMR (400.1 MHz, $CDCl_3$): δ / ppm 7.20–6.75 (9H, m, Ar), 3.38 (3H, s, CH_3), 2.24 (3H, s, CH_3).

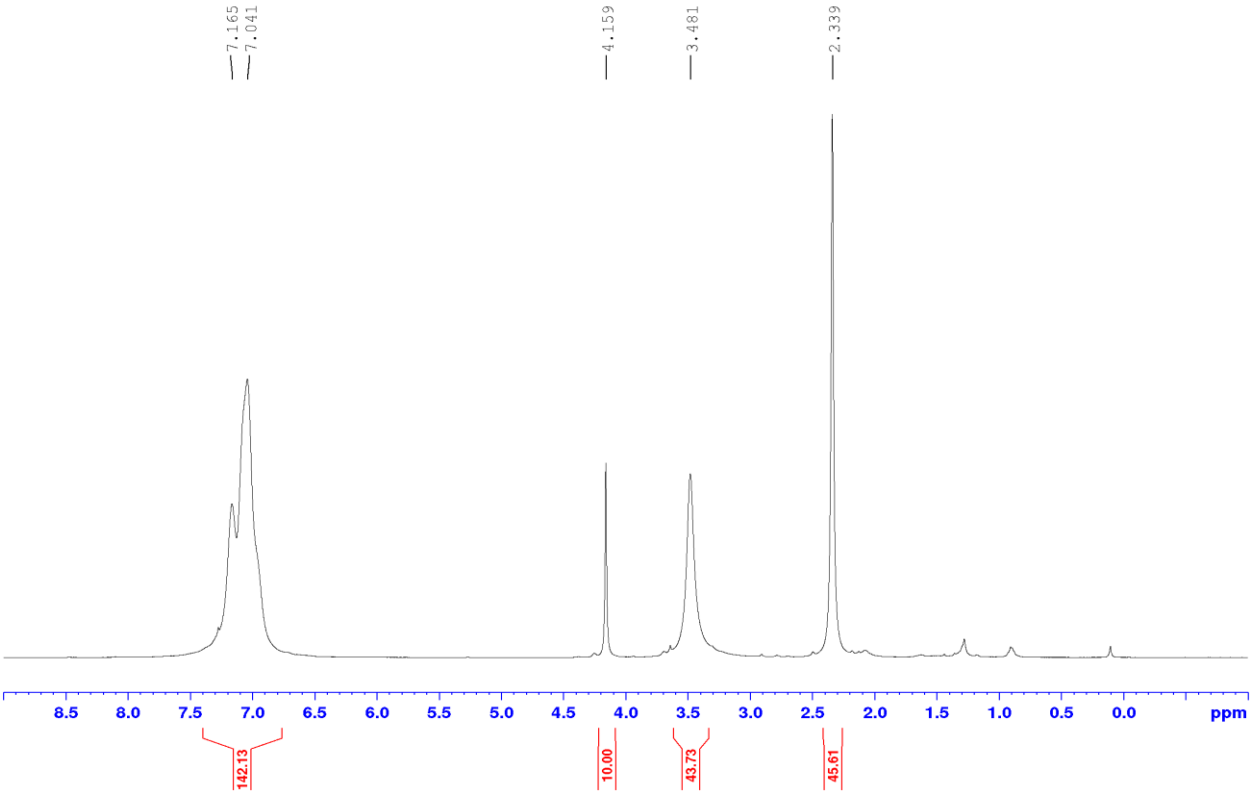

Figure 39 ^{1}H NMR spectrum (400.1 MHz, $CDCl_3$) of Table 3, Entry **3i**, 60%. $FeCp_2$ (40 μmol, 4 mol%).

N-Methyl-*N*-phenylfuran-3-carboxamide **3j**. Spectral data were in accord with published data.[8]

^{1}H NMR (400.1 MHz, $CDCl_3$): δ / ppm 7.44–7.30 (9H, m, Ar), 7.24–7.15 (9H, m, Ar), 7.15–7.06 (9H, m, Ar), 6.92–6.82 (9H, m, Ar), 3.39 (3H, s, CH_3).

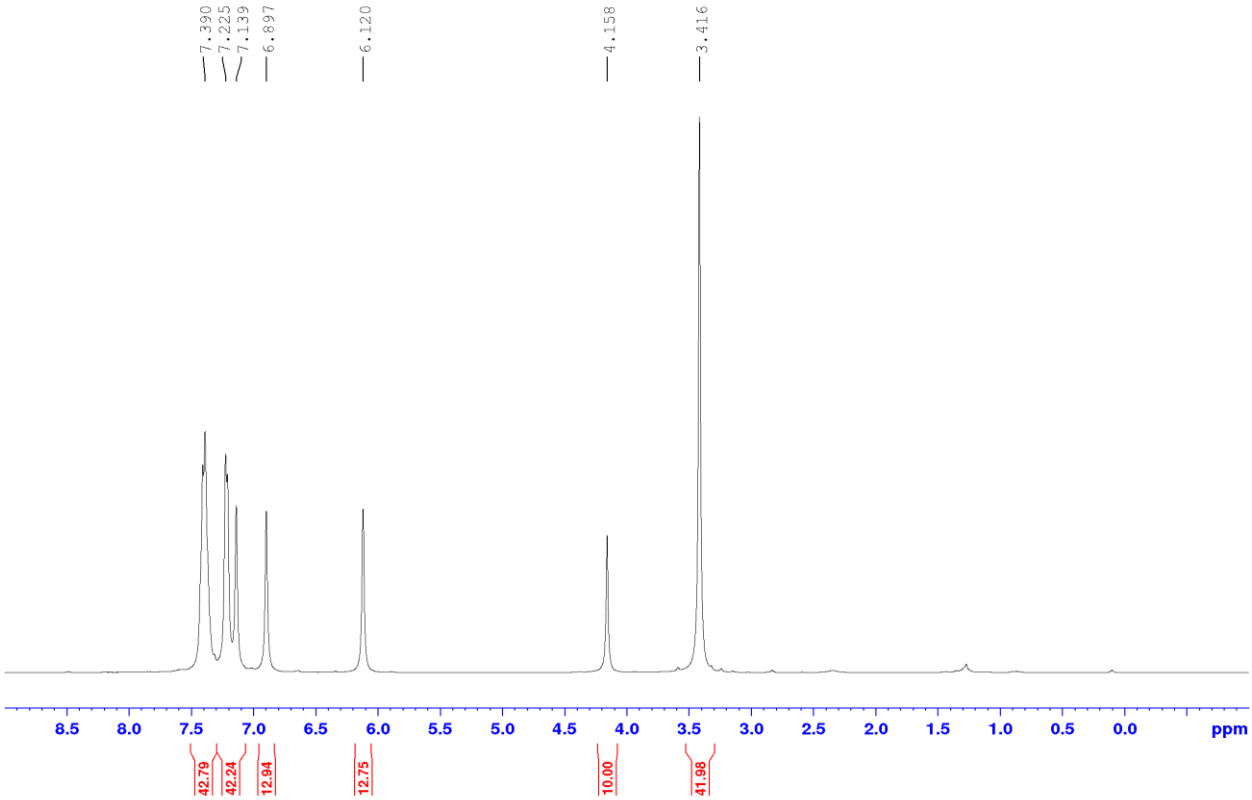

Figure 40 ^{1}H NMR spectrum (400.1 MHz, $CDCl_3$) of Table 3, Entry **3j**, 78%. $FeCp_2$ (52 μmol, 5.2 mol%).

N-Methyl-*N*-phenylnicotinamide **3k**.

^{1}H NMR (400.1 MHz, $CDCl_3$): δ / ppm 8.43 (1H, d, *J* = 1.7 Hz, Ar), 8.37 (1H, dd, *J* = 4.9 Hz, 1.6 Hz, Ar), 7.53 (1H, *J* = 8.0 Hz, 2.0 Hz, Ar), 7.18 (t, *J* = 7.5 Hz, Ar), 7.10 (tt, J = 7.3, 2.0 Hz, Ar), 7.03 (1H, dd, *J* = 8.0 Hz, 4.8 Hz, Ar), 6.98 (2H, d, J = 7 Hz, Ar), 3.43 (3H, s, C*H*$_3$)

^{13}C{^{1}H} NMR (100.6 MHz, $CDCl_3$): δ / ppm 168.0 (*C*O), 150.2 (Ar), 149.5 (Ar), 144.1 (Ar_{ipso}), 136.0 (Ar), 131.7 (Ar_{ipso}), 129.4 (Ar), 127.1 (Ar), 127.0 (Ar), 38.3 (CH_3).

HR-MS found: 212.09376; calculated for [M^+] ($C_{13}H_{12}ON_2^+$): 212.09441 (error -0.65 ppm).

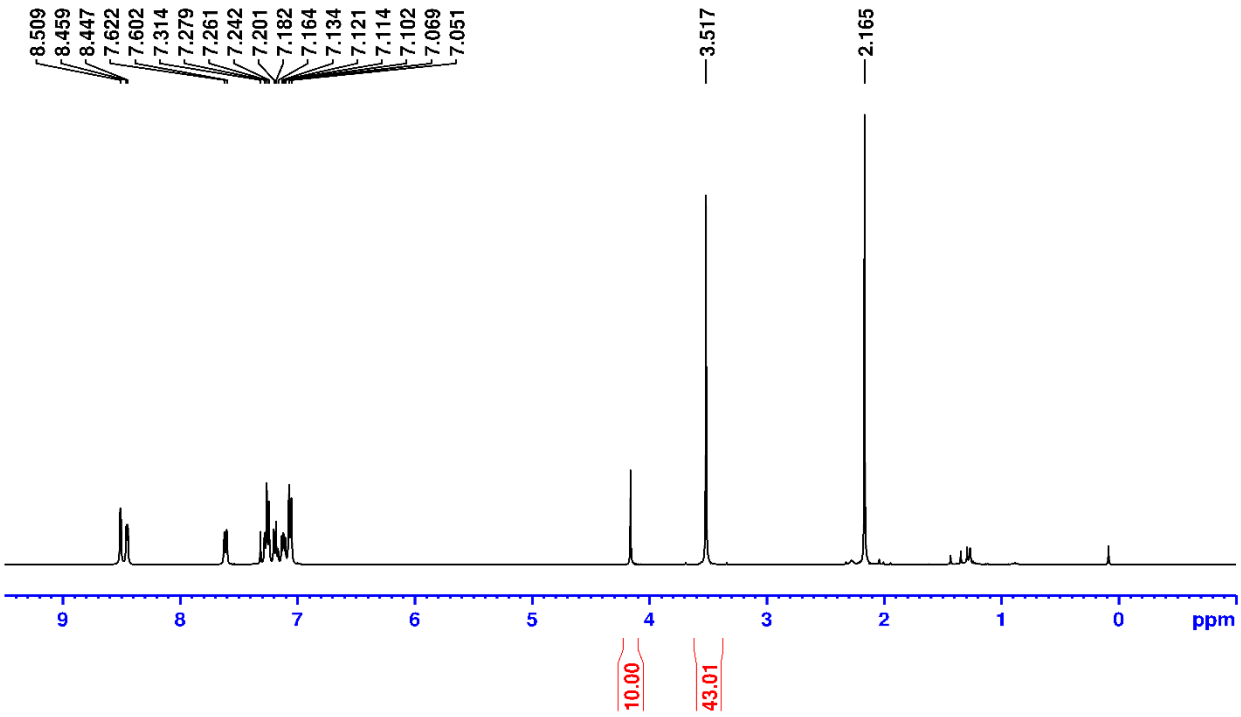

Figure 41 ^{1}H NMR spectrum (400.1 MHz, $CDCl_3$) of Table 3, Entry **3k**, 72%. $FeCp_2$ (50 µmol, 5 mol%).

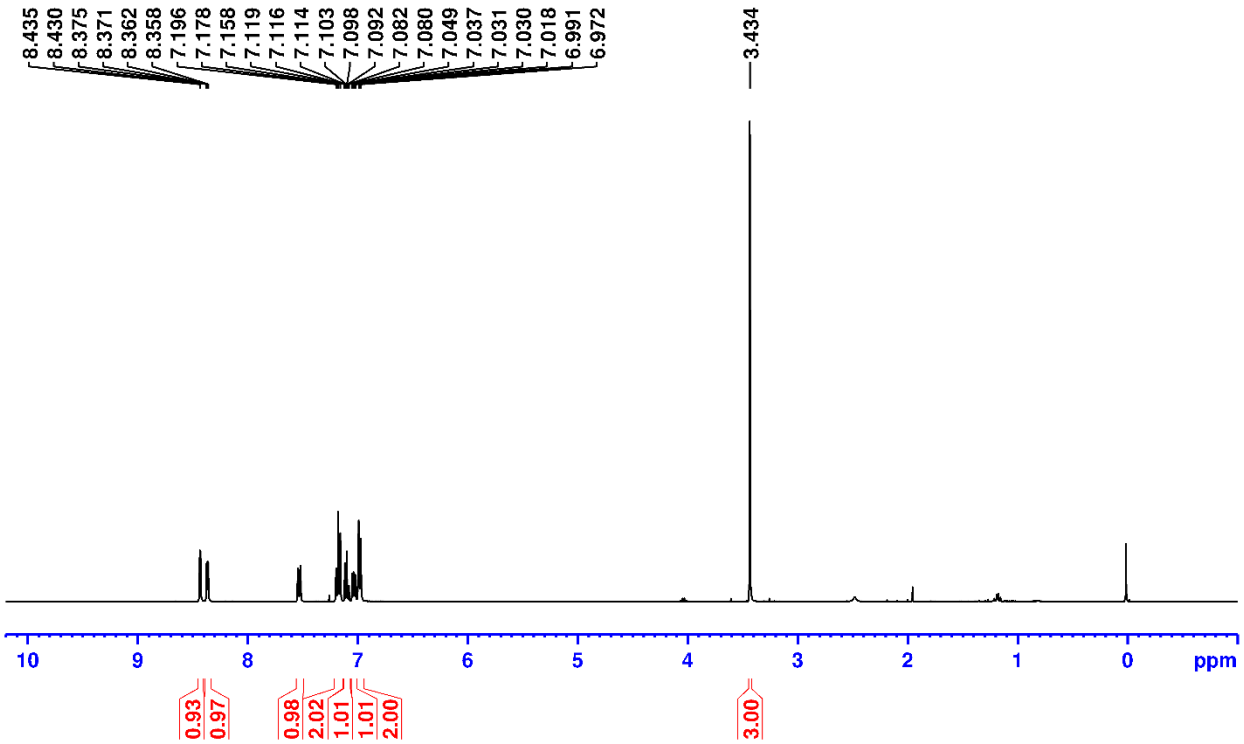

Figure 42 ^{1}H NMR spectrum of **3k** in $CDCl_3$

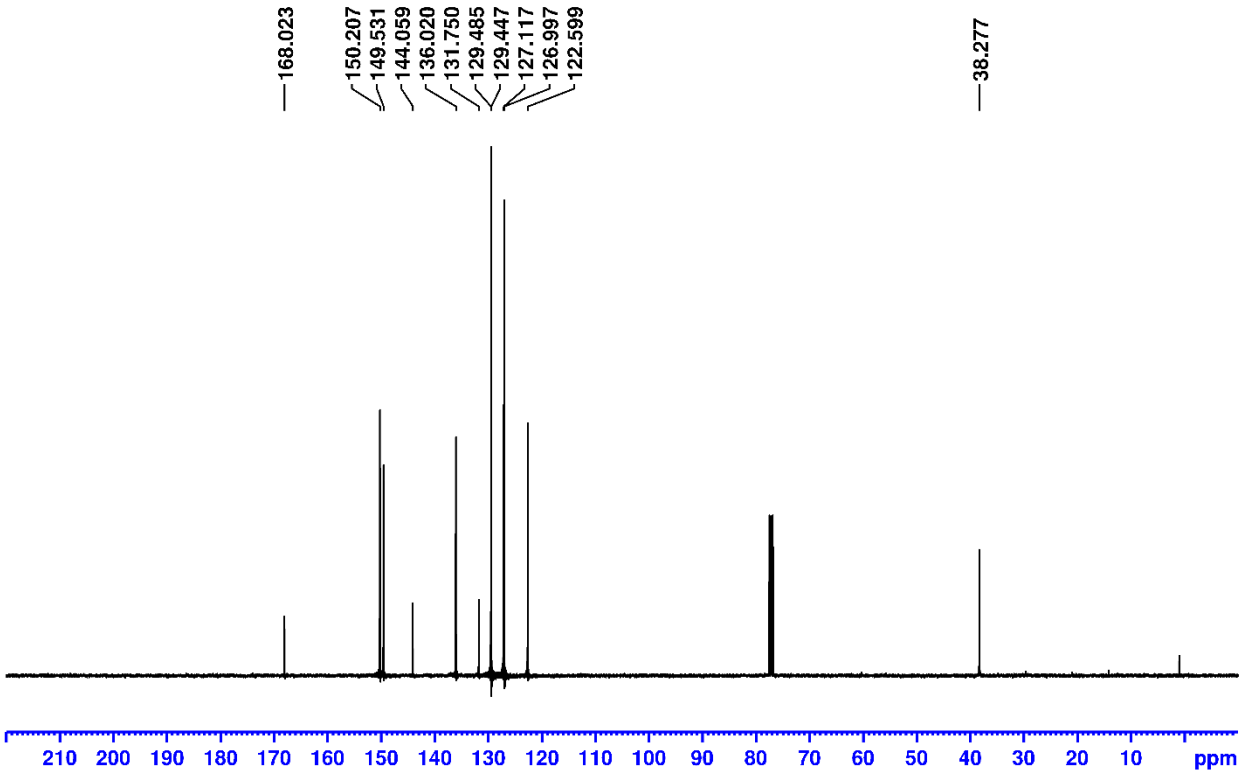

Figure 43 $^{13}C\{^{1}H\}$ NMR spectrum of **3k** in $CDCl_3$

N-Methyl-*N*-phenylcyclohexanecarboxamide **3l**. Spectral data were in accord with published data.[9]

^{1}H NMR (400.1 MHz, $CDCl_3$): δ / ppm 7.42 (2H, t, *J* = 7.2 Hz, Ar), 7.35 (1H, t, *J* = 7.2 Hz, Ar), 7.17 (2H, d, *J* = 7.2 Hz, Ar), 3.24 (3H, s, CH_3), 2.17–2.09 (1H, s, C*H*), 1.75–1.44 (7H, s, CH_2), 1.27–1.08 (1H, s, CH_2), 1.08–0.84 (2H, s, CH_2).

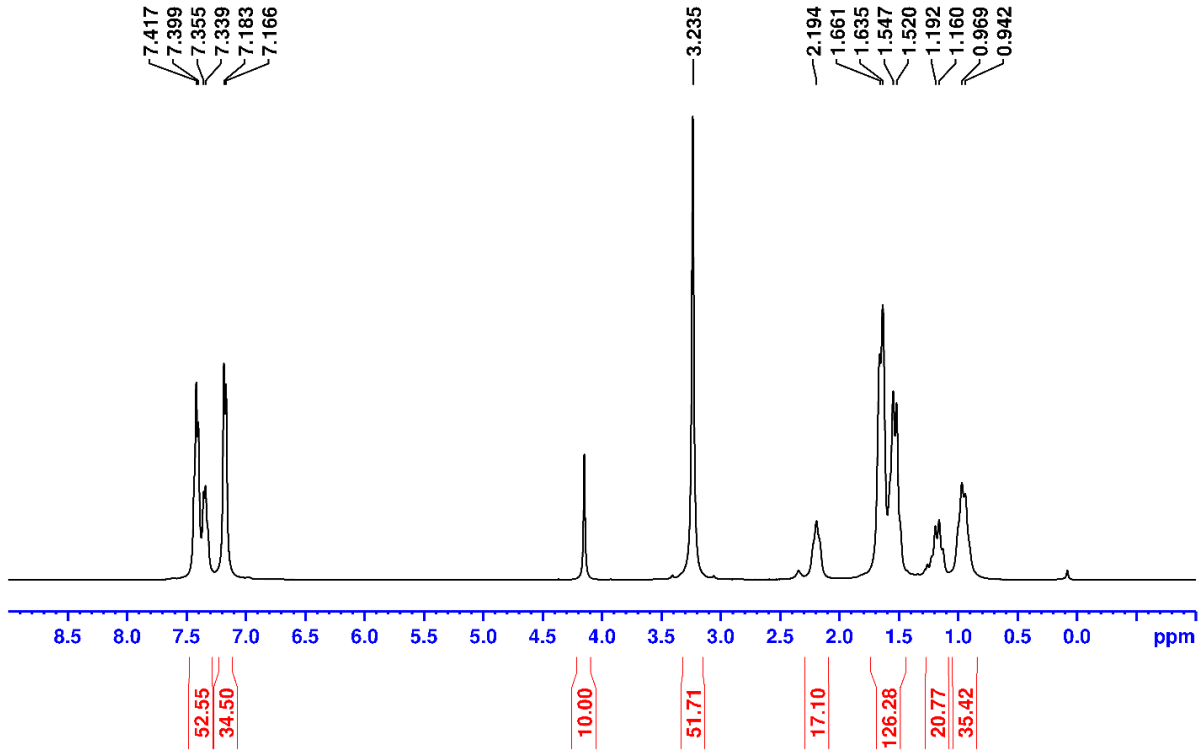

Figure 44 ^{1}H NMR spectrum (400.1 MHz, $CDCl_3$) of Table 3, Entry **3l**, 72%. $FeCp_2$ (42 µmol, 4.2 mol%).

N-Methyl-*N*-phenyloctanamide **3m**. Spectral data were in accord with published data.[9]

^{1}H NMR (400.1 MHz, $CDCl_3$): δ / ppm 7.42 (2H, t, *J* = 7.4 Hz, Ar), 7.34 (1H, t, *J* = 7.4 Hz, Ar), 7.18 (2H, t, *J* = 7.4 Hz, Ar), 3.27 (3H, s, CH_3), 2.07 (2H, t, *J* = 6.6 Hz, CH_2), 1.57 (2H, qui, *J* = 6.6 Hz, CH_2), 1.30–1.09 (8H, m, CH_2), 0.85 (3H, t, *J* = 6.5 Hz, CH_3).

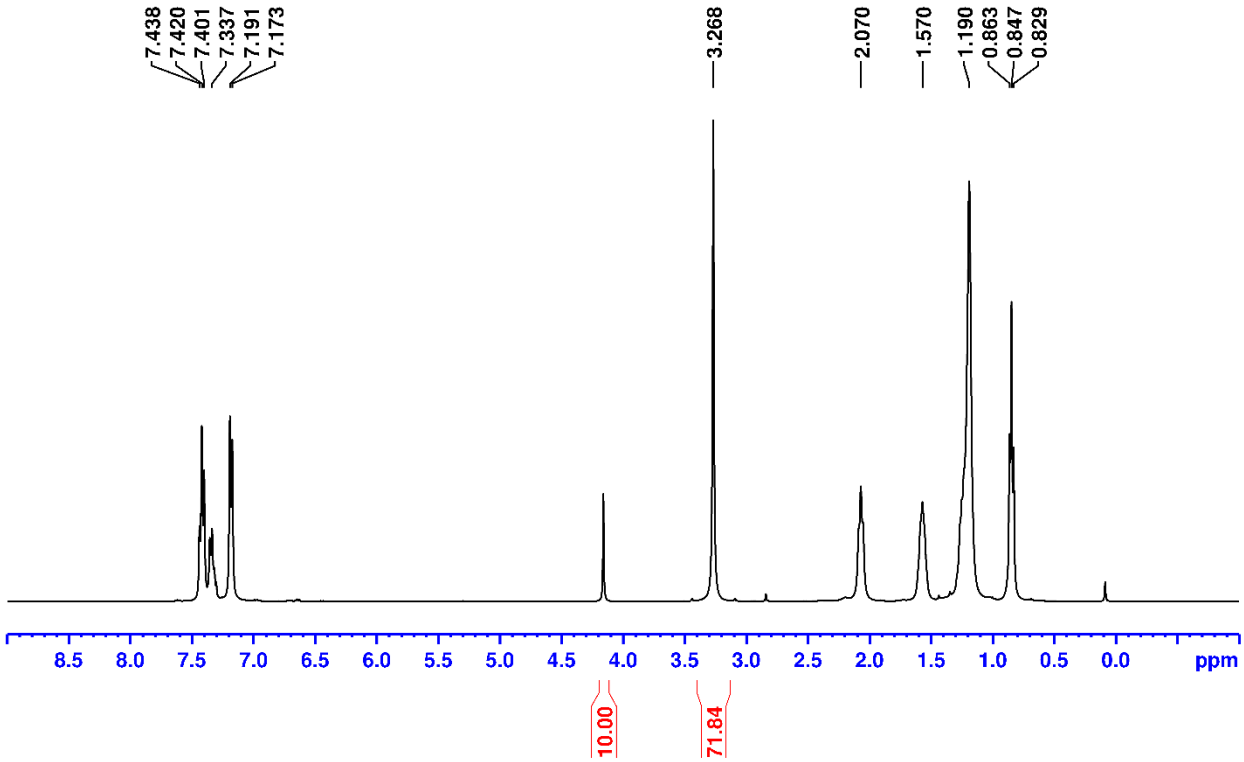

Figure 45 ^{1}H NMR spectrum (400.1 MHz, $CDCl_3$) of Table 3, Entry **3m**, 39%. $FeCp_2$ (16 µmol, 1.6 mol%).

Variation of Li-Amide for Transamidation (**5b-5h'**) – Table 4

Additions were performed under air at room temperature in an open Schlenk flask (25 mL) and 1 g of 2-MeTHF. Lithium amide **2a-j** (1.5 mL, 1.0 M in 2-MeTHF) was added to a stirring solution of ester **1a/1n** (1 mmol). After 20 s the reaction was quenched by the addition of saturated Rochelle's salt solution (sodium potassium tartrate tetrahydrate, 5 mL) before being extracted into 2-MeTHF (3 x 10 mL). Extracts were combined, dried over $MgSO_4$ and concentrated under vacuum.

Crude products were purified by silica column chromatography, eluted by hexane:EtOAc (10:1 – 2:1 gradient). Products were identified by GCMS and ^{1}H NMR. Yields were obtained by ^{1}H NMR spectroscopy by integration against ferrocene as an internal standard as described in General Methods.

N-Methyl-*N*-phenylbenzamide **3a**. Spectral data were in accord with published data.[3]

^{1}H NMR (400.1 MHz, $CDCl_3$): δ / ppm 7.34–7.28 (2H, m, Ar), 7.24–7.09 (6H, m, Ar), 7.06–7.01 (2H, m, Ar), 3.49 (3H, s, C*H*$_3$).

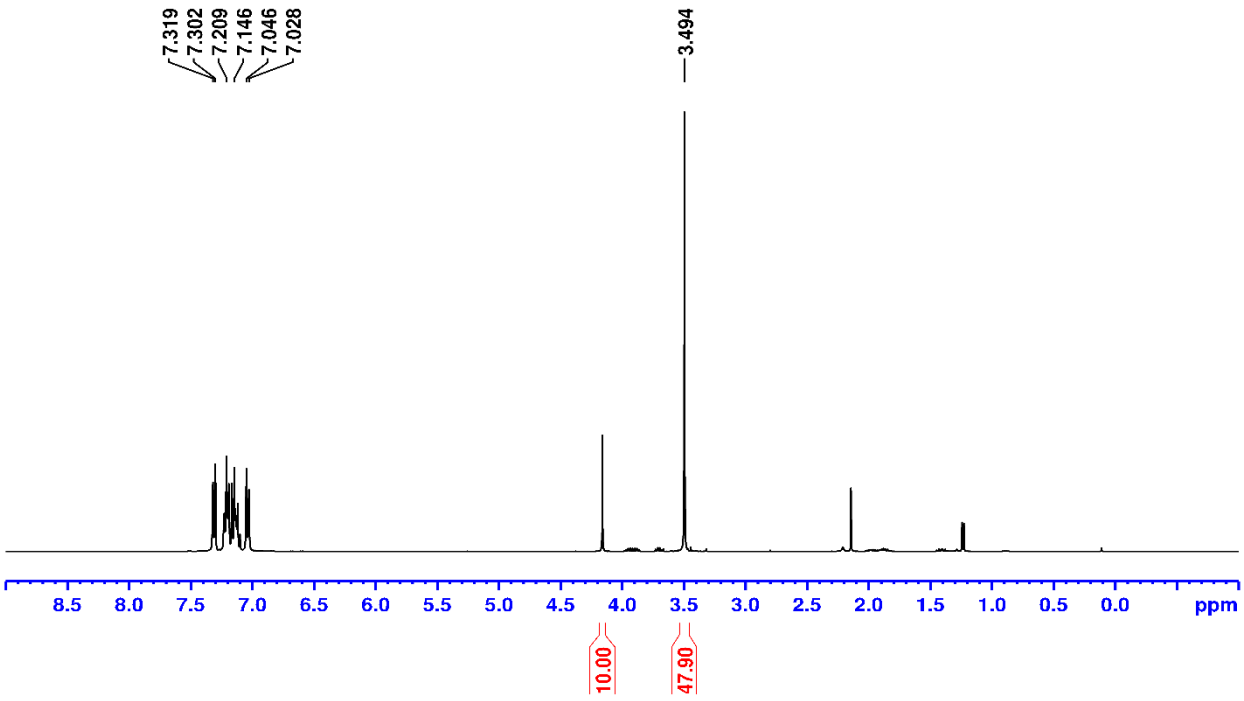

Figure 46 ^{1}H NMR spectrum (400.1 MHz, $CDCl_3$) of Table 4, Entry **3a**, 81%. $FeCp_2$ (51 µmol, 5.1 mol%).

N-Phenylbenzamide **5b**. Spectral data were in accord with published data.[3]

*3 equivalents of lithium anilide (**2b**) were employed.

^{1}H NMR (400.1 MHz, $CDCl_3$): δ / ppm 7.93 (1H, br. s, N*H*), 7.86 (2H, d, *J* = 7.5 Hz, Ar), 7.65 (2H, d, *J* = 7.8 Hz, Ar), 7.54 (1H, t, *J* = 7.8 Hz, Ar), 7.47 (2H, t, *J* = 7.5 Hz, Ar), 7.37 (2H, t, *J* = 7.8 Hz, Ar), 7.15 (1H, t, *J* = 7.5 Hz, Ar).

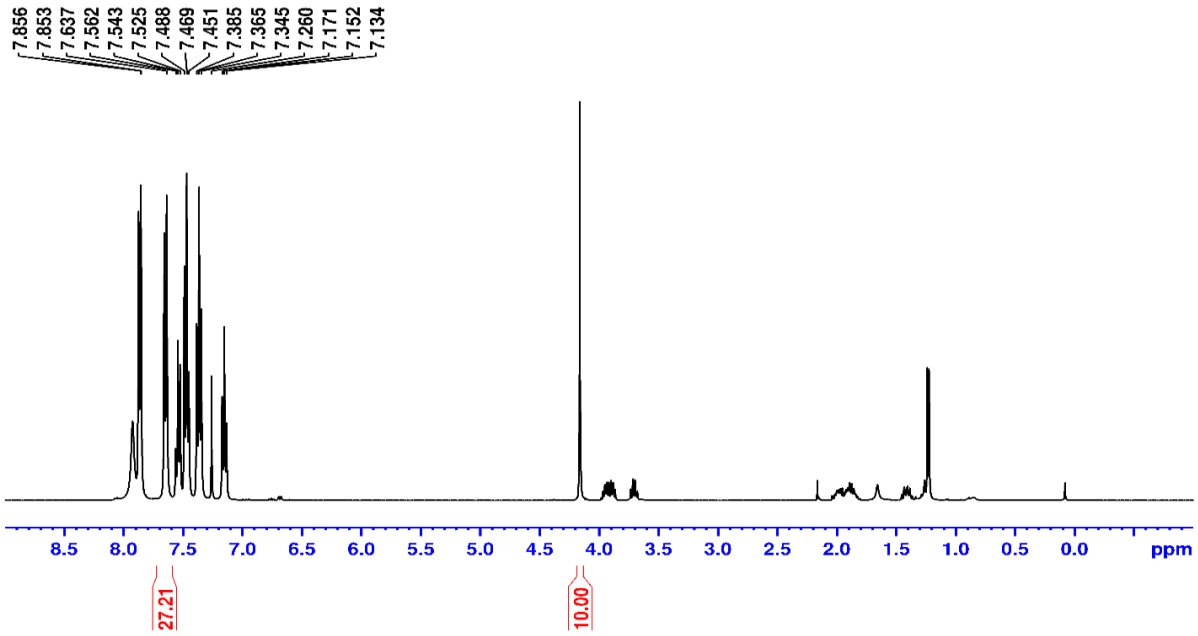

Figure 47 ^{1}H NMR spectrum (400.1 MHz, $CDCl_3$) of Table 4, Entry **5b**, 71%. $FeCp_2$ (52 μmol, 5.2 mol%).

N,*N*-Dibutylbenzamide **5c**. Spectral data were in accord with published data.[6]

^{1}H NMR (400.1 MHz, $CDCl_3$): δ / ppm 7.43–7.31 (5H, m, Ar), 3.61–3.36 (2H, m, CH_2), 3.34–3.05 (2H, m, CH_2), 1.76–1.57 (2H, m, CH_2), 1.57–1.34 (4H, m, CH_2), 1.20–1.07 (2H, m, CH_2), 1.06–0.91 (3H, m, CH_3), 0.87–0.71 (2H, m, CH_2).

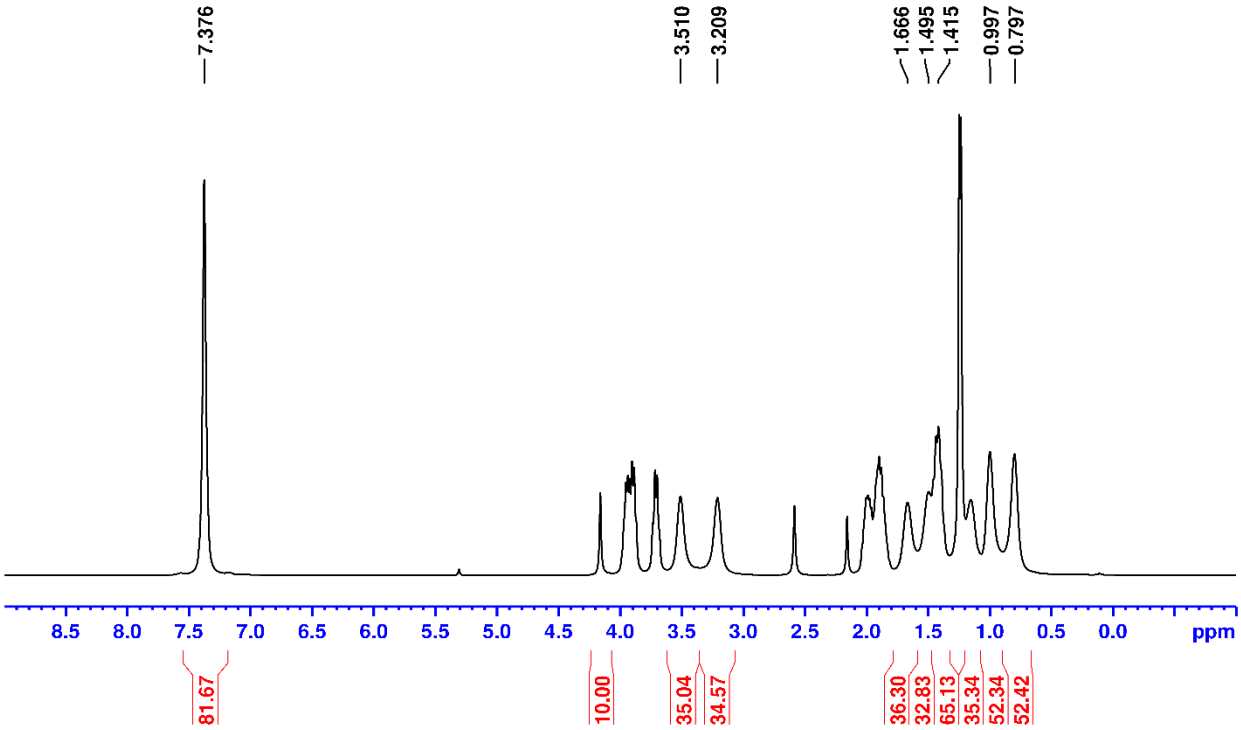

Figure 48 ^{1}H NMR spectrum (400.1 MHz, $CDCl_3$) of Table 4, Entry **5c**, 77%. $FeCp_2$ (45 µmol, 4.5 mol%). Additional peaks correspond to remaining 2-MeTHF.

Morpholino(phenyl)methanone **5d**. Spectral data were in accord with published data.[11]

*0.08 M lithium morpholide (**2d**) solution in 2-MeTHF was employed due to limited solubility.

^{1}H NMR (400.1 MHz, $CDCl_3$): δ / ppm 7.45–7.32 (5H, m, Ar), 3.96–3.56 (6H, m, CH_2), 3.56–3.28 (2H, m, CH_2).

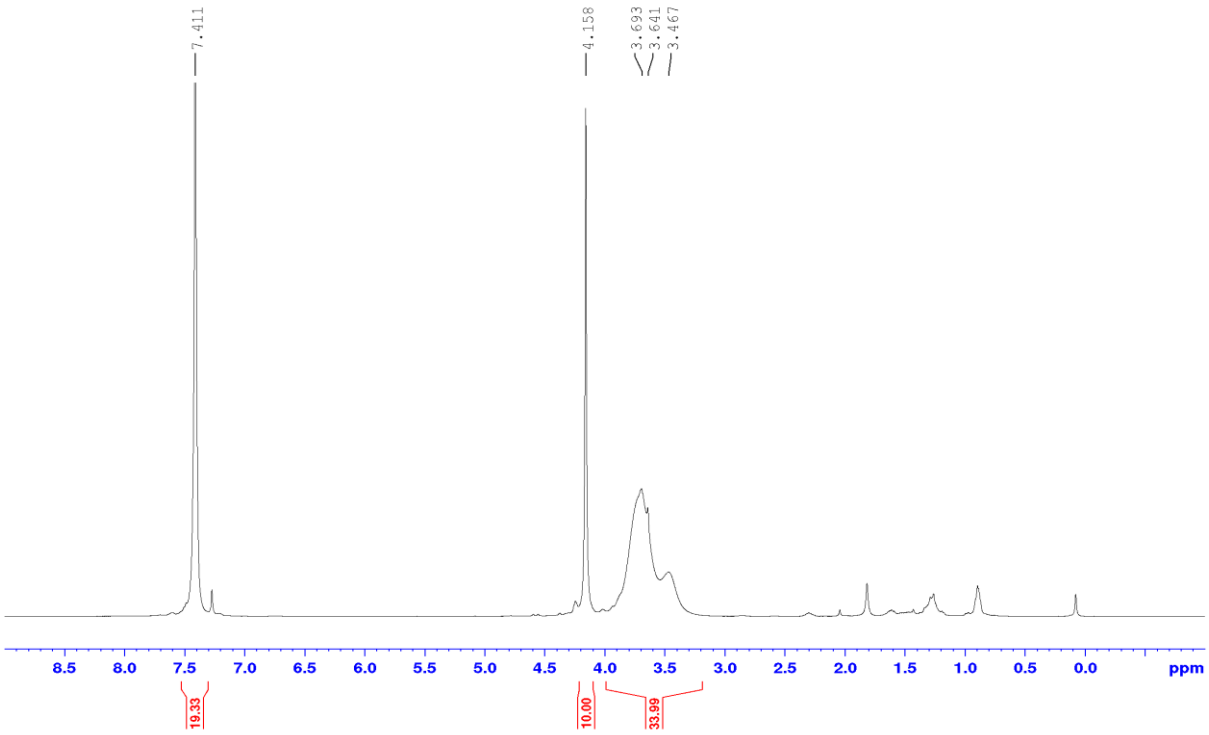

Figure 49 ^{1}H NMR spectrum (400.1 MHz, $CDCl_3$) of Table 4, Entry **5d**, 17%. $FeCp_2$ (40 µmol, 4 mol%).

Phenyl(pyrrolidin-1-yl)methanone **5e**. Spectral data were in accord with published data.[8, 12]

^{1}H NMR (400.1 MHz, $CDCl_3$): δ / ppm 7.60–7.47 (2H, m, Ar), 7.45–7.33 (3H, m, Ar), 3.70–3.54 (2H, m, CH_2), 3.50–3.31 (2H, m, CH_2), 2.07–1.80 (6H, m, CH_2).

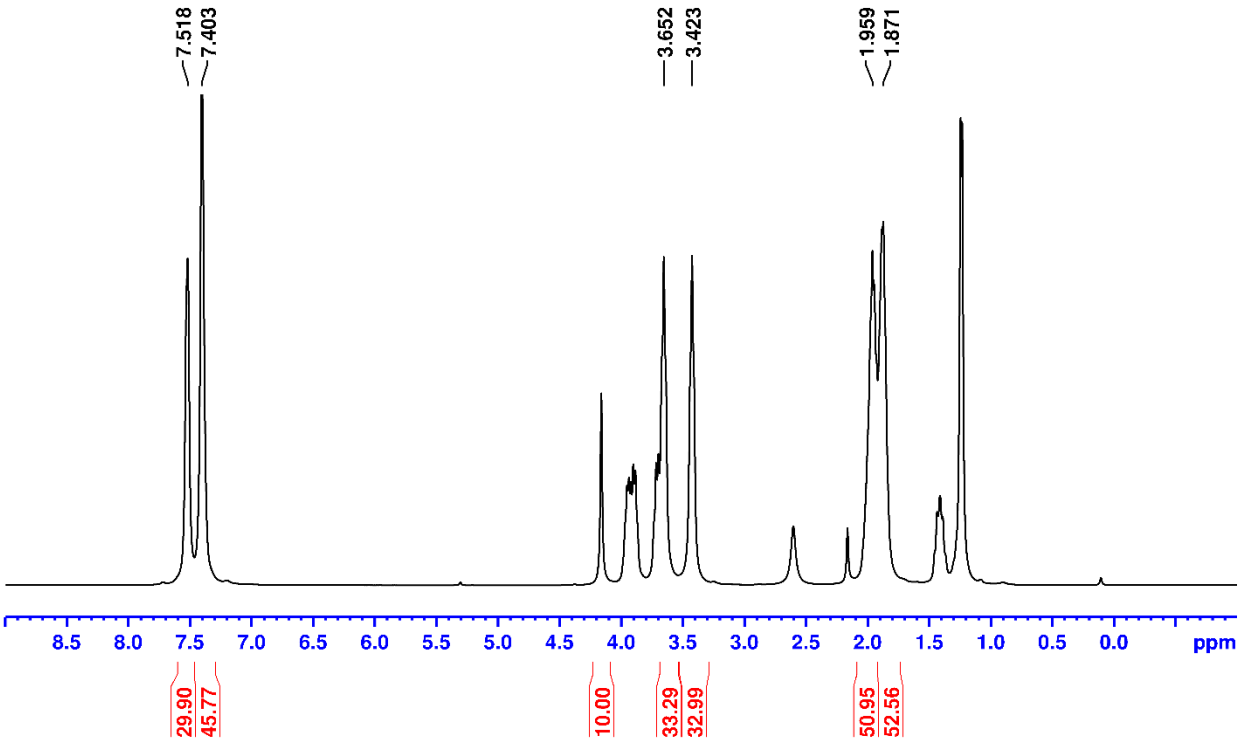

Figure 50 ^{1}H NMR spectrum (400.1 MHz, $CDCl_3$) of Table 4, Entry **5e**, 79%. $FeCp_2$ (48 µmol, 4.8 mol%). Additional peaks correspond to remaining 2-MeTHF.

Phenyl(piperidin-1-yl)methanone **5f**. Spectral data were in accord with published data.[13]

^{1}H NMR (400.1 MHz, $CDCl_3$): δ / ppm 7.34 (5H, m, Ar), 3.78–3.55 (2H, m, CH_2), 3.40–3.17 (2H, m, CH_2), 1.74–1.54 (4H, m, CH_2), 1.54–1.38 (2H, m, CH_2).

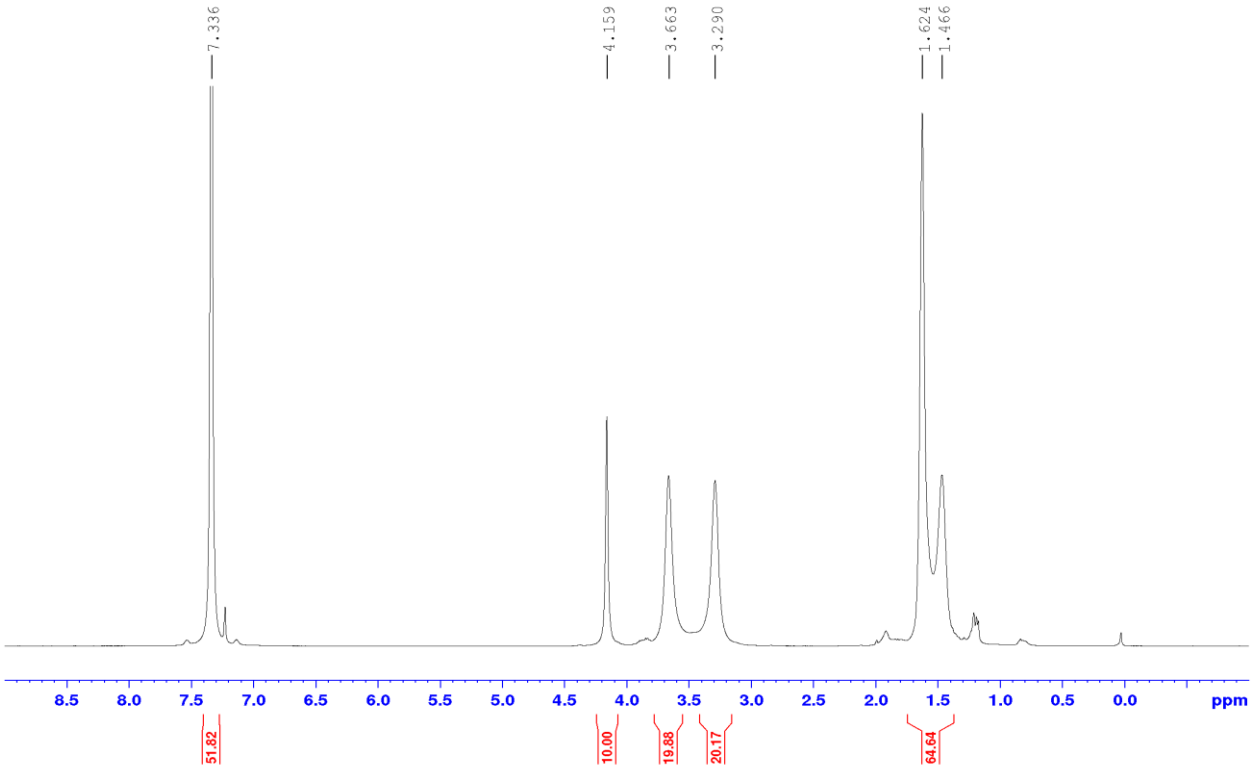

Figure 51 ^{1}H NMR spectrum (400.1 MHz, $CDCl_3$) of Table 4, Entry **5f**, 58%. $FeCp_2$ (57 µmol, 5.7 mol%).

(2,6-Dimethylpiperidin-1-yl)(phenyl)methanone **5g**. Spectral data were in accord with published data.[9, 14]

^{1}H NMR (400.1 MHz, $CDCl_3$): δ / ppm 7.43–7.36 (3H, m, Ar), 7.36–7.30 (2H, m, Ar), 5.00–4.25 (2H, m, C*H*), 1.90–1.81 (1H, m, CH_2), 1.75–1.62 (2H, m, CH_2), 1.62–1.46 (3H, m, CH_2), 1.29 (3H, s, CH_3), 1.27 (3H, s, CH_3).

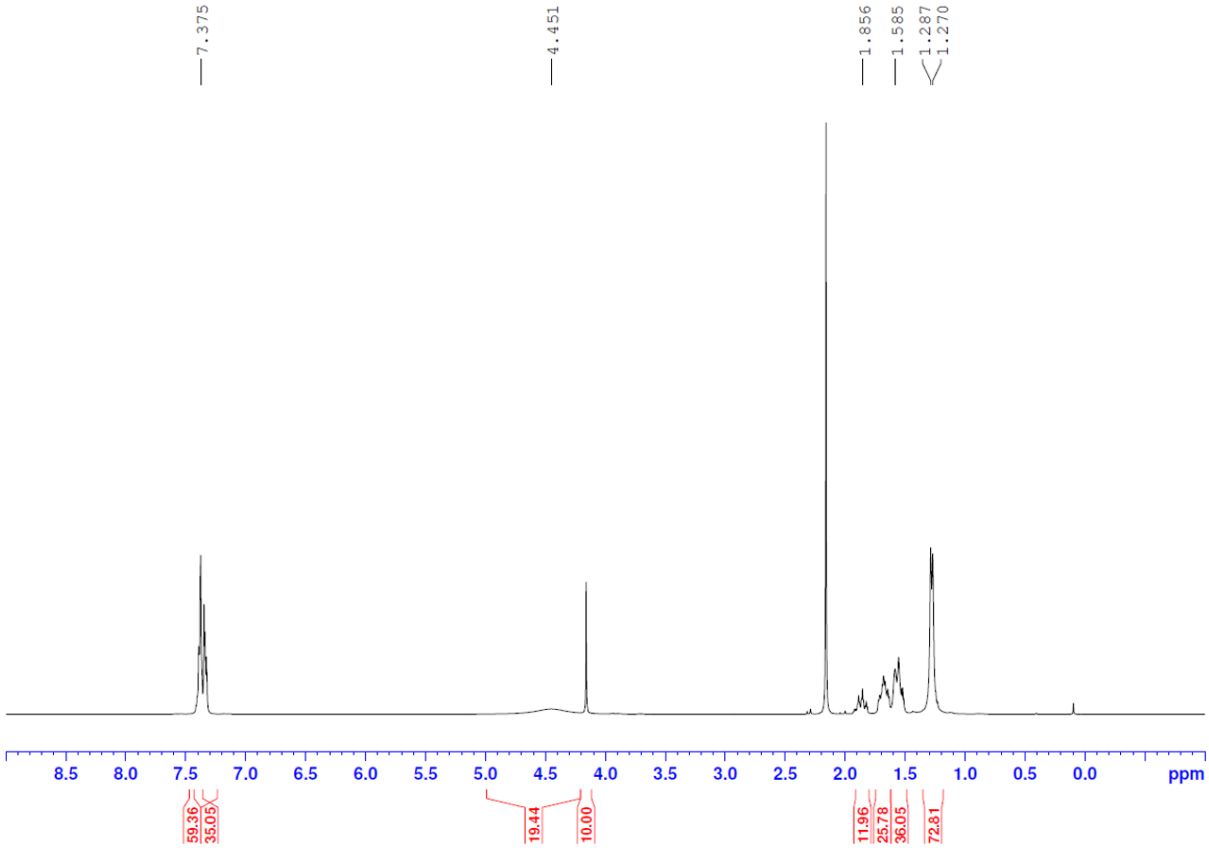

Figure 52 ^{1}H NMR spectrum (400.1 MHz, $CDCl_3$) of Table 4, Entry **5g**, 63%. $FeCp_2$ (52 µmol, 5.2 mol%).

N,*N*-Diphenylbenzamide **5h**. Spectral data were in accord with published data.[15]

^{1}H NMR (400.1 MHz, $CDCl_3$): δ / ppm 8.20–6.83 (15H, m, Ar).

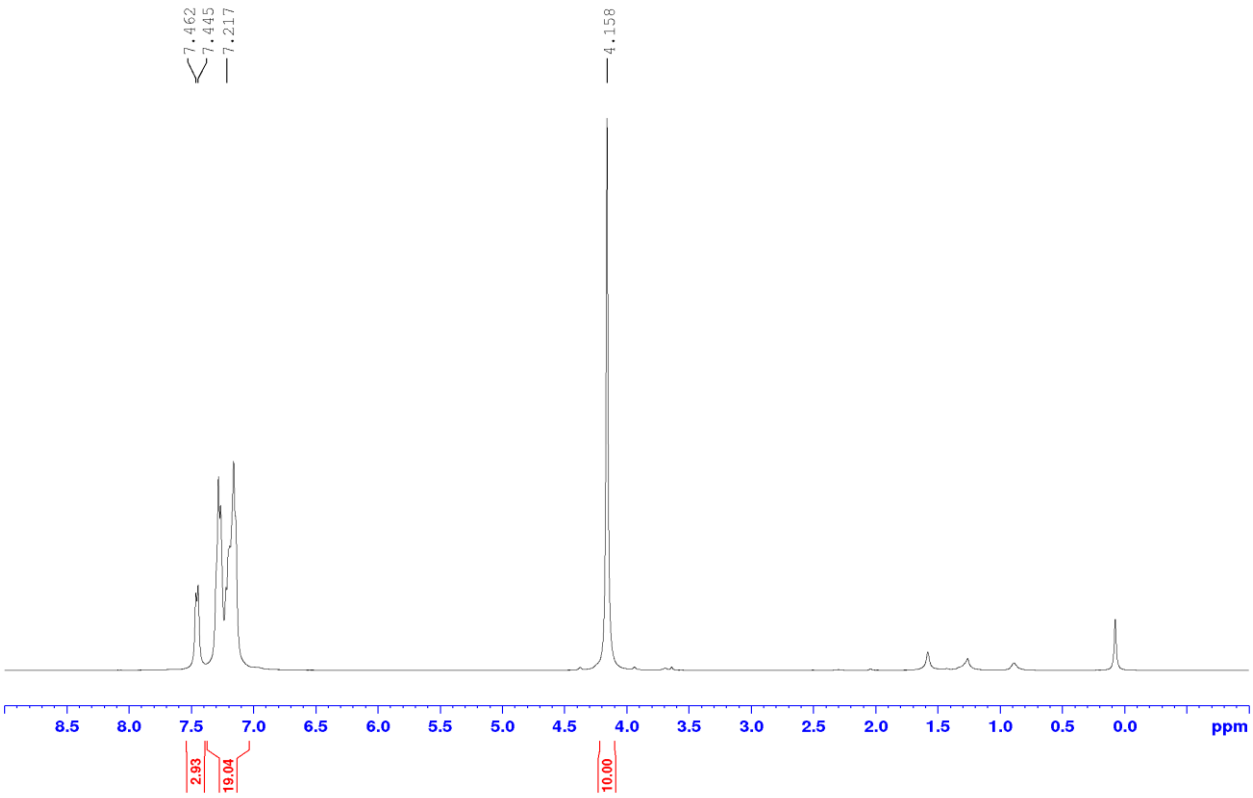

Figure 53 ^{1}H NMR spectrum (400.1 MHz, $CDCl_3$) of Table 4, Entry **5h**, 6%. $FeCp_2$ (40 µmol, 4 mol%).

2,2,2-Trifluoro-*N*,*N*-diphenylacetamide **5h'**.

^{1}H NMR (400.1 MHz, $CDCl_3$): δ / ppm 7.41 (3H, br. s, Ar), 7.39 (2H, br. s, Ar), 7.32 (5H, br. s, Ar)

$^{13}C\{^{1}H\}$ NMR (100.6 MHz, $CDCl_3$): δ / ppm 157.0 (q, J = 36 Hz, *C*O), 141.7 (br, Ar_{ipso}), 128.8 (br, Ar), 127.8 (br, Ar), 126.2 (br, Ar), 115.2 (q, *J* = 289 Hz, *C*F_3)

^{19}F NMR (128.4 MHz, $CDCl_3$): δ / ppm -66.9 (s, C*F*$_3$)

HR-MS found: 265.07087; calculated for [M^+] ($C_{14}H_{10}ONF_3^+$): 265.07090 (error -0.03 ppm).

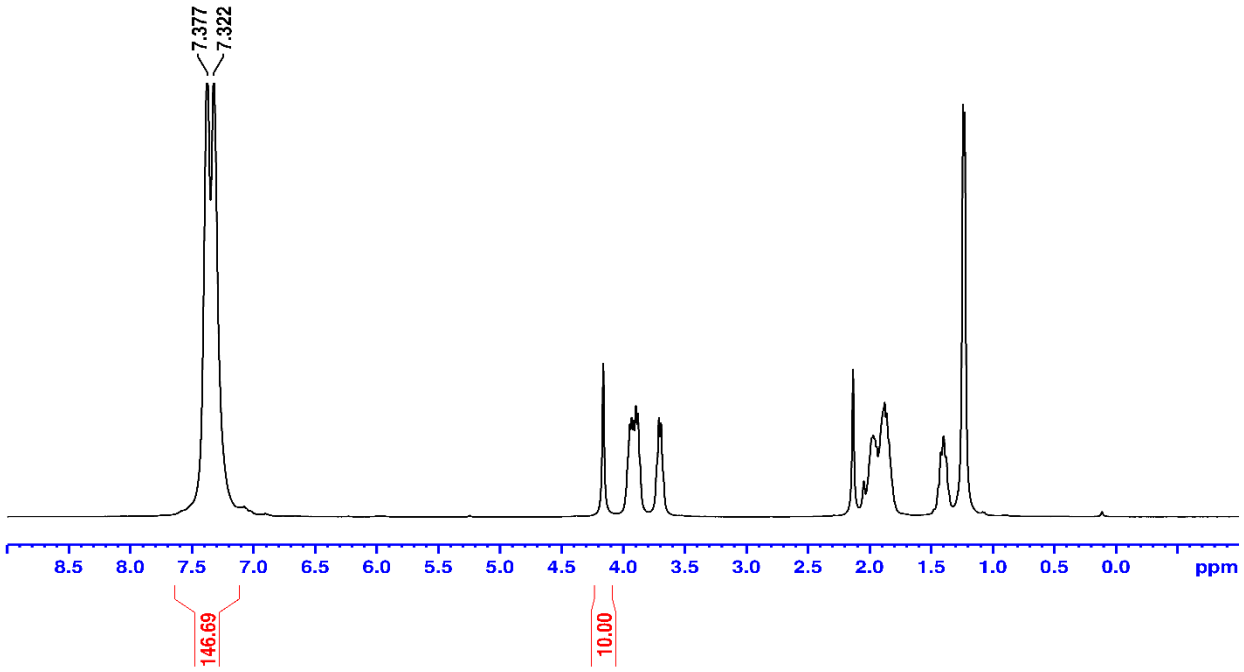

Figure 54 ^{1}H NMR spectrum (400.1 MHz, $CDCl_3$) of Table 4, Entry **5h'**, 70%. $FeCp_2$ (48 μmol, 4.8 mol%). Additional peaks correspond to remaining 2-MeTHF.

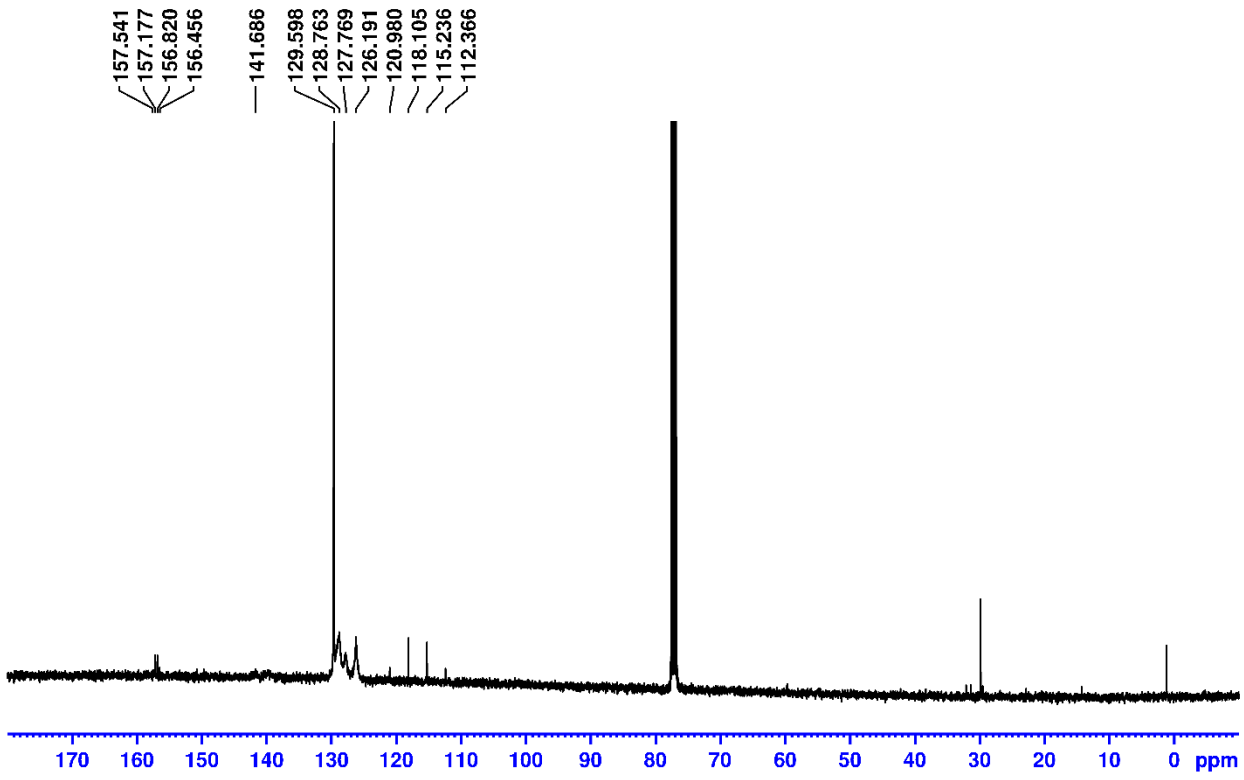

Figure 55 $^{13}C\{^{1}H\}$ NMR spectrum of Table 4, **5h'** in $CDCl_3$

Procedure for the Addition of Li-N(H)Ph (**2b**) to Ethylbenzoate (**1a**) Under Inert Conditions

To a nitrogen-flushed 25 mL Schlenk flask, 1 g (1.16 mL) of dry 2-MeTHF and 1 mmol (144 μL) of ethylbenzoate were added and stirred at room temperature. To this, 1.5 equivalents (1.5 mL, 1.0 M solution in 2-MeTHF) of Li-N(H)Ph (**2b**) was added. After 20 s, the reaction was quenched by the addition of saturated Rochelle's salt solution (sodium potassium tartrate tetrahydrate, 5 mL) before being extracted into 2-MeTHF (3 x 10 mL). Extracts were combined, dried over $MgSO_4$ and concentrated under vacuum.

The crude product (**5b**) was purified by silica column chromatography, eluted by hexane:EtOAc (10:1 – 2:1 gradient). The yield was obtained by ^{1}H NMR spectroscopy by integration against ferrocene as an internal standard as described in General Methods. The yield of **5b** was calculated to be 59%.

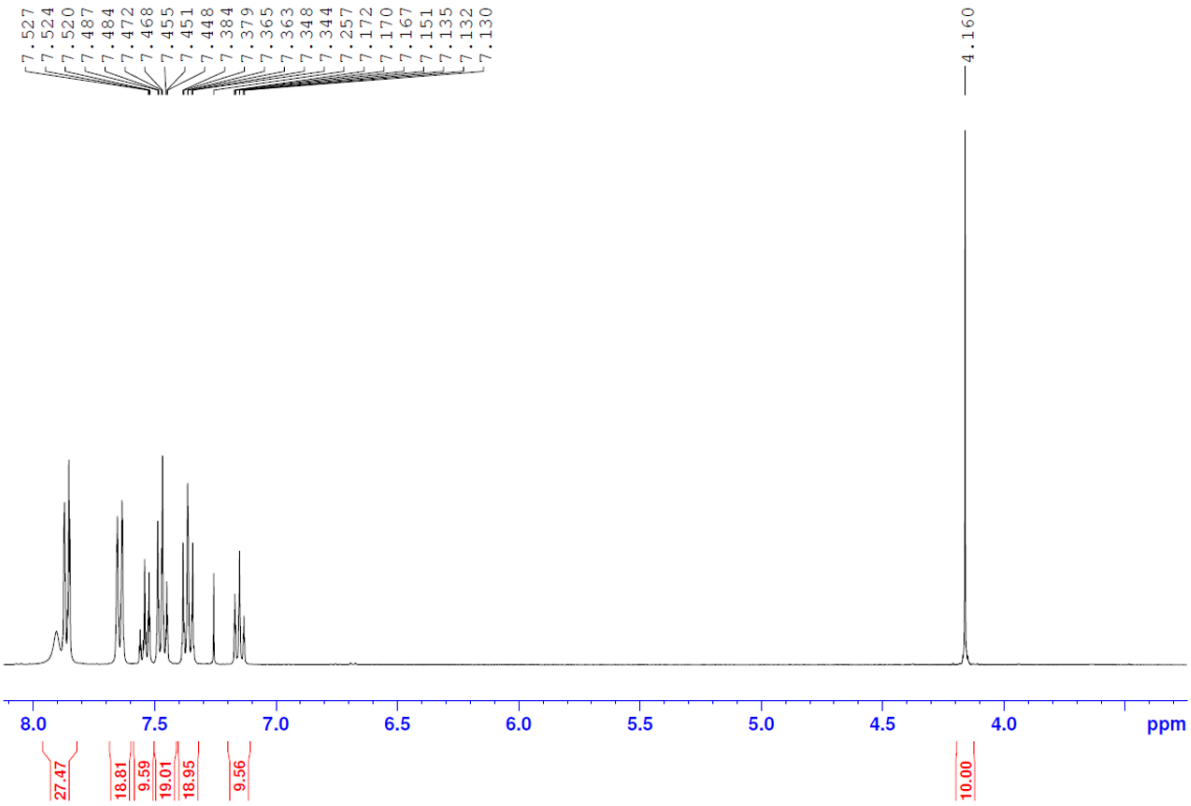

Figure 56 ^{1}H NMR spectrum (400.1 MHz, $CDCl_3$) of **5b** from amidation of ethylbenzoate (**1a**) by Li-N(H)Ph (**2b**) under nitrogen atmosphere, 59%. $FeCp_2$ (63 μmol, 6.3 mol%).

Procedure for the Addition of Li-Amides to *N,N*-di(Boc)-benzamide – Table 5

Additions were performed under air at room temperature in an open Schlenk flask (25 mL) and 1 g of solvent. Lithium amide **2a, 2c, 2e, 2f-h** (1.5 mL, 1.0 M in 2-MeTHF) was added to a stirring solution of *N,N*-di(Boc)-benzamide **6** (1 mmol). After 20 s the reaction was quenched by the addition of saurated Rochelle's salt solution (sodium potassium tartrate tetrahydrate, 5 mL) before being extracted into 2-MeTHF (3 x 10 mL). Extracts were combined, dried over $MgSO_4$ and concentrated under vacuum.

Crude products were purified by silica column chromatography, eluted by hexane:EtOAc (10:1 – 2:1 gradient). Products were identified by GCMS and ^{1}H NMR. Yields were obtained by ^{1}H NMR spectroscopy by integration against ferrocene as an internal standard as described in General Methods.

N-Methyl-*N*-phenylbenzamide **3a**. Spectral data were in accord with published data.[3]

^{1}H NMR (400.1 MHz, $CDCl_3$): δ / ppm 7.34–7.28 (2H, m, Ar), 7.24–7.09 (6H, m, Ar), 7.06–7.01 (2H, m, Ar), 3.49 (3H, s, CH_3).

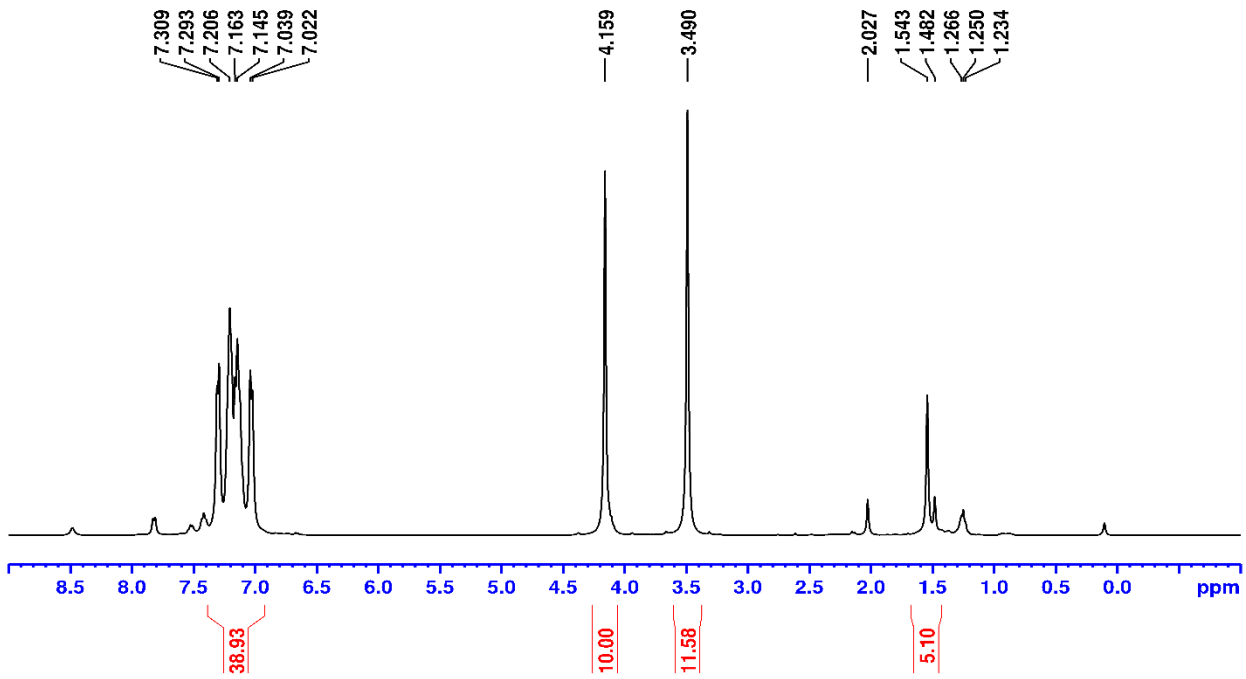

Figure 57 ^{1}H NMR spectrum (400.1 MHz, $CDCl_3$) of Table 5, Entry **3a**, 77%. $FeCp_2$ (200 μmol, 20 mol%).

N,*N*-Dibutylbenzamide **5c**. Spectral data were in accord with published data.[6]

^{1}H NMR (400.1 MHz, $CDCl_3$): δ / ppm 7.43–7.31 (5H, m, Ar), 3.61–3.36 (2H, m, CH_2), 3.34–3.05 (2H, m, CH_2), 1.76–1.57 (2H, m, CH_2), 1.57–1.34 (4H, m, CH_2), 1.20–1.07 (2H, m, CH_2), 1.06–0.91 (3H, m, CH_3), 0.87–0.71 (2H, m, CH_2).

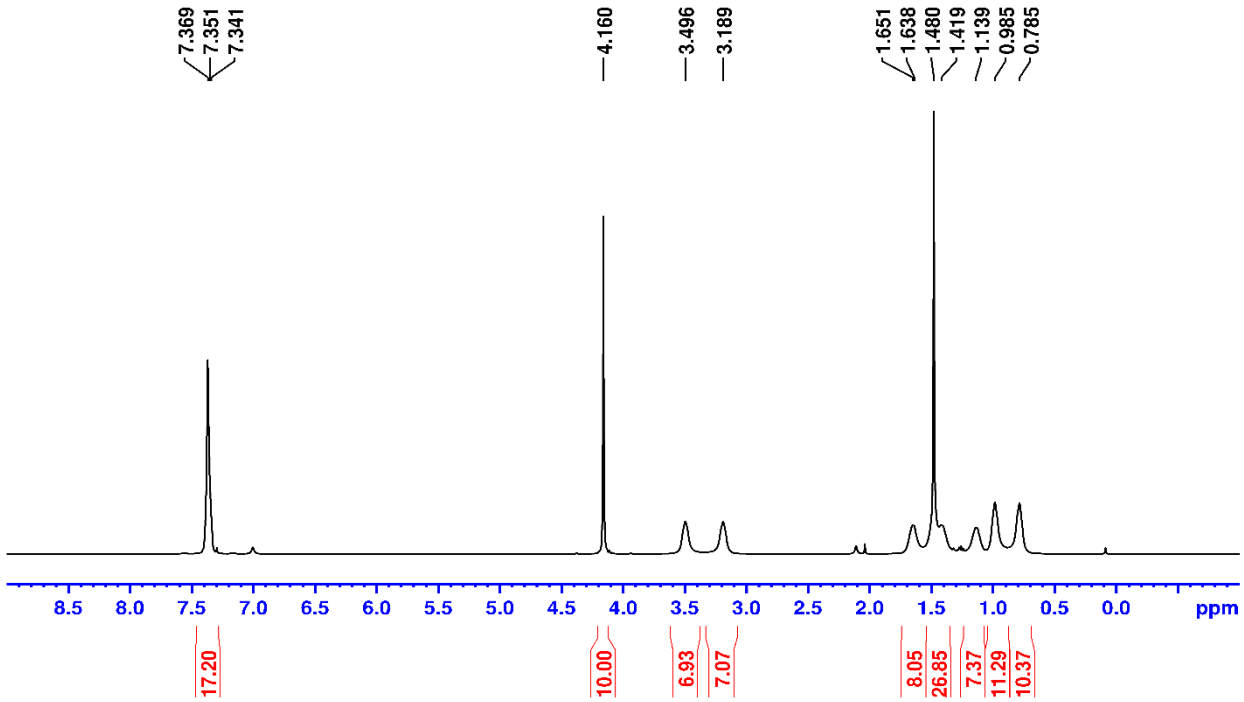

Figure 58 ^{1}H spectrum (400.1 MHz, $CDCl_3$) of Table 5, Entry **5c**, 70%. $FeCp_2$ (200 μmol, 20 mol%).

Phenyl(pyrrolidin-1-yl)methanone **5e**. Spectral data were in accord with published data.[8, 12]

^{1}H NMR (400.1 MHz, $CDCl_3$): δ / ppm 7.60–7.47 (2H, m, Ar), 7.45–7.33 (3H, m, Ar), 3.70–3.54 (2H, m, CH_2), 3.50–3.31 (2H, m, CH_2), 2.07–1.80 (6H, m, CH_2).

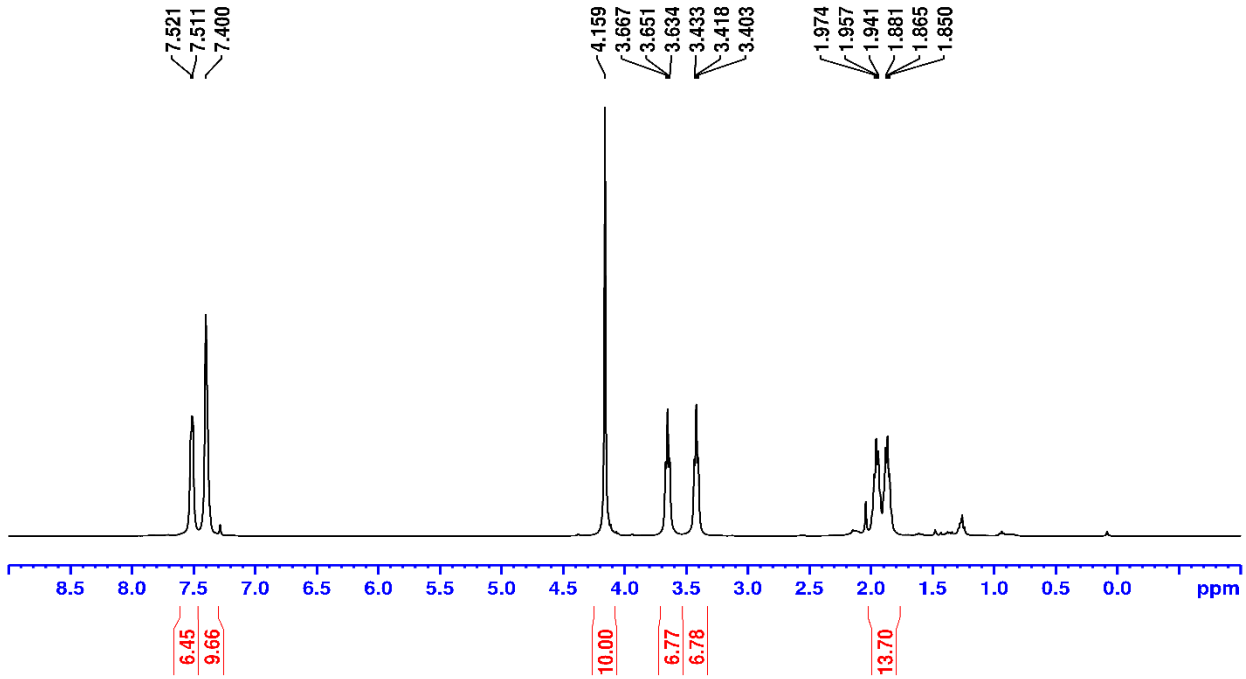

Figure 59 ^{1}H spectrum (400.1 MHz, $CDCl_3$) of Table 5, Entry **5e**, 65%. $FeCp_2$ (200 μmol, 20 mol%).

Phenyl(piperidin-1-yl)methanone **5f**. Spectral data were in accord with published data.[13]

^{1}H NMR (400.1 MHz, $CDCl_3$): δ / ppm 7.34 (5H, m, Ar), 3.78–3.55 (2H, m, CH_2), 3.40–3.17 (2H, m, CH_2), 1.74–1.54 (4H, m, CH_2), 1.54–1.38 (2H, m, CH_2).

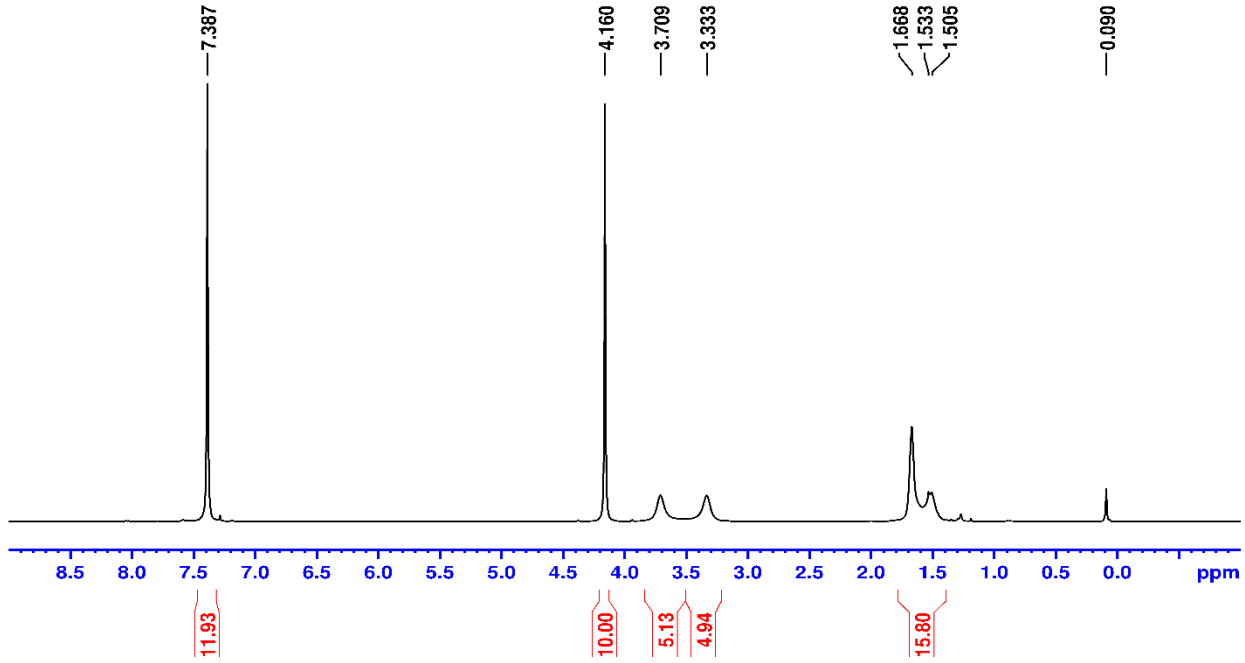

Figure 60 ^{1}H spectrum (400.1 MHz, $CDCl_3$) of Table 5, Entry **5f**, 53%. $FeCp_2$ (200 μmol, 20 mol%).

(2,6-Dimethylpiperidin-1-yl)(phenyl)methanone **5g**. Spectral data were in accord with published data.[9, 14]

^{1}H NMR (400.1 MHz, $CDCl_3$): δ / ppm 7.43–7.36 (3H, m, Ar), 7.36–7.30 (2H, m, Ar), 5.00–4.25 (2H, m, C*H*), 1.90–1.81 (1H, m, CH_2), 1.75–1.62 (2H, m, CH_2), 1.62–1.46 (3H, m, CH_2), 1.29 (3H, s, CH_3), 1.27 (3H, s, CH_3).

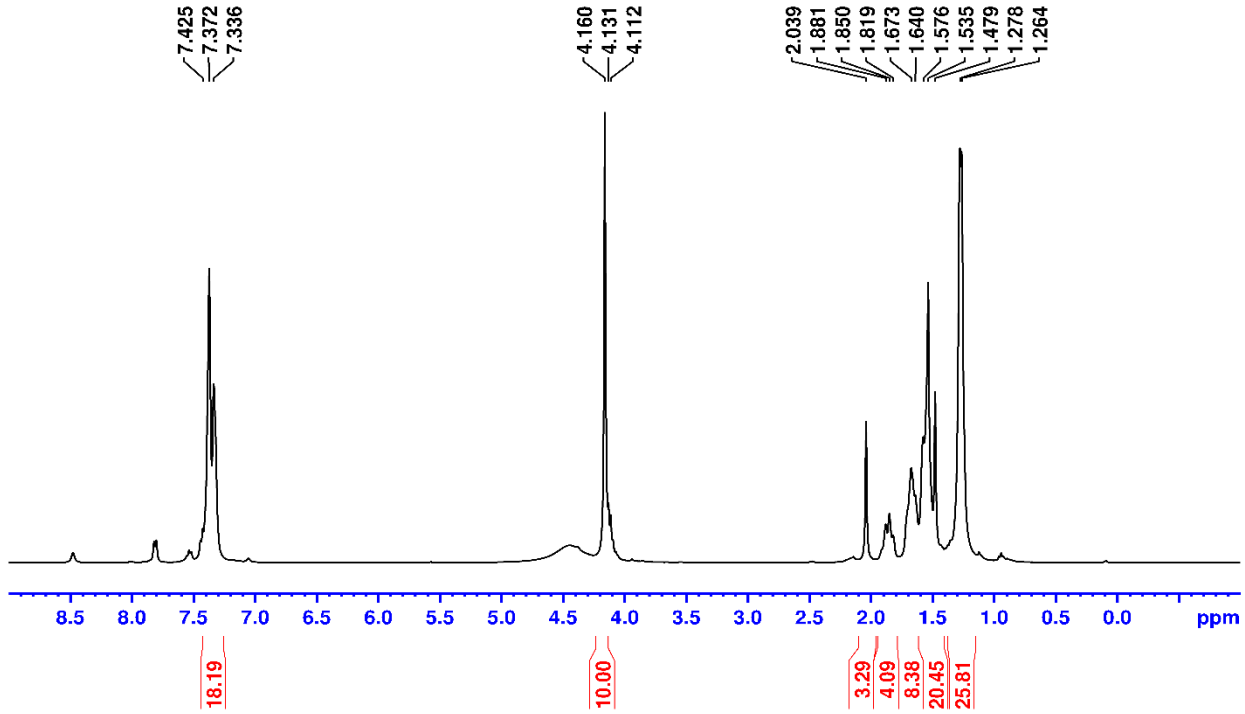

Figure 61 ^{1}H spectrum (400.1 MHz, $CDCl_3$) of Table 5, Entry **5g**, 73%. $FeCp_2$ (200 μmol, 20 mol%).

N,*N*-Diphenylbenzamide **5h**. Spectral data were in accord with published data.[15]

^{1}H NMR (400.1 MHz, $CDCl_3$): δ / ppm 8.20–6.83 (15H, m, Ar), 7.15 (N-*H*, HNBoc), 1.48 (C*H*$_3$, *t*Bu, HNBoc).

*HNBoc present in approximately 21%.

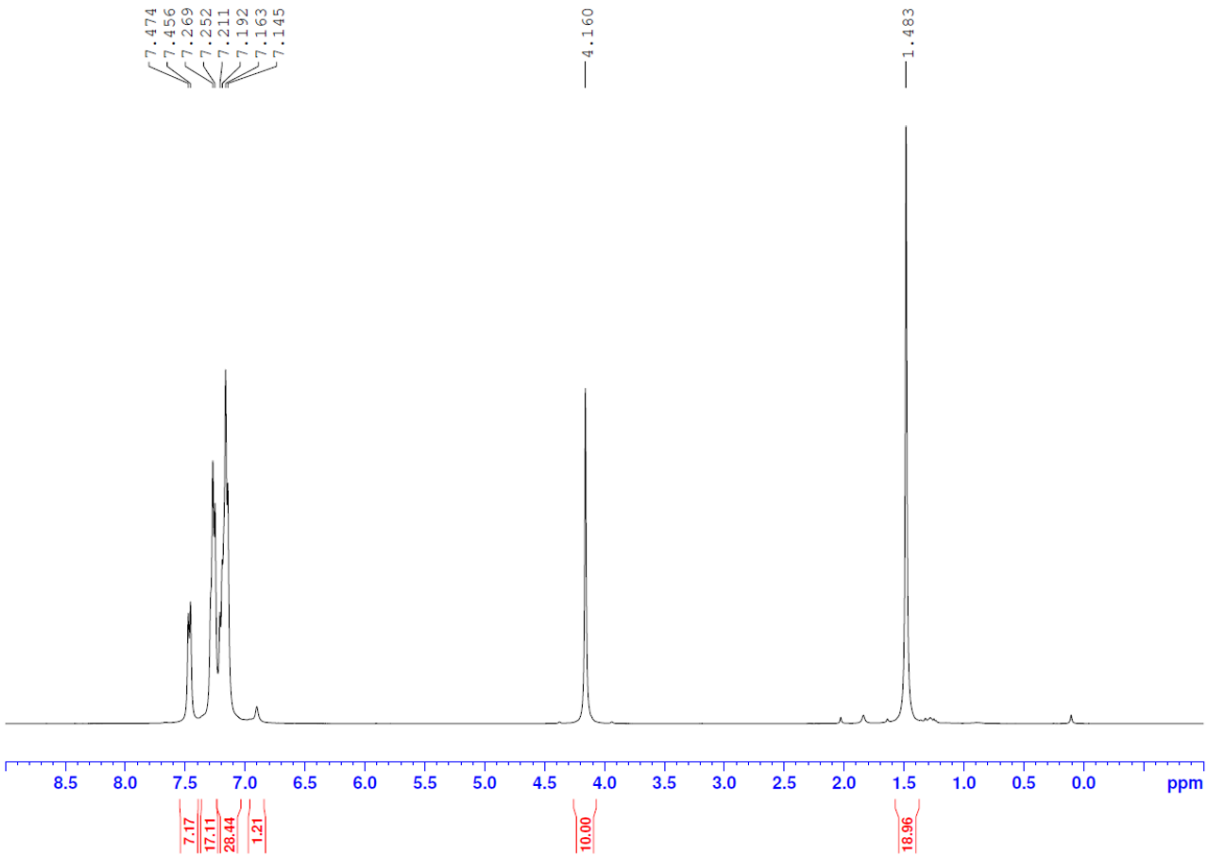

Figure 62 ^{1}H spectrum (400.1 MHz, $CDCl_3$) of Table 5, Entry **5h**, 72%. $FeCp_2$ (200 μmol, 20 mol%).

Procedure for Addition of LiN(Me)Ph (**2a)** to Ethylbenzoate (**1a)** Under Inert Conditions

To an argon-flushed Schlenk flask (25 mL), 1.16 mL of dry 2-MeTHF was measured – the solvent was then degassed using freeze-pump-thaw cycles. 1 mmol (144 μL, 1 mmol) of ethylbenzoate (**1a**) was then added followed by 1.5 equivalents (1.5 mL, 1.0 M solution in 2-MeTHF) of Li-N(Me)Ph (**2a**) and the reaction mixture stirred at room temperature. After 20 s the reaction was quenched by the addition of saturated Rochelle's salt solution (sodium potassium tartrate tetrahydrate, 5 mL) before being extracted into 2-MeTHF (3 x 10 mL). Extracts were combined, dried over $MgSO_4$ and concentrated under vacuum.

Crude products were purified by silica column chromatography, eluted by hexane:EtOAc (10:1 – 2:1 gradient). **3a** was identified by GCMS and ^{1}H NMR. The yield was obtained by ^{1}H NMR spectroscopy by integration against ferrocene as an internal standard as described in General Methods to give a yield of 85%.

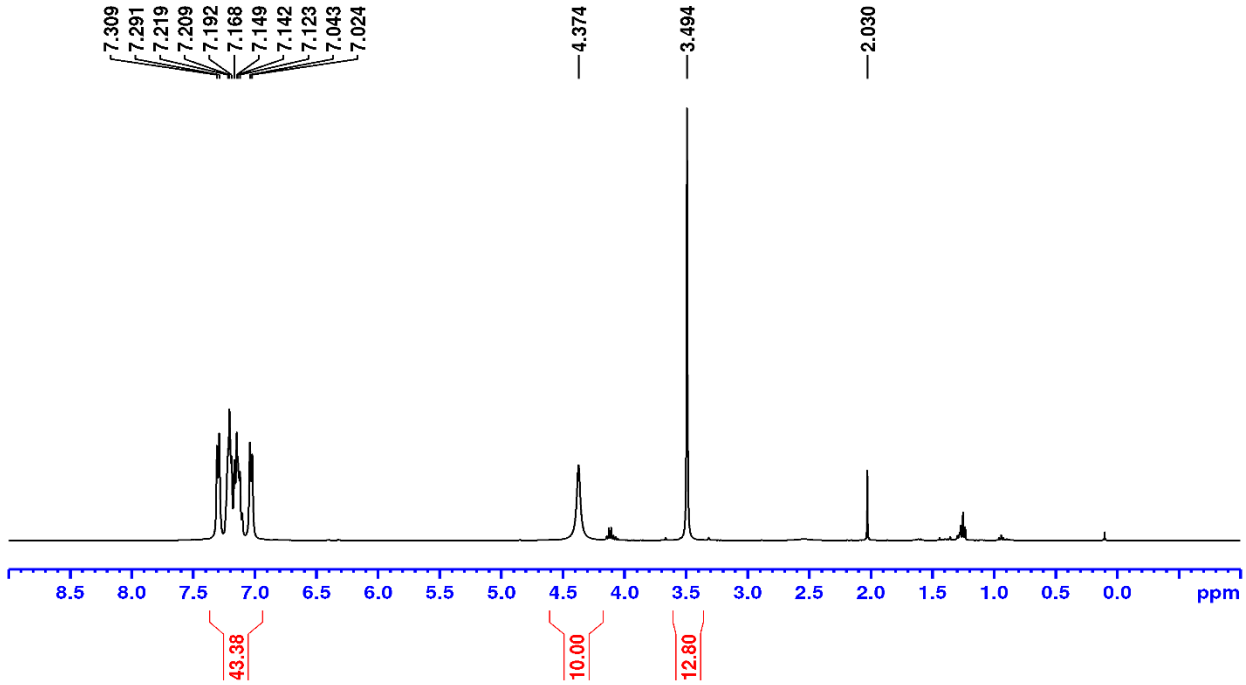

Figure 63 ^{1}H spectrum (400.1 MHz, $CDCl_3$) of **3a** (dry and degassed conditions, 85%). $FeCp_2$ (200 μmol, 20 mol%).

Synthesis of Lithium Amides

n-BuLi (19 mL, 30 mmol) was added dropwise to a stirring solution of amine (30 mmol) in hexane (60 mL) and left to stir for 1 h. The resultant suspension was filtered and washed with hexane (3 x 10 mL) before being dried under vacuum. The white solid product obtained was stored in an argon filled glovebox and analysed by multinuclear NMR spectroscopy (^{1}H, ^{7}Li and ^{13}C{^{1}H}.

Lithium *N*-methylanilide (**2a**)

^{1}H-NMR (400.1 MHz, D$_8$-THF, 300 K): δ / ppm 6.81 (t, 2H, C-*H*$_{meta}$), 6.28 (d, 2H, C-*H*$_{ortho}$), 5.93 (t, 1H, C-*H*$_{para}$), 2.81 (s, 3H, N-C*H*$_3$).

^{7}Li-NMR (155.5 MHz, D$_8$-THF, 300 K): δ / ppm 0.51 (*Li*-N(H)Ph).

^{13}C{^{1}H}-NMR (100.6 MHz, D$_8$-THF, 300 K): δ / ppm 164.1 (*C*$_q$-N), 129.2 (*C*$_{meta}$-H and *C*$_{ortho}$-H)‡, 108.3 (*C*$_{para}$-H), 37.6 (N-*C*H$_3$).

‡Confirmed by [^{1}H,^{13}C]-HSQC NMR spectrum

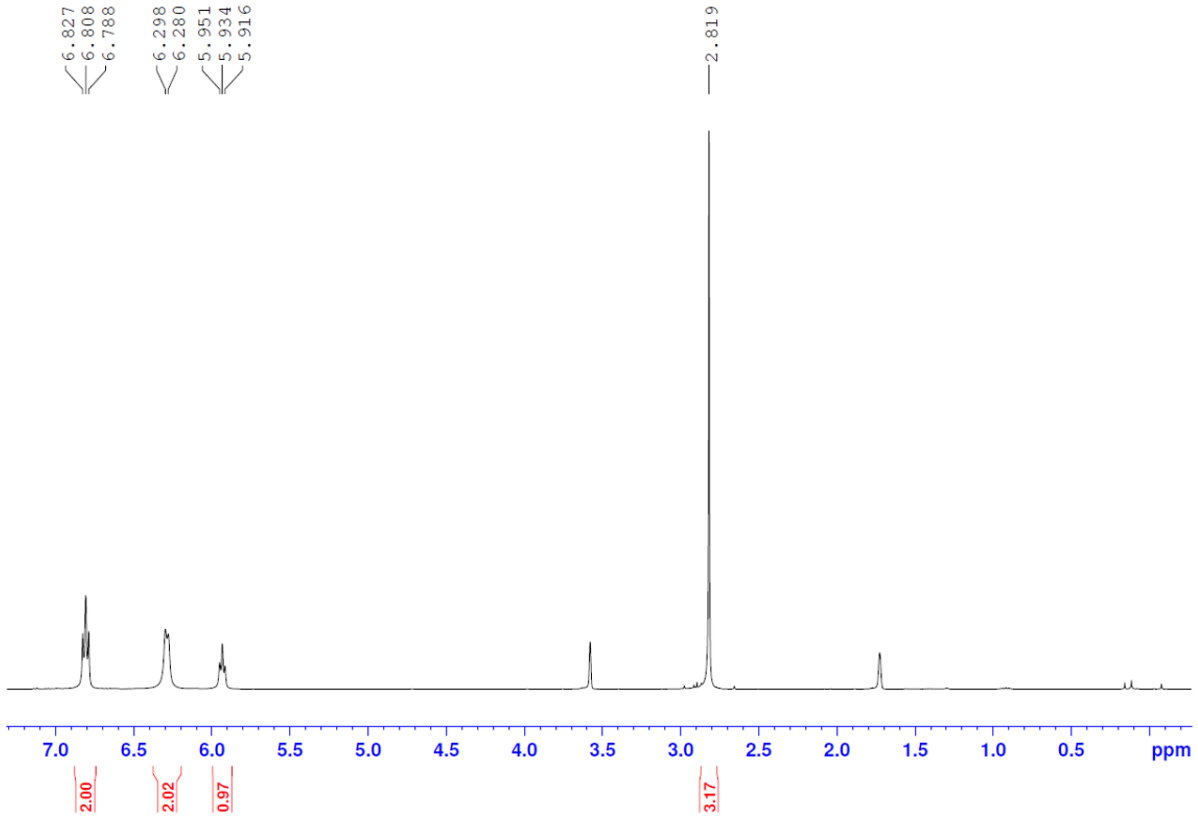

Figure 64 ^{1}H NMR spectrum of compound **2a** in D$_8$-THF

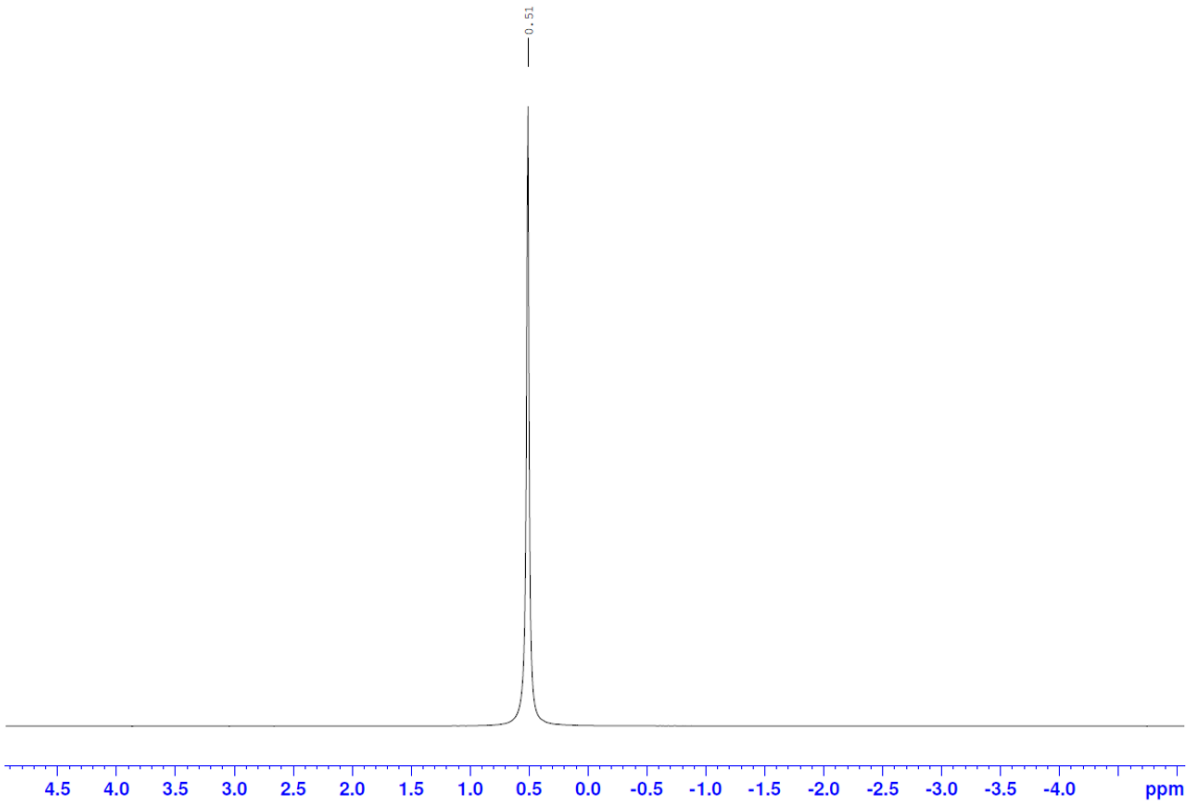

Figure 65 ^{7}Li NMR spectrum of **2a** in D_8-THF

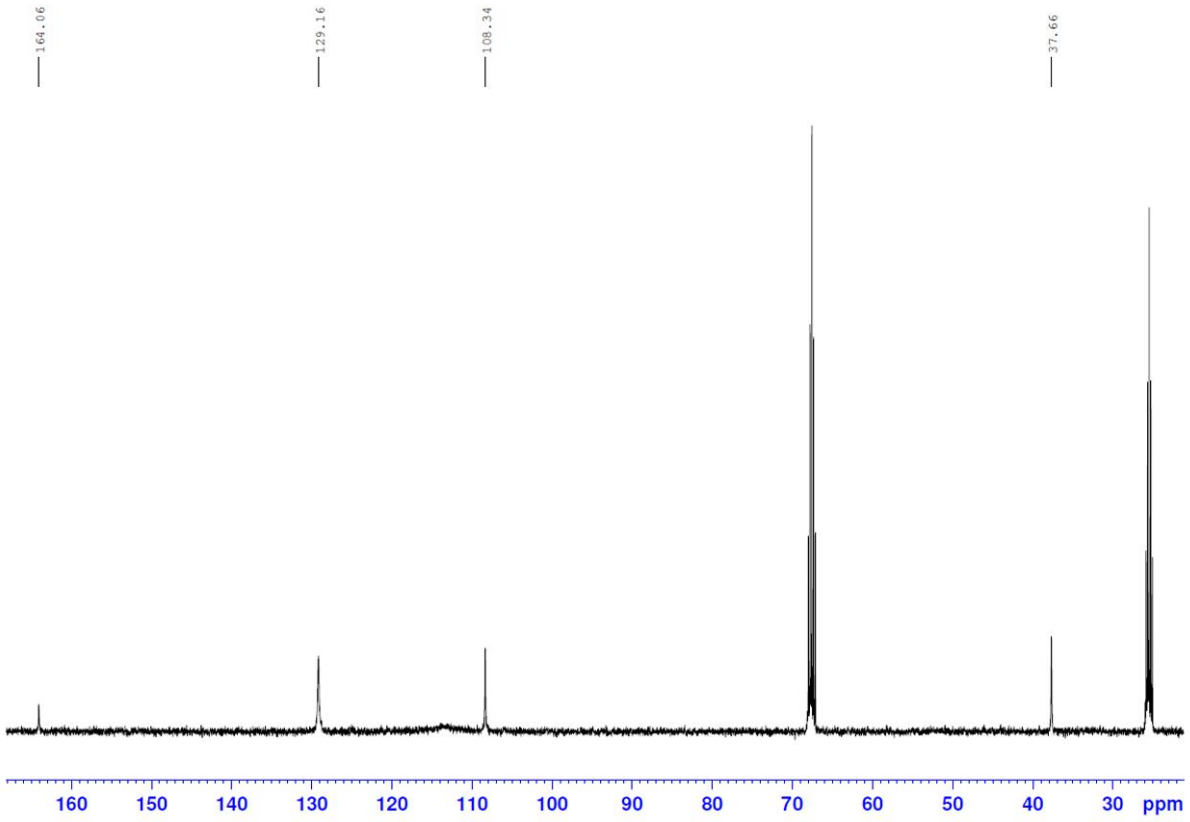

Figure 66 $^{13}C\{^{1}H\}$ NMR spectrum of compound **2a** in D_8-THF

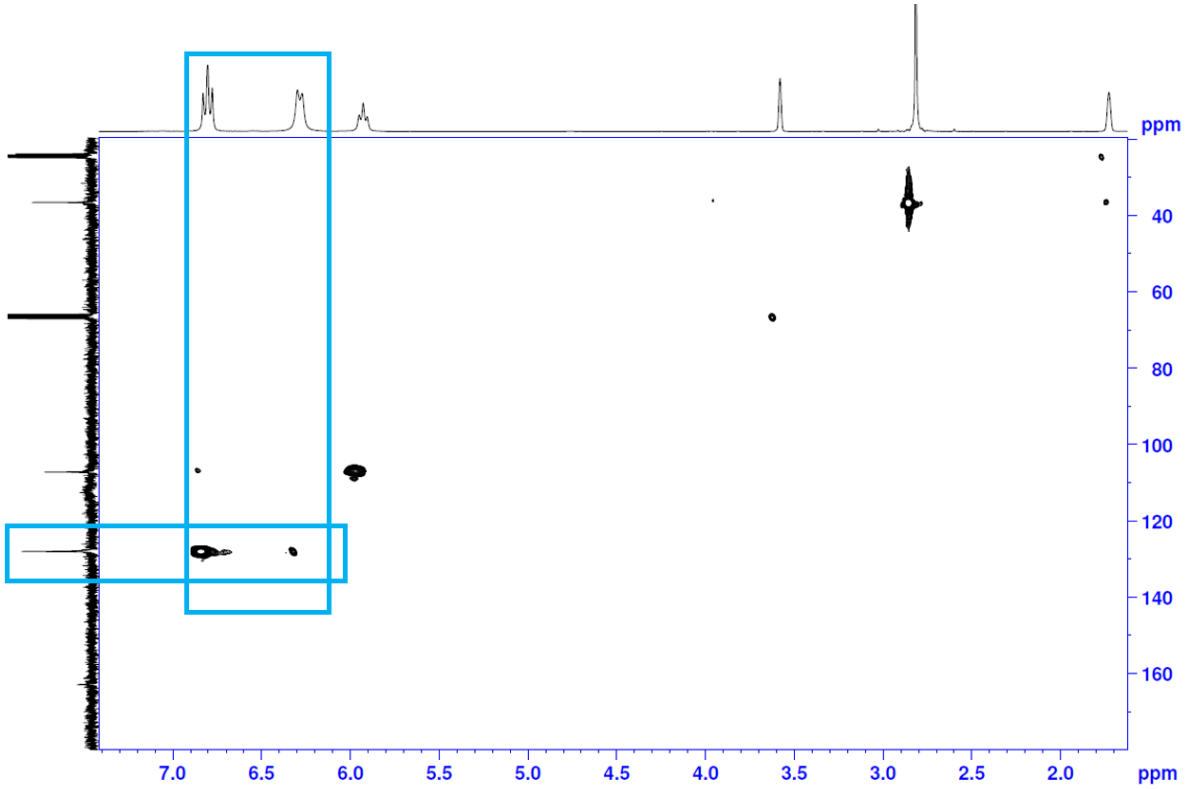

Figure 67 [^{1}H,^{13}C]-HSQC NMR spectrum of **2a** in D_8-THF

Lithium anilide (**2b**)

^{1}H-NMR (300.1 MHz, D_8-THF, 300 K): δ / ppm 6.64 (t, 2H, C-*H*$_{meta}$), 6.24 (d, 2H, C-*H*$_{ortho}$), 5.85 (t, 1H, C-*H*$_{para}$), 2.72 (br. s, 1H, N-*H*).

^{7}Li-NMR (116.6 MHz, D_8-THF, 300 K): δ / ppm 0.87 (*Li*-N(H)Ph).

^{13}C{^{1}H}-NMR (75.5 MHz, D_8-THF, 300 K): δ / ppm 164.3 (*C*$_{q}$-N), 128.8 (*C*$_{meta}$-H), 115.9 (*C*$_{ortho}$-H), 108.3 (*C*$_{para}$-H).

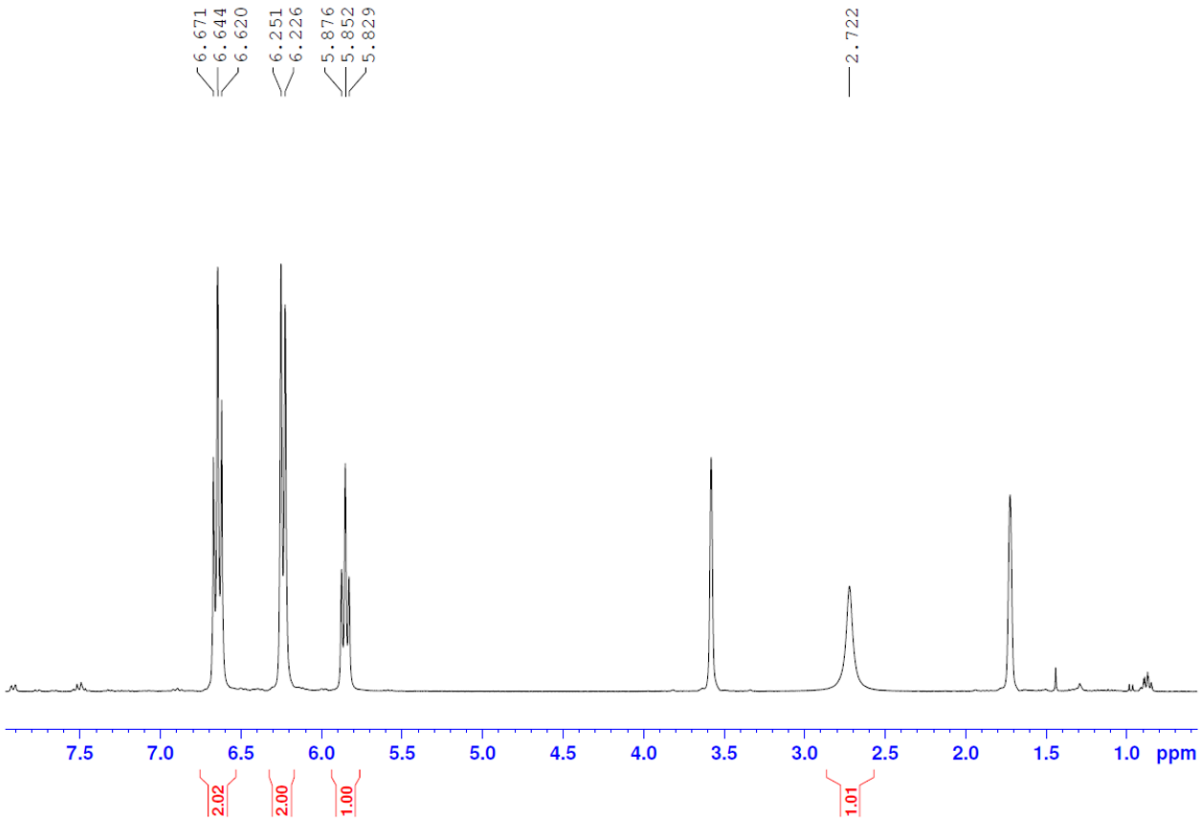

Figure 68 ^{1}H NMR spectrum of compound **2b** in D_8-THF

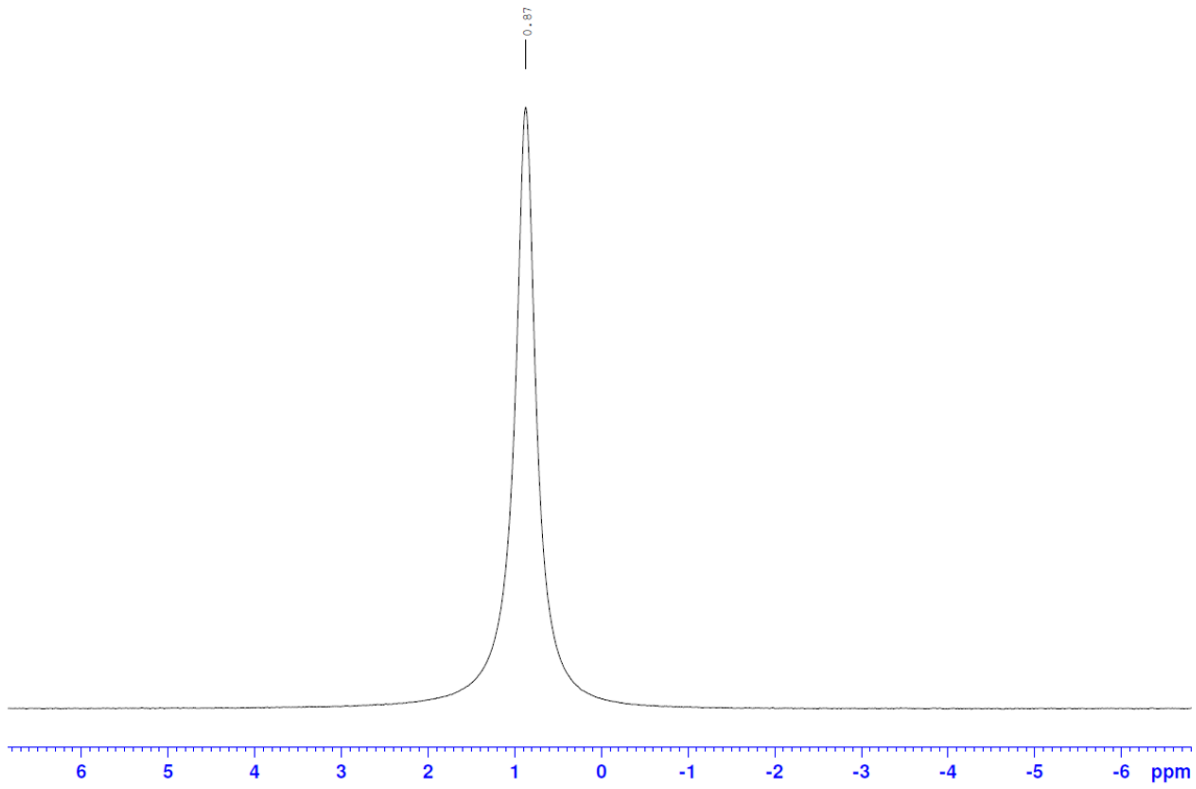

Figure 69 ^{7}Li NMR spectrum of compound **2b** in D_8-THF

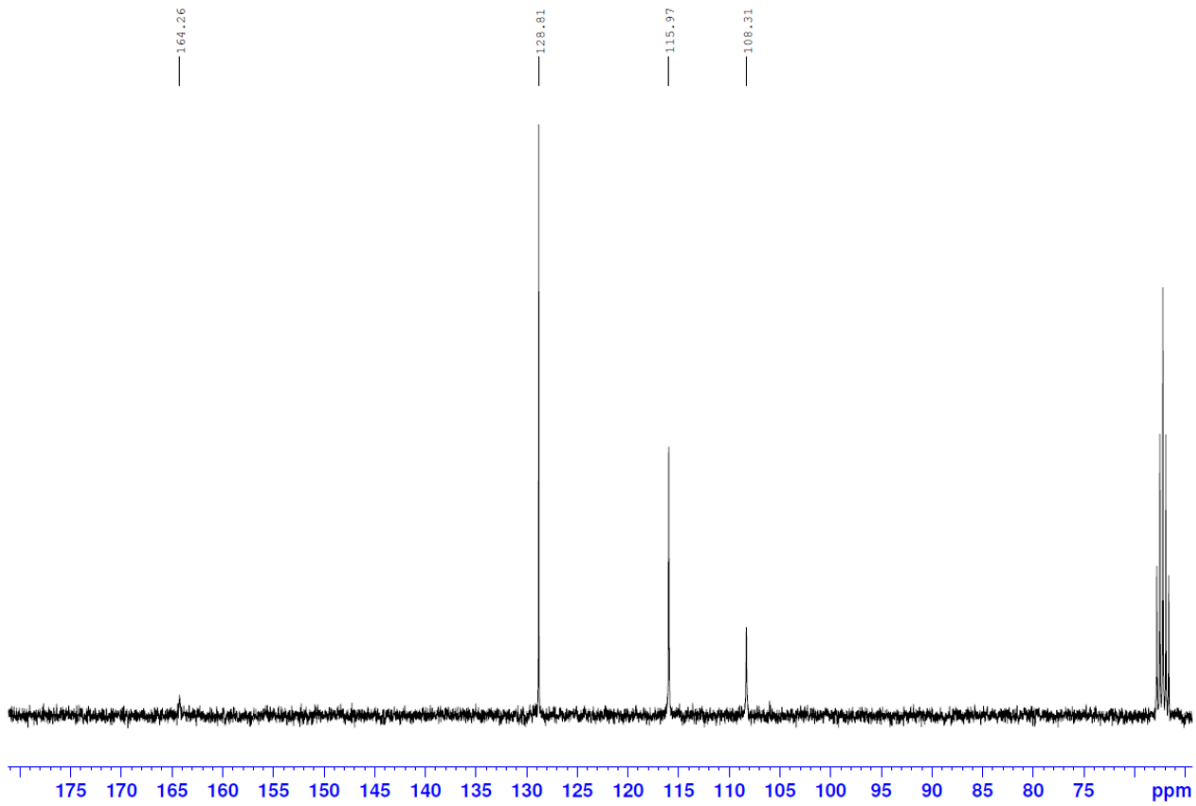

Figure 70 $^{13}C\{^{1}H\}$ NMR spectrum of compound **2b** in D_8-THF

Lithium di-*n*-butylamide (**2c**)

^{1}H-NMR (300.1 MHz, D_8-THF, 300 K): δ / ppm 2.85 (br. t, 4H, N-C*H*$_2$), 1.47-1.24 (br. m, 8H, N-CH$_2$(C*H*$_2$)$_2$CH$_3$), 0.90 (br. t, 6H, C*H*$_3$).

^{7}Li-NMR (116.6 MHz, D_8-THF, 300 K): δ / ppm 1.63 (*Li*-N*n*Bu$_2$).

^{13}C{^{1}H}-NMR (75.5 MHz, D_8-THF, 300 K): δ / ppm 59.4 (N-*C*H$_2$), 37.3 (N-CH$_2$(C*H*$_2$)$_2$CH$_3$), 22.4 (N-CH$_2$(C*H*$_2$)$_2$CH$_3$), 14.9 (*C*H$_3$).

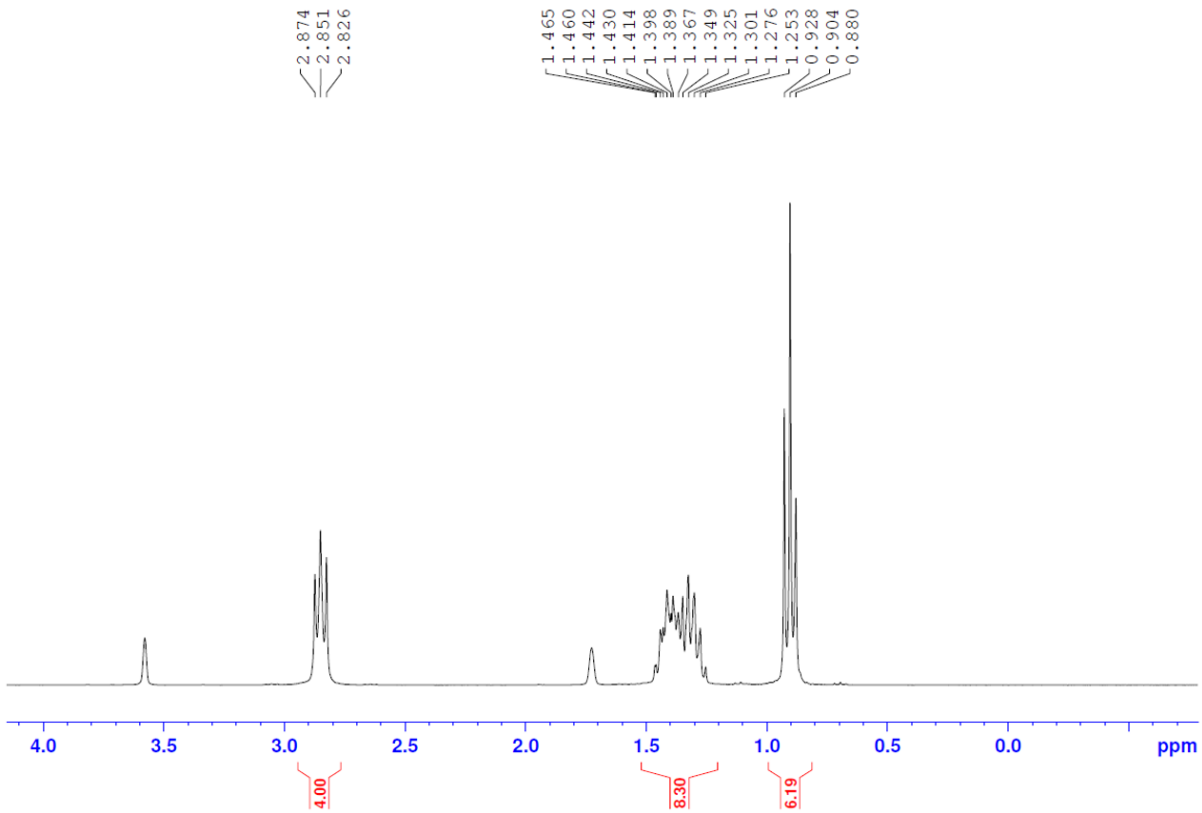

Figure 71 ^{1}H NMR spectrum of compound **2c** in D_8-THF

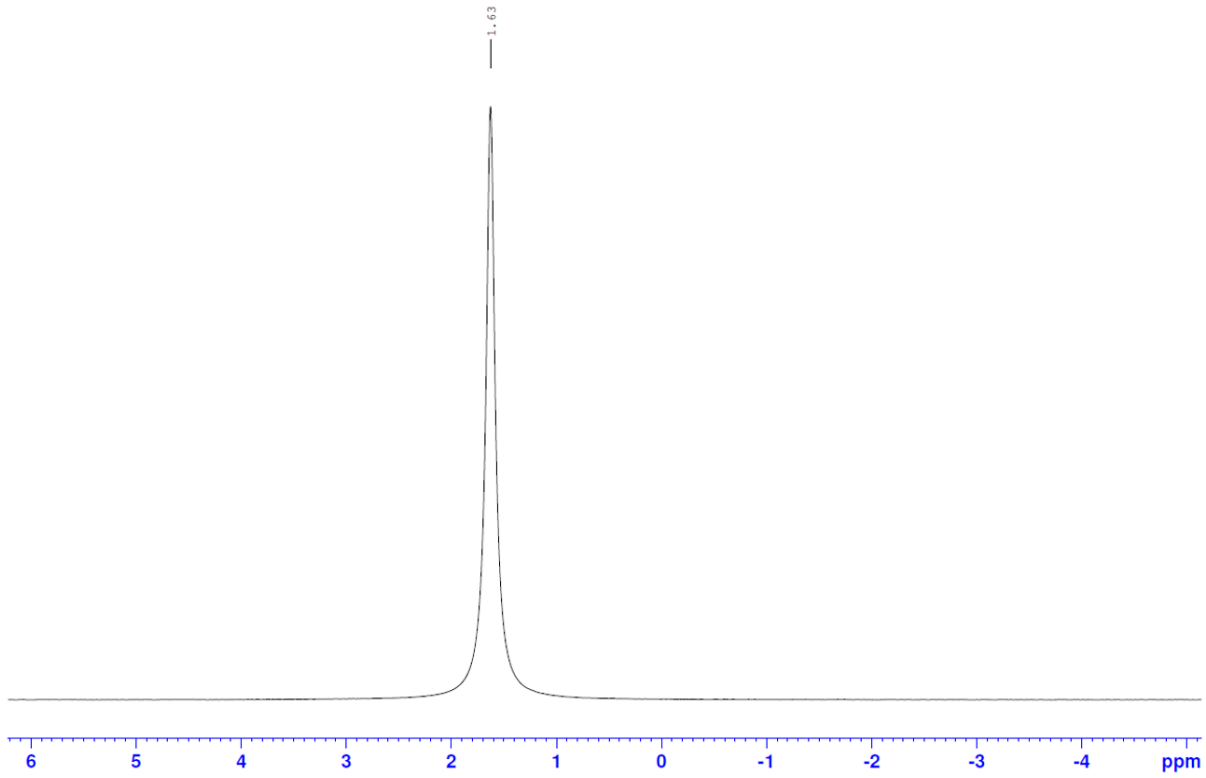

Figure 72 ^{7}Li NMR spectrum of compound **2c** in D_8-THF

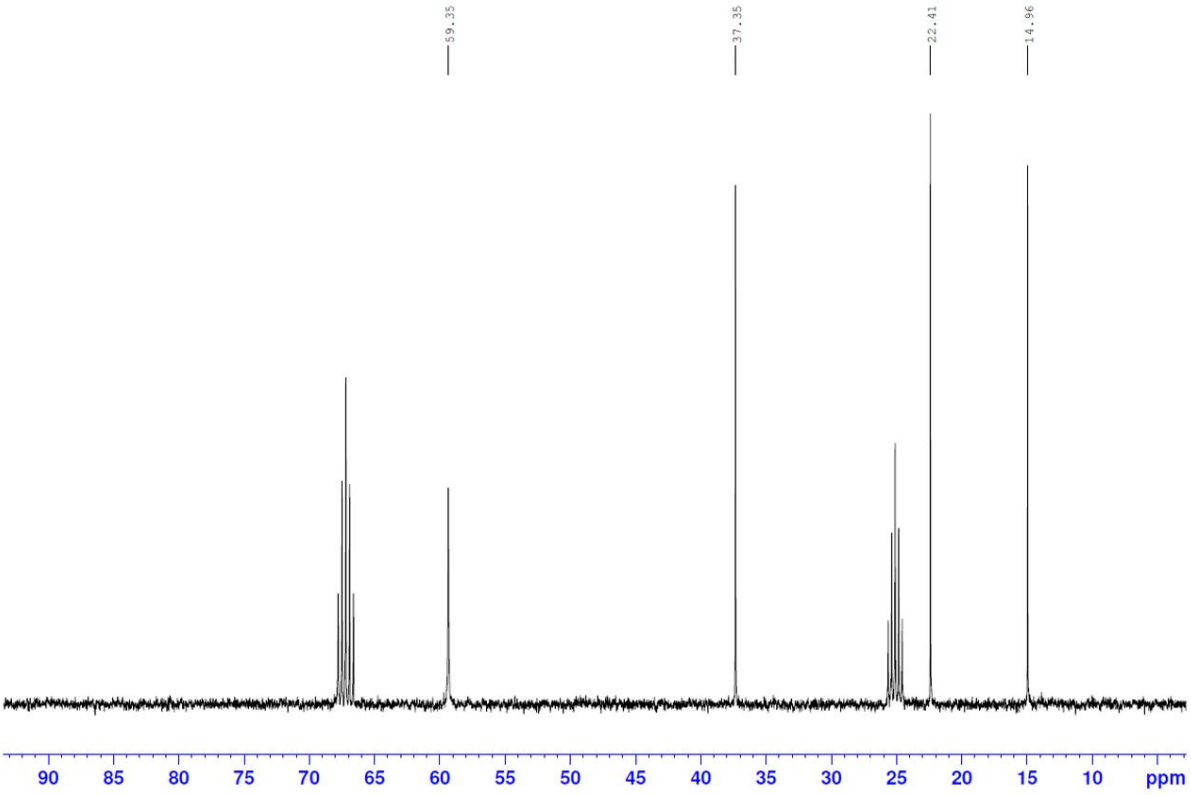

Figure 73 $^{13}C\{^{1}H\}$ NMR spectrum for compound **2c** in D_8-THF

Lithium morpholide (**2d)**

^{1}H-NMR (300.1 MHz, D_8-THF, 300 K): δ / ppm 3.32 (br. t, 4H, O(C*H*$_2$)$_2$), 2.93 (br. t, 4H, N(C*H*$_2$)$_2$).

^{7}Li-NMR (116.6 MHz, D_8-THF, 300 K): δ / ppm 0.74 (*Li*-N(CH$_2$)$_2$(CH$_2$)$_2$O).

^{13}C{^{1}H}-NMR (75.5 MHz, D_8-THF, 300 K): δ / ppm 71.9 (O(*C*H$_2$)$_2$), 55.3 (N(*C*H$_2$)$_2$).

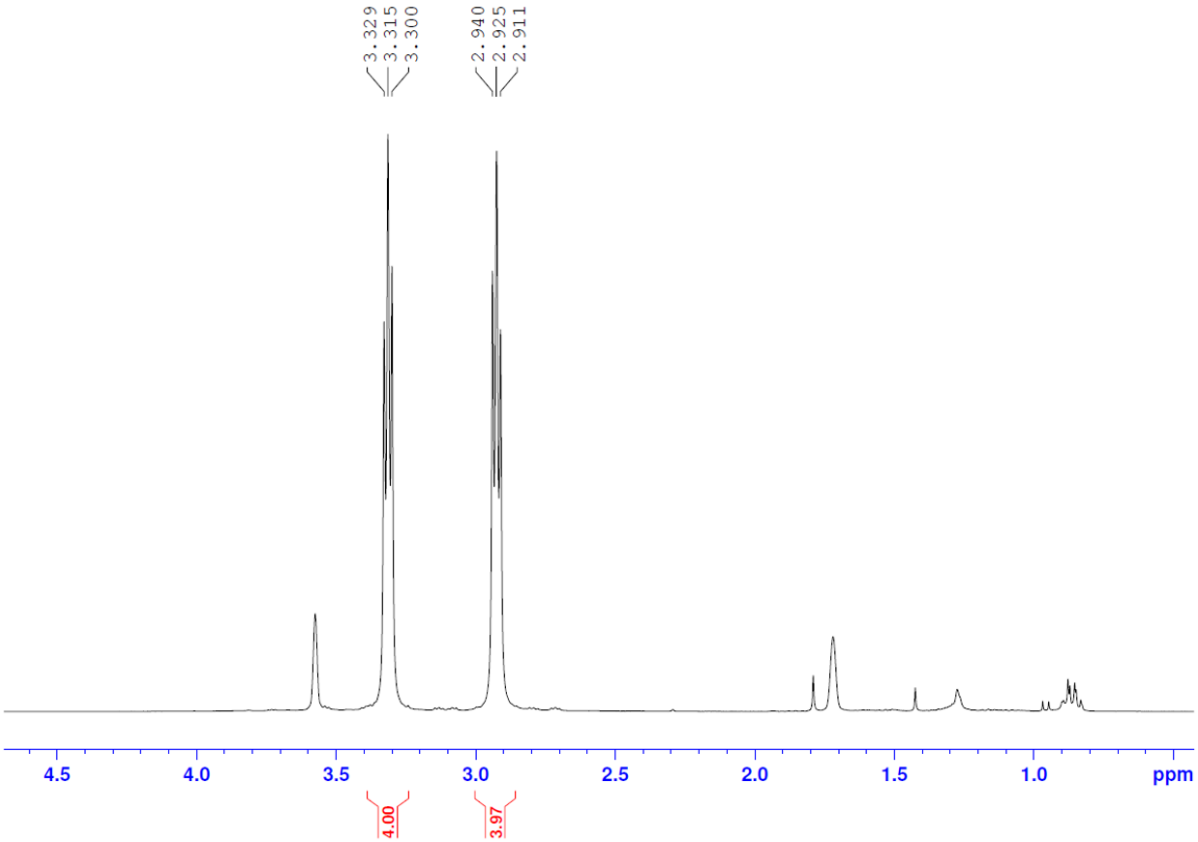

Figure 74 ^{1}H NMR spectrum of compound **2d** in D_8-THF

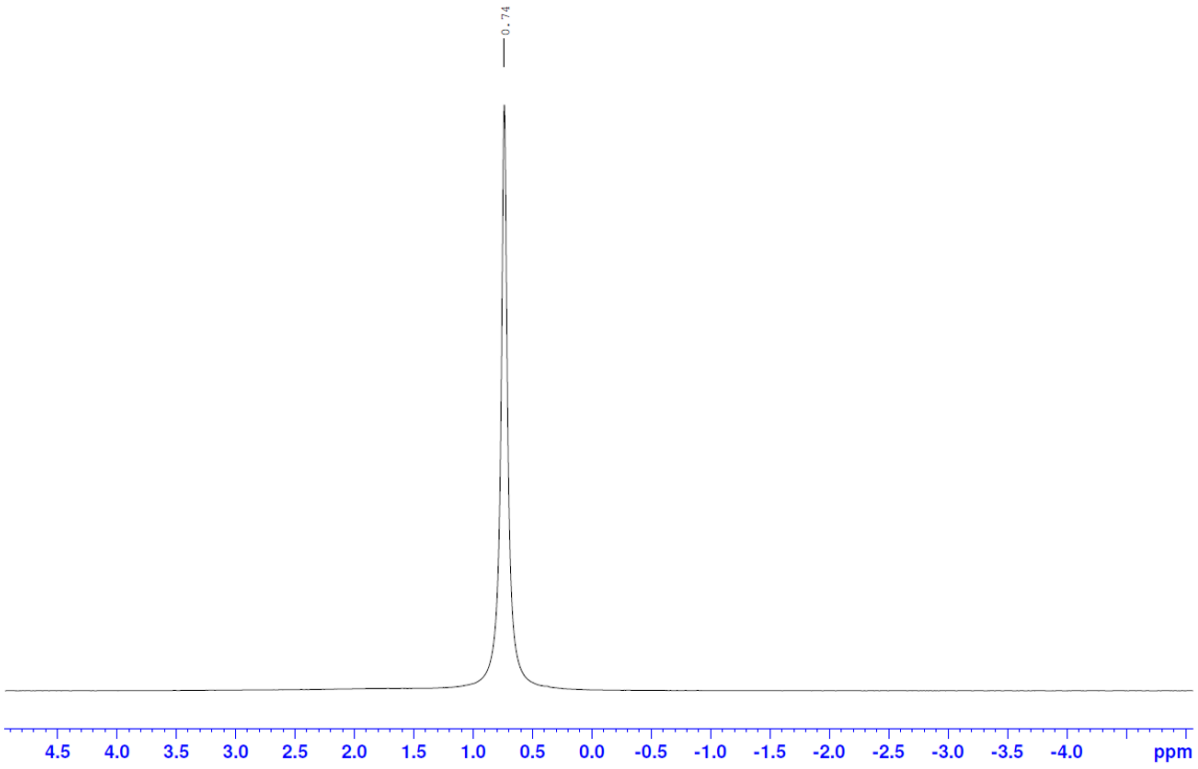

Figure 75 ^{7}LI NMR spectrum of compound **2d** in D_8-THF

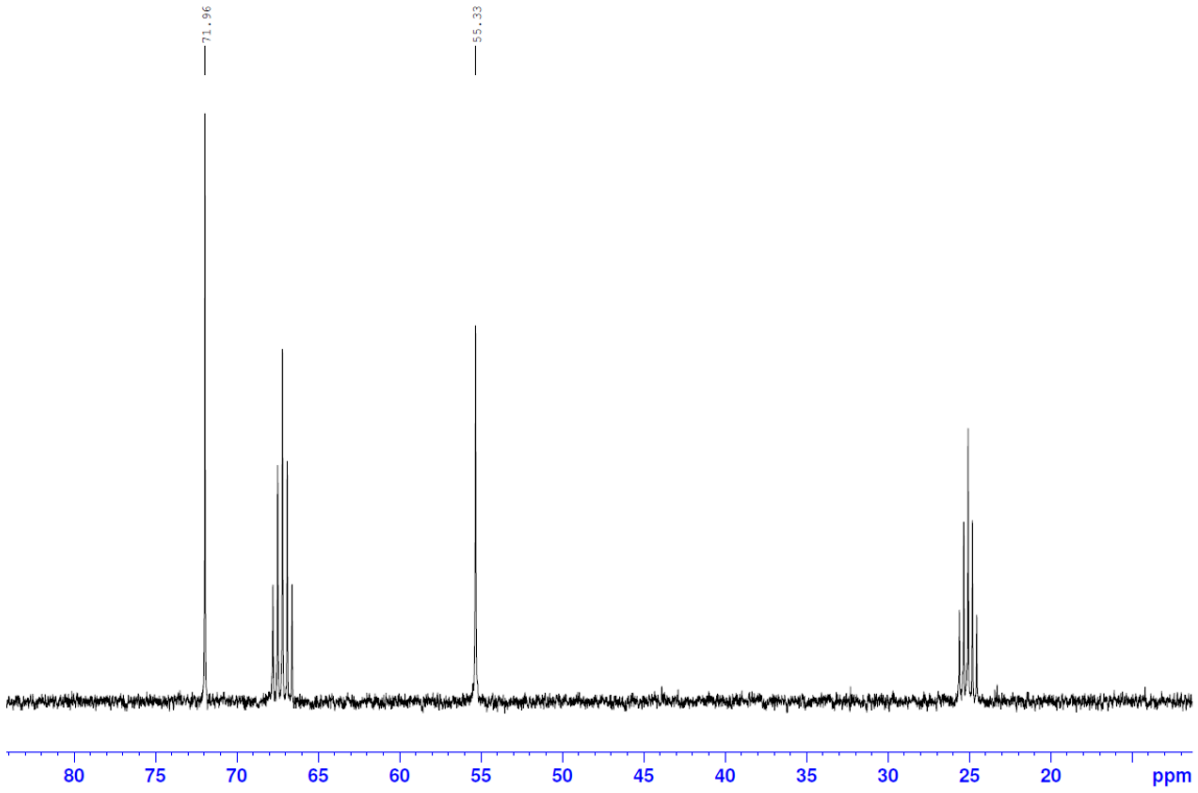

Figure 76 $^{13}C\{^{1}H\}$ NMR spectrum of compound **2d** in D_8-THF

Lithium pyrrolidide (**2e**)

^{1}H-NMR (400.1 MHz, D_8-THF, 300 K): δ / ppm 2.96 (br. t, 4H, N(C*H*$_2$)$_2$), 1.28 (br. t, 4H, N(CH$_2$)$_2$(C*H*$_2$)$_2$).

^{7}Li-NMR (155.5 MHz, D_8-THF, 300 K): δ / ppm 1.02 (*Li*-N(CH$_2$)$_2$(CH$_2$)$_2$O).

^{13}C{^{1}H}-NMR (100.6 MHz, D_8-THF, 300 K): δ / ppm 55.4 (N(*C*H$_2$)$_2$), 27.9 (N(CH$_2$)$_2$(*C*H$_2$)$_2$).

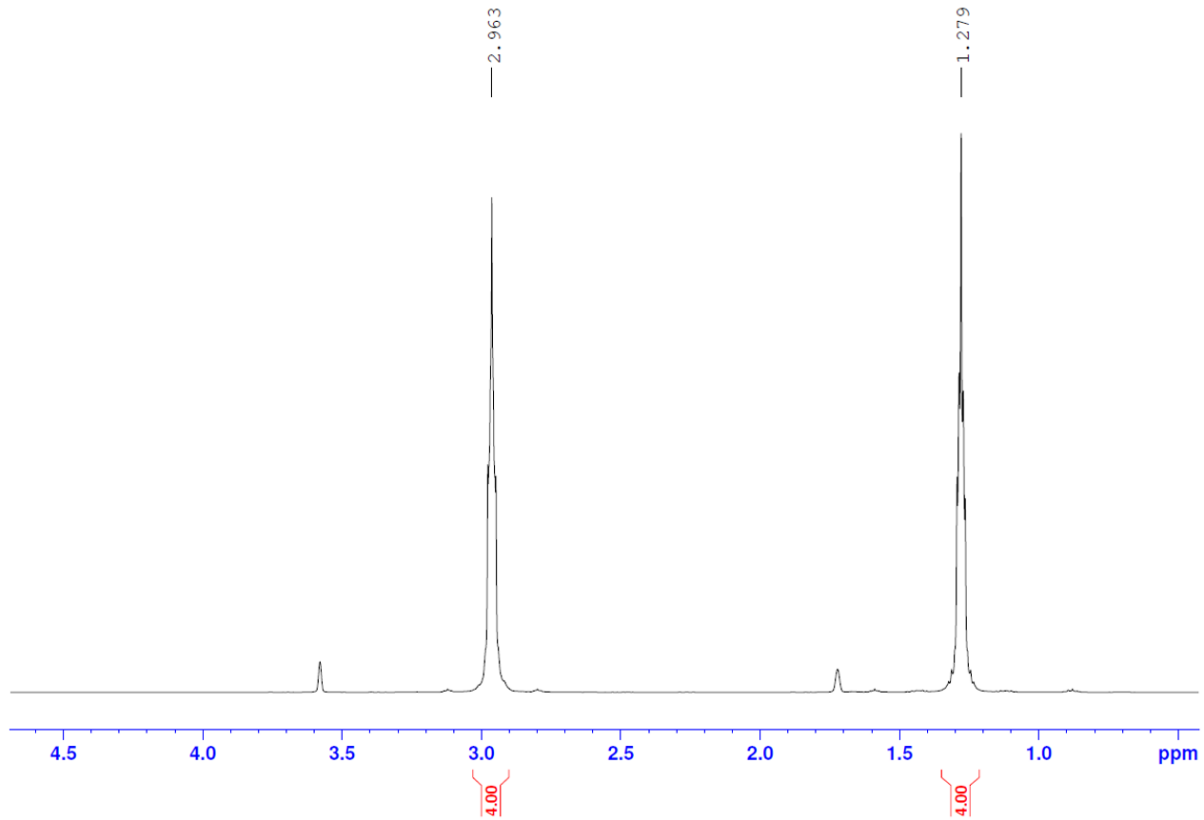

Figure 77 ^{1}H NMR spectrum of compound **2e** in D_8-THF

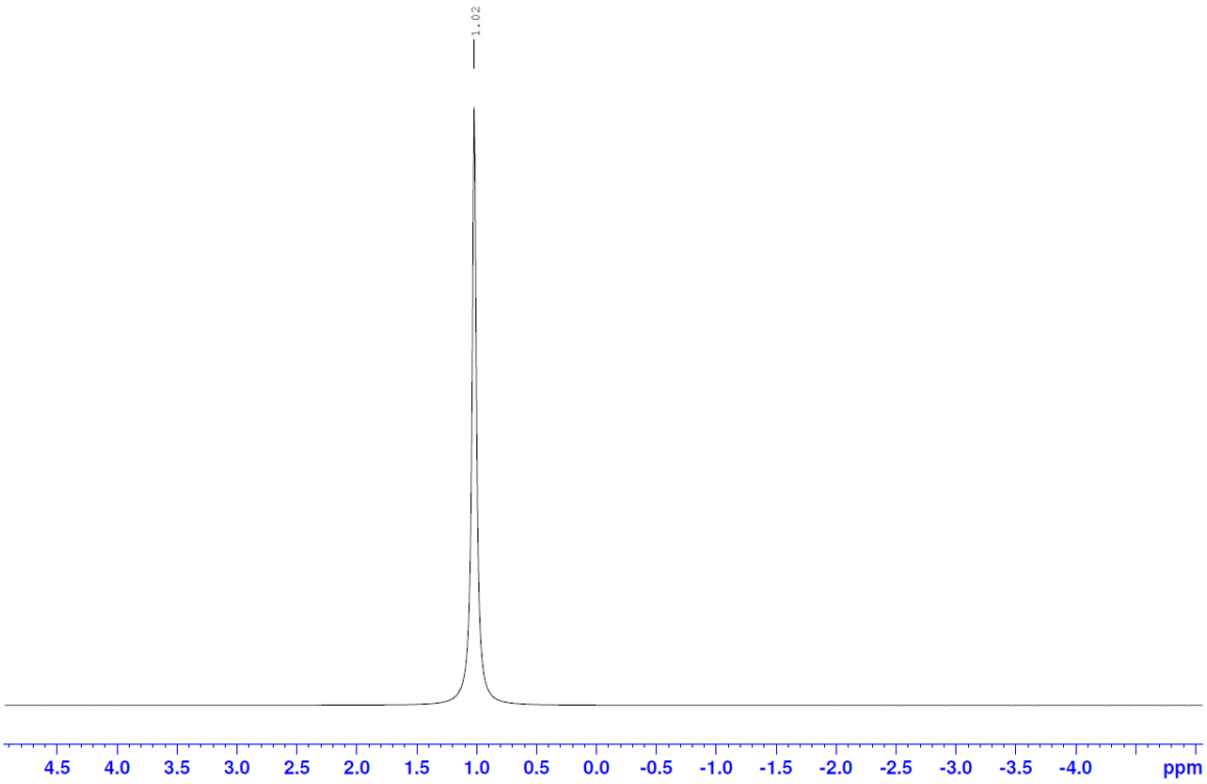

Figure 78 ^{7}Li NMR spectrum of **2e** in D_8-THF

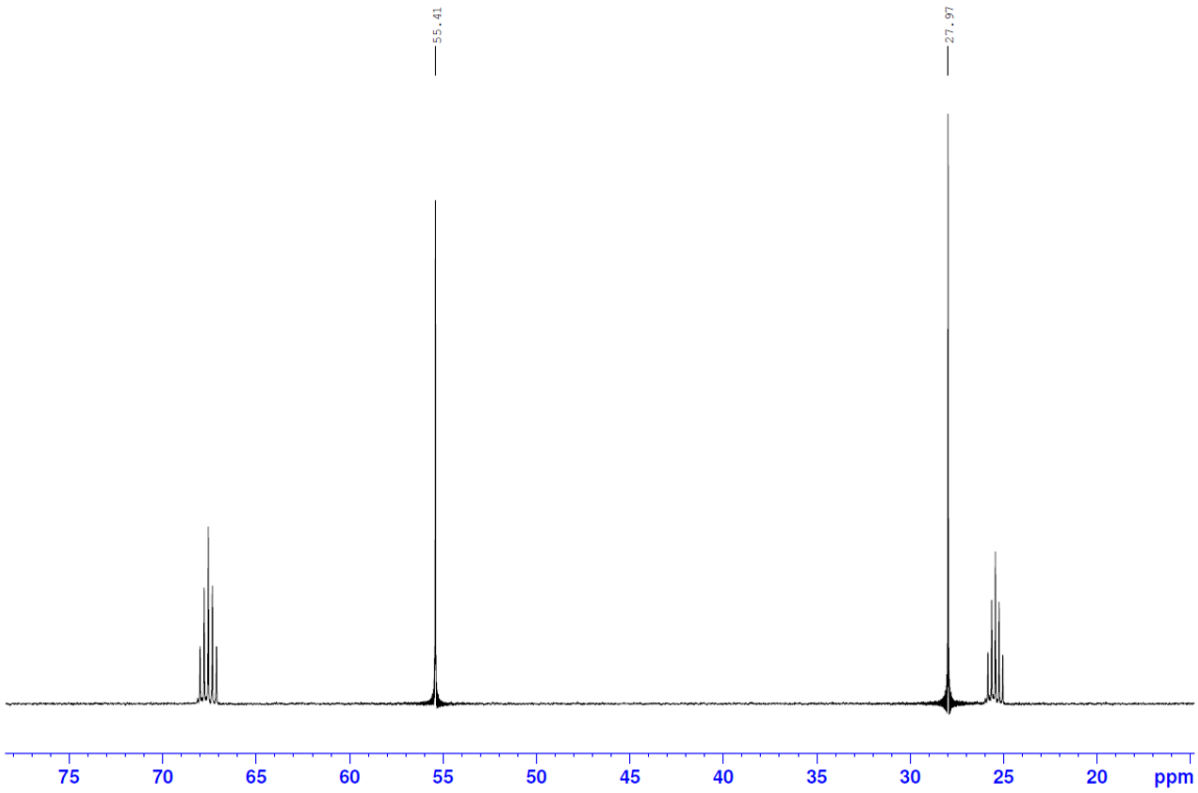

Figure 79 $^{13}C\{^{1}H\}$ NMR spectrum of **2e** in D_8-THF

Lithium piperidide (**2f**)

^{1}H-NMR (300.1 MHz, D_8-THF, 300 K): δ / ppm 2.99 (br. t, 4H, N-(C*H*$_2$)$_2$, 1.50 (br. m, 2H, N(CH$_2$)$_2$(CH$_2$)$_2$C*H*$_2$), 1.23 (br. m, 4H, N(CH$_2$)$_2$(C*H*$_2$)$_2$CH$_2$).

^{7}Li-NMR (116.6 MHz, D_8-THF, 300 K): δ / ppm 0.79 (*Li*-piperidide)

^{13}C{^{1}H}-NMR (75.5 MHz, D_8-THF, 300 K): δ / ppm 56.5 (N(*C*H$_2$)$_2$(CH$_2$)$_2$CH$_2$), 32.6 (N(CH$_2$)$_2$(CH$_2$)$_2$*C*H$_2$), 28.8 (N(CH$_2$)$_2$(*C*H$_2$)$_2$CH$_2$).

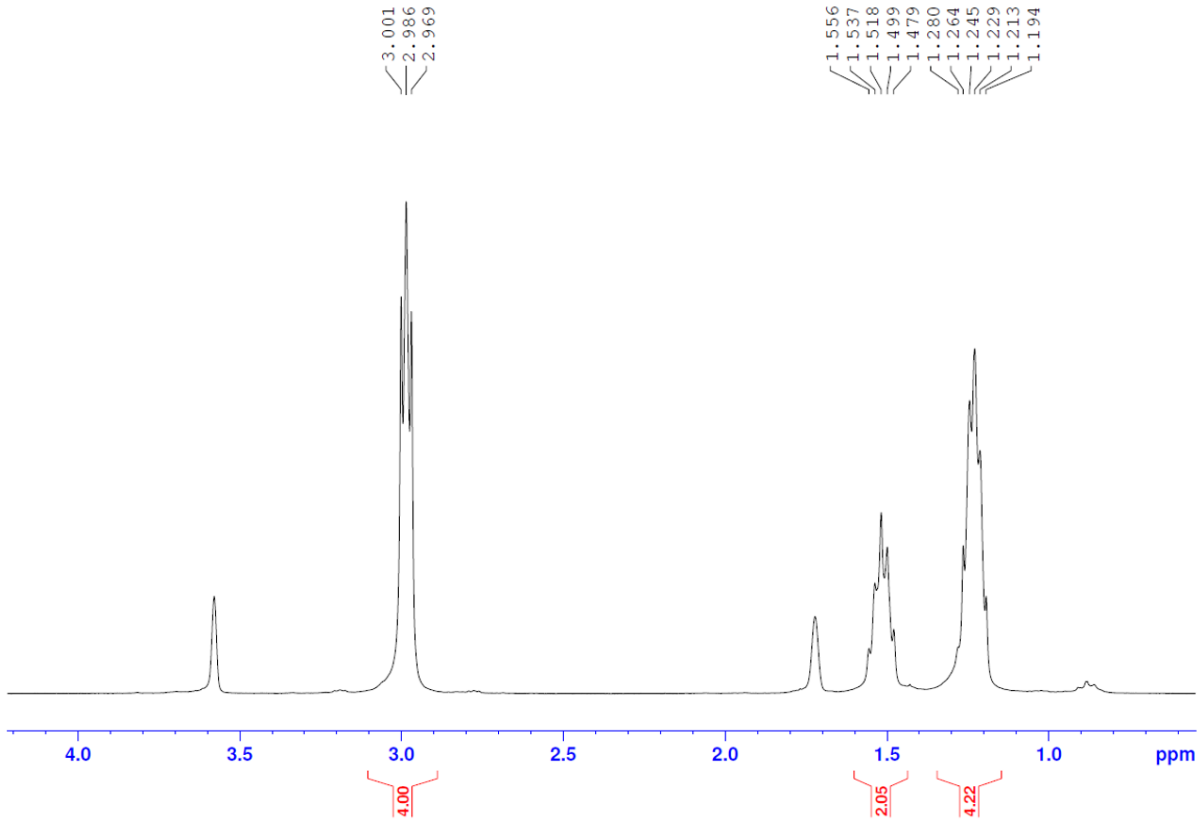

Figure 80 ^{1}H NMR spectrum of compound **2f** in D_8-THF

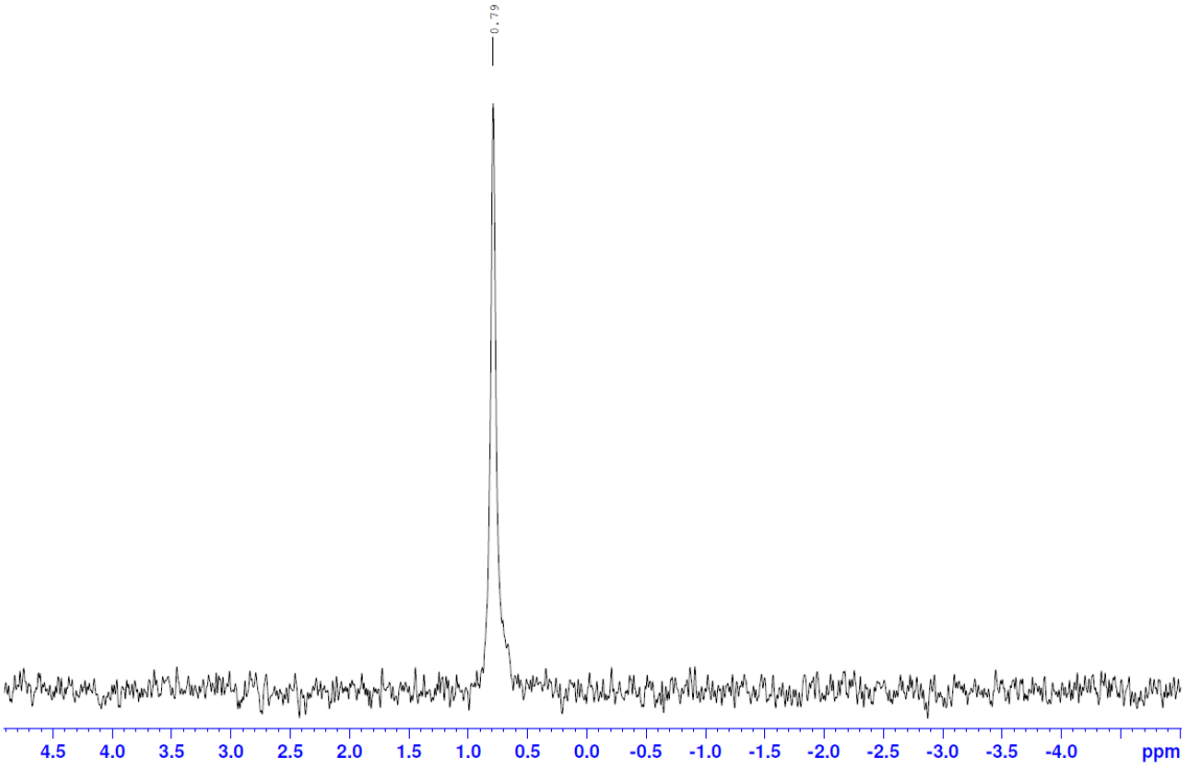

Figure 81 ^{7}Li NMR spectrum of compound **2f** in D_8-THF

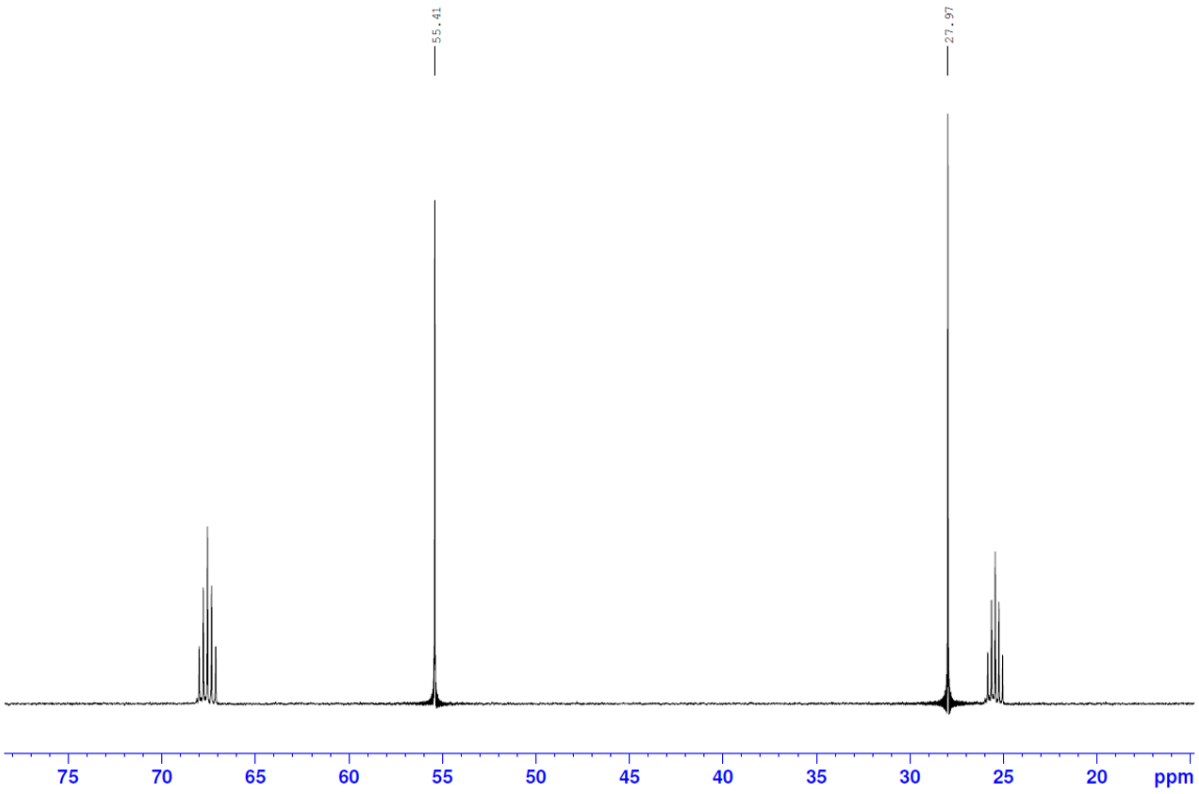

Figure 82 $^{13}C\{^{1}H\}$ NMR spectrum of compound **2f** in D_8-THF

Lithium 2,6-dimethylpiperidide (**2g**) Spectral data were in accord with published data[16]

^{1}H-NMR (400.1 MHz, D_8-THF, 300 K): δ / ppm 3.06–2.95 (2H, m, C*H*), 2.16–2.06 (1H, m, C*H*), 1.91–1.82 (1H, m, C*H*), 1.83–1.73 (2H, m, CH_2), 0.94–0.80 (2H, m, CH_2)

^{7}Li-NMR (155.5 MHz, D_8-THF, 300 K): δ / ppm 0.39 (*Li*-NPh$_2$).

Lithium diphenylamide (**2h**)

^{1}H-NMR (300.1 MHz, D_8-THF, 300 K): δ / ppm 6.79 (br. t, 4H, C-H_{meta}), 6.68 (br. d, 4H, C-H_{ortho}), 6.13 (br. t, 2H, C-H_{para}).

^{7}Li-NMR (116.6 MHz, D_8-THF, 300 K): δ / ppm 0.39 (*Li*-NPh$_2$).

^{13}C{^{1}H}-NMR (75.5 MHz, D_8-THF, 300 K): δ / ppm 159.6 (C_q-N), 128.7 (C_{meta}-H), 119.4 (C_{ortho}-H), 112.3 (C_{para}-H).

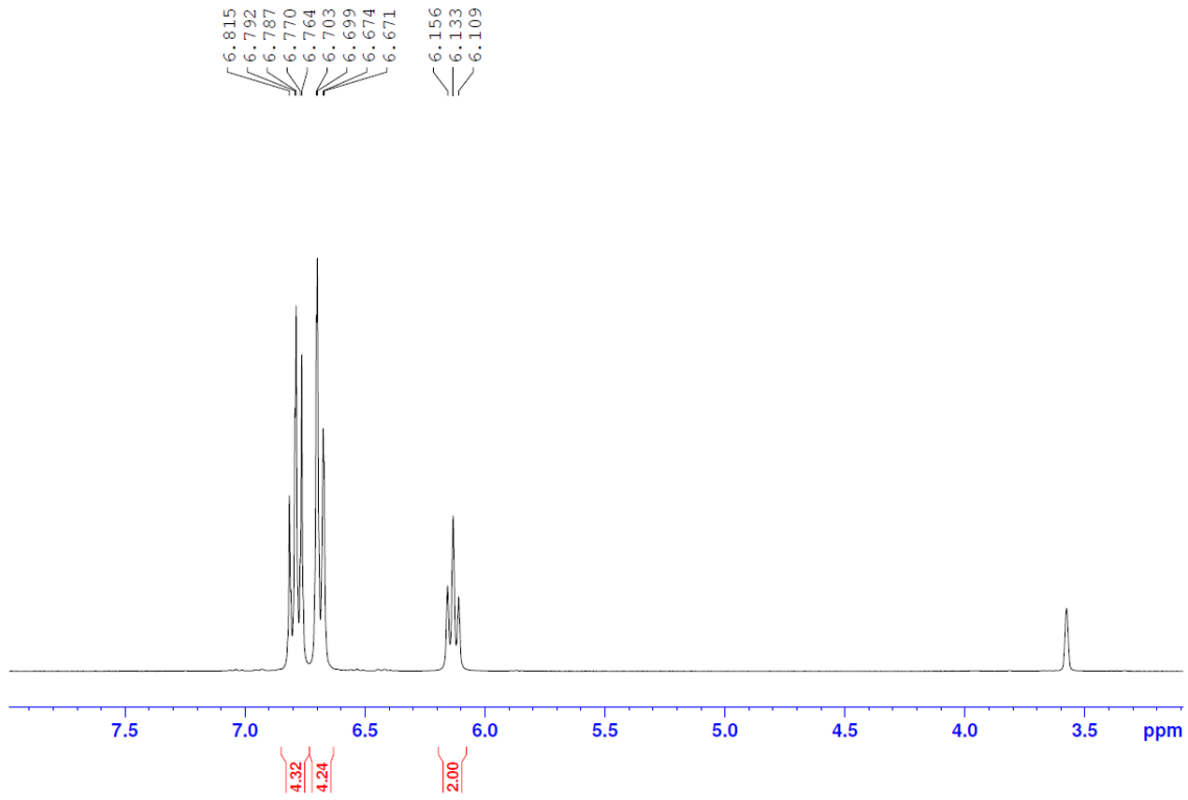

Figure 83 ^{1}H NMR spectrum of compound **2h** in D_8-THF

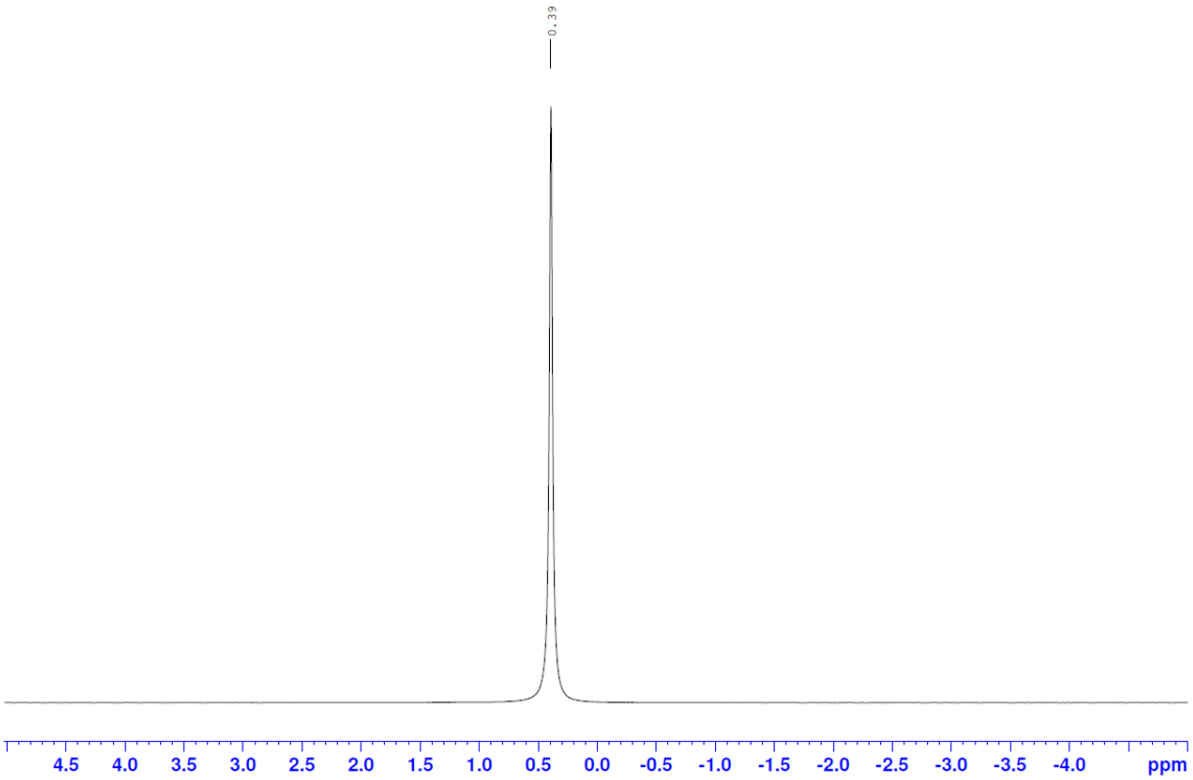

Figure 84 ^{7}Li NMR spectrum of compound **2h** in D_8-THF

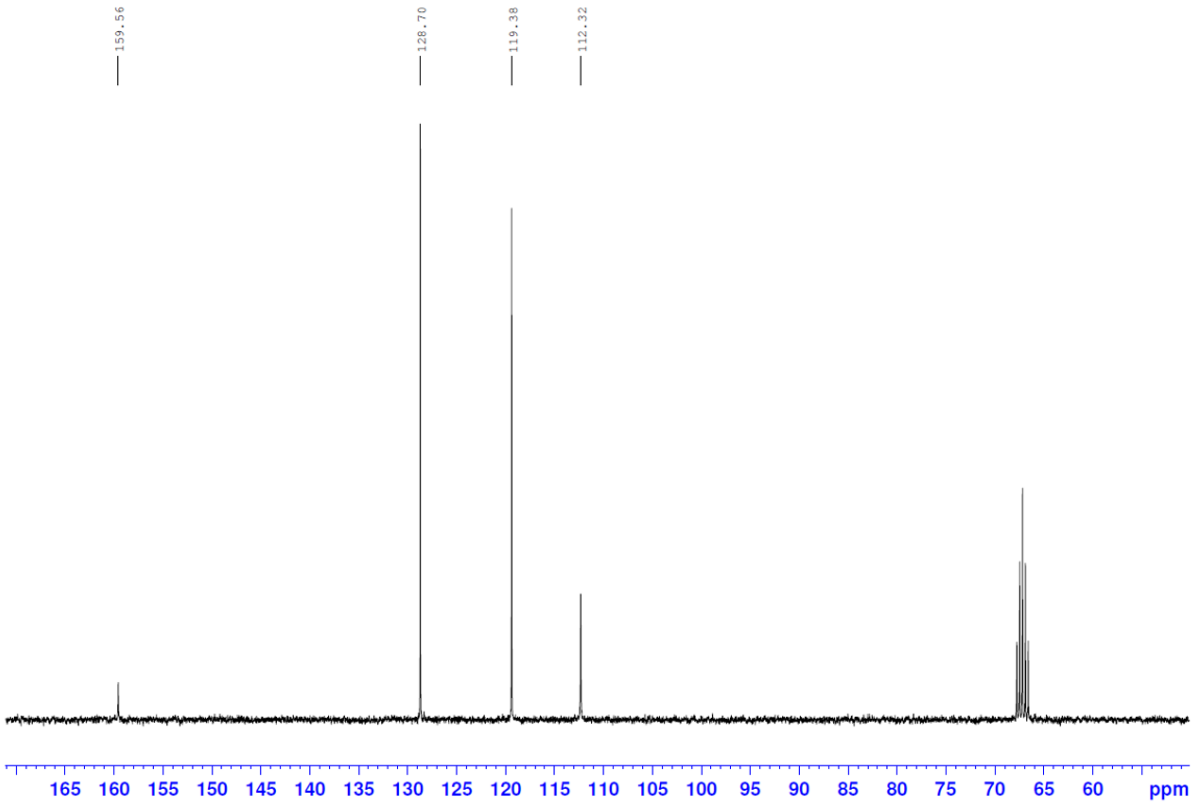

Figure 85 $^{13}C\{^{1}H\}$ NMR spectrum of **2h** in D_8-THF

Synthesis and Characterisation of Crystalline Compounds - Lithium Amides (**2b-*S*$_4$**, **2h-*S*$_3$** and **2i-*S*$_2$**) and of [{LiNPh$_2$}(O=CPh(NMe$_2$)]$_2$ (**8**)

Lithium anilide (**2b-*S*$_4$**)

To an argon-flushed Schlenk flask, 2 mmoles (0.2 mL) of aniline was added to 23 mL of dry hexane. To this, an equimolar amount of *n*BuLi (1.26 mL, 1.6 M in hexane) was added affording a thick, white suspension. The suspension was stirred at room temperature for 1 hour and then solubilized with the addition of 2.5mL of dry 2-MeTHF and gentle heating. Cooling the solution to -18°C over a period of 24 hours afforded a crop of colourless crystals in a 21% yield.

^{1}H-NMR (300.1 MHz, D$_8$-THF, 300 K): δ / ppm 6.76 (t, 2H, C-*H*$_{meta}$), 6.35 (d, 2H, C-*H*$_{ortho}$), 6.13 (t, 1H, C-*H*$_{para}$), 3.9-3.6 (br. m, N-*H*, 2x *H*$_α$, 2-MeTHF + C-*H*, 2-MeTHF), 1.93 (m, 1x *H*$_β$, 2-MeTHF), 1.82 (m, 1x *H*$_β$ + 1x *H*γ, 2-MeTHF), 1.32 (m, 1x *H*γ of 2-MeTHF), 1.13 (d, C*H*$_3$, 2-MeTHF).

^{7}Li-NMR (116.6 MHz, D$_8$-THF, 300 K): δ / ppm 0.82 (*Li*-N(H)Ph).

^{13}C{^{1}H}-NMR (75.5 MHz, D$_8$-THF, 300 K): δ / ppm 165.4 (*C*$_q$-N), 129.1 (*C*$_{meta}$-H), 116.4 (*C*$_{ortho}$-H), 108.2 (*C*$_{para}$-H), 75.7 (*C*(H)CH$_3$, 2-MeTHF), 68.1 (O*C*H$_2$, 2-MeTHF), 34.0 (*C*γ-H$_2$, 2-MeTHF), 26.7 (*C*$_β$-H$_2$, 2-MeTHF), 21.4 (*C*H$_2$, 2-MeTHF).

*Ratio of 2-MeTHF to **2b** varies from the solid state structure – 2-MeTHF could have been partially removed under reduced pressure during isolation of crystalline material.

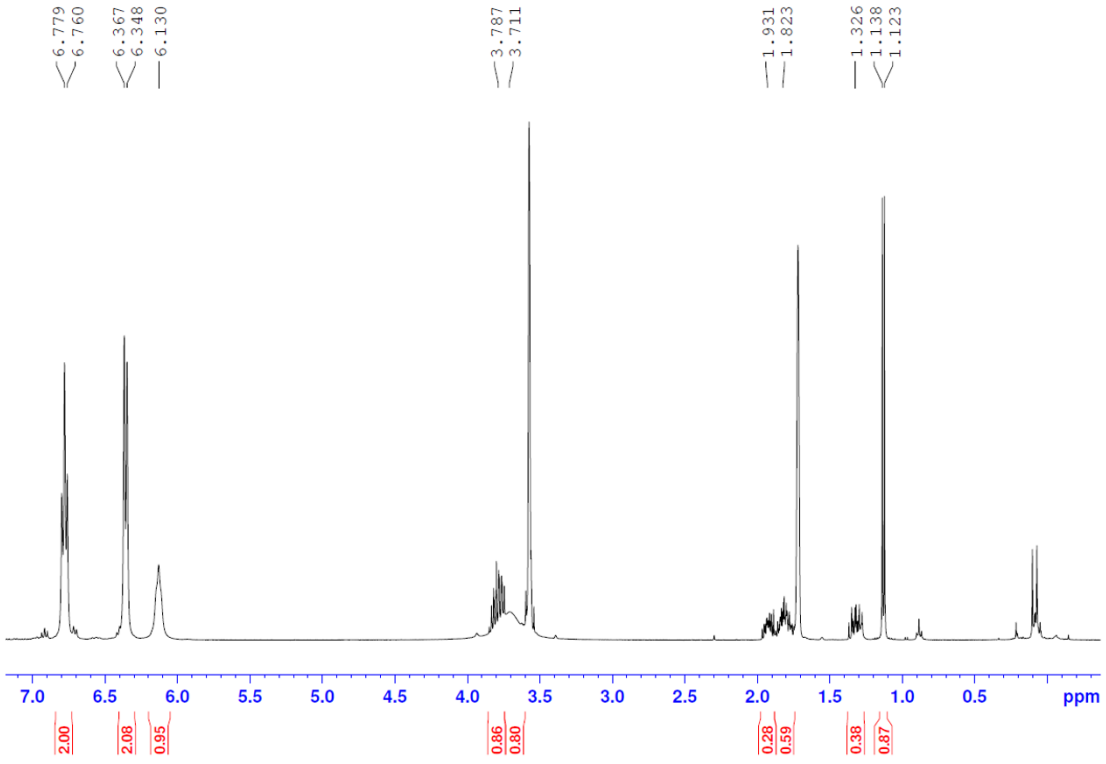

Figure 86 ^{1}H NMR spectrum of compound **2b-*S*$_4$** in D$_8$-THF

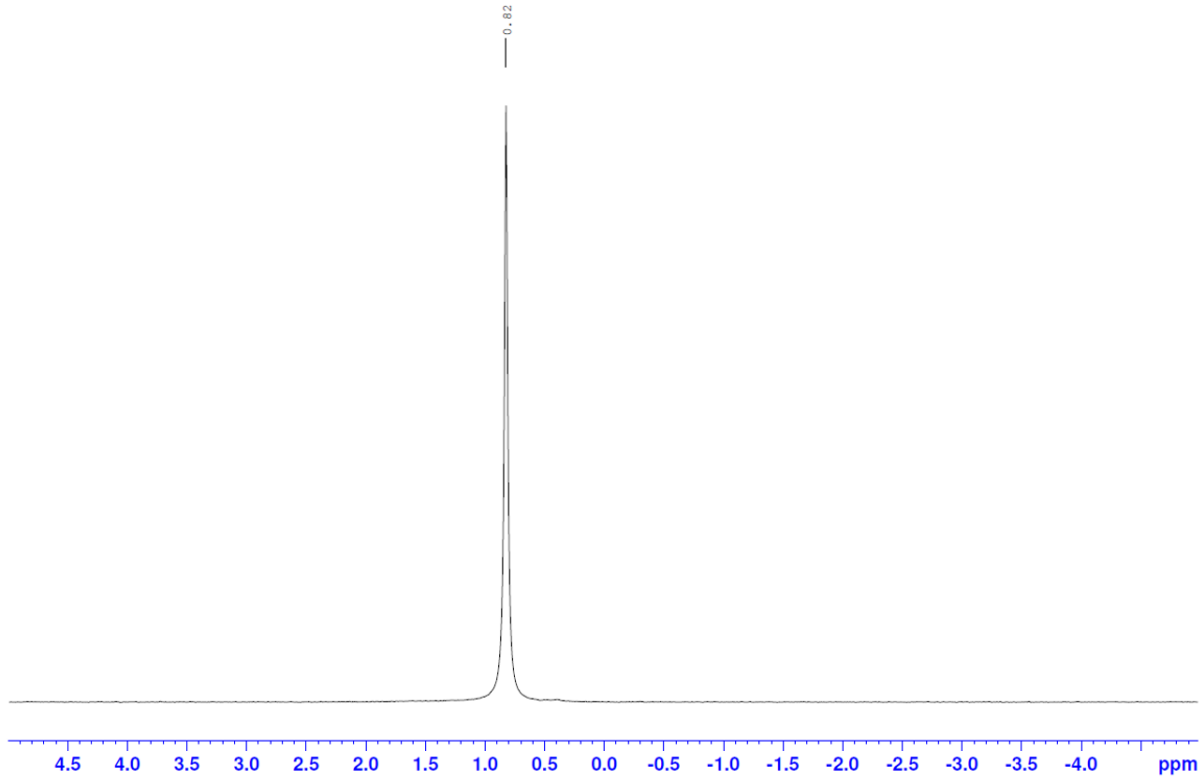

Figure 87 ^{7}Li NMR spectrum of compound **2b-*S*$_4$** in D_8-THF

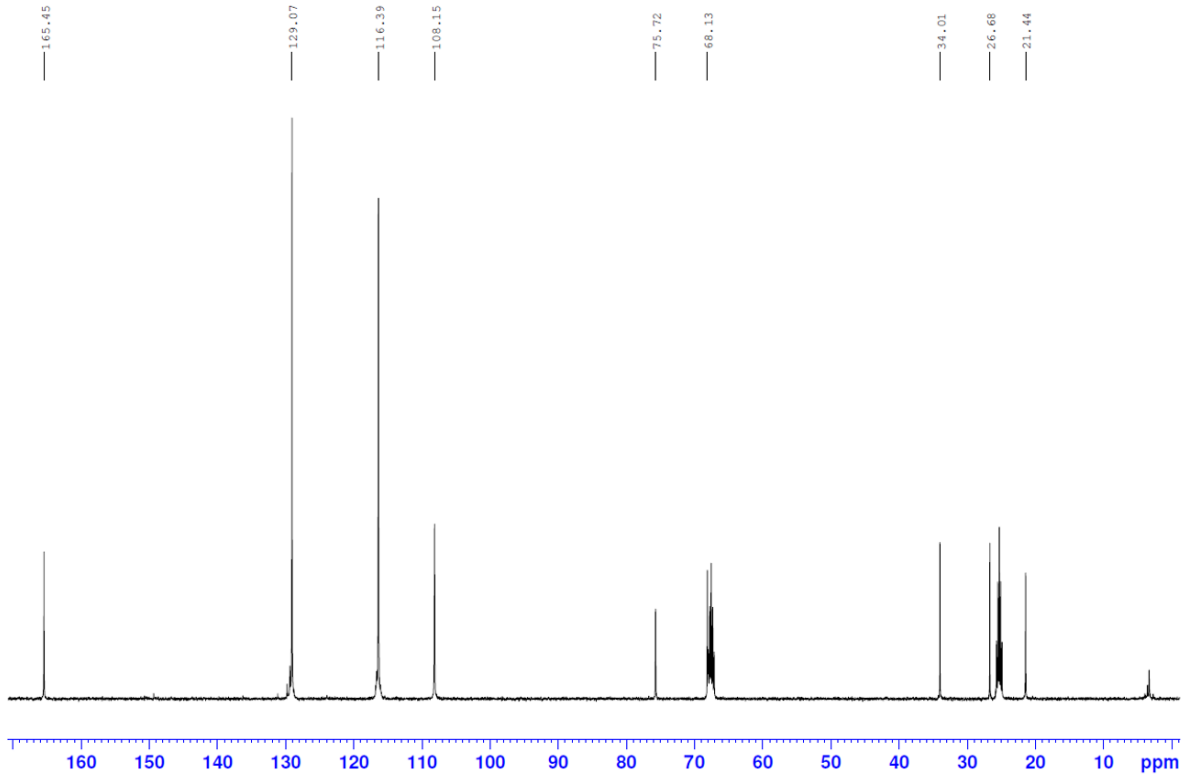

Figure 88 ^{13}C{^{1}H} NMR spectrum of compound **2b-*S*$_4$** in D_8-THF

Lithium diphenylamide (**2h-S_3**)

To an argon-flushed Schlenk flask, 2 mmol (340 mg) of diphenylamine was added to 23 mL of dry hexane. To this, an equimolar amount of *n*BuLi (1.26 mL, 1.6 M in hexane) was added affording a thick, white suspension. The suspension was stirred at room temperature for 1 hour and then solubilized with the addition of 0.3 mL of dry 2-MeTHF and gentle heating. Cooling the solution to -33°C over a period of 24 hours afforded a crop of colourless crystals in a 54% yield.

^{1}H-NMR (300.1 MHz, D_8-THF, 300 K): δ / ppm 6.84 (br. t, 4H, C-H_{meta}), 6.74 (br. d, 4H, C-H_{ortho}), 6.18 (br. t, 2H, C-H_{para}), 3.89-3.78 (br. m, 2x H_α, 2-MeTHF), 3.60 (CH_3, 2-MeTHF), 1.93 (m, 1x H_β, 2-MeTHF), 1.83 (m, 1x H_β + 1x $H\gamma$, 2-MeTHF), 1.35 (m, 1x $H\gamma$ of 2-MeTHF), 1.17 (d, CH_3, 2-MeTHF).

^{7}Li-NMR (116.6 MHz, D_8-THF, 300 K): δ / ppm 0.39 (*Li*-NPh_2).

^{13}C{^{1}H}-NMR (75.5 MHz, D_8-THF, 300 K): δ / ppm 159.4 (C_q-N), 128.7 (C_{meta}-H), 119.3 (C_{ortho}-H), 112.4 (C_{para}-H), 75.4 (*C*(H)CH_3, 2-MeTHF), 67.7 (OCH_2, 2-MeTHF), 33.7 ($C\gamma$-H_2, 2-MeTHF), 26.3 (C_β-H_2, 2-MeTHF), 21.1 (CH_2, 2-MeTHF).

*Ratio of 2-MeTHF to **2h** varies from the solid state structure – 2-MeTHF could have been partially removed under reduced pressure during isolation of crystalline material.

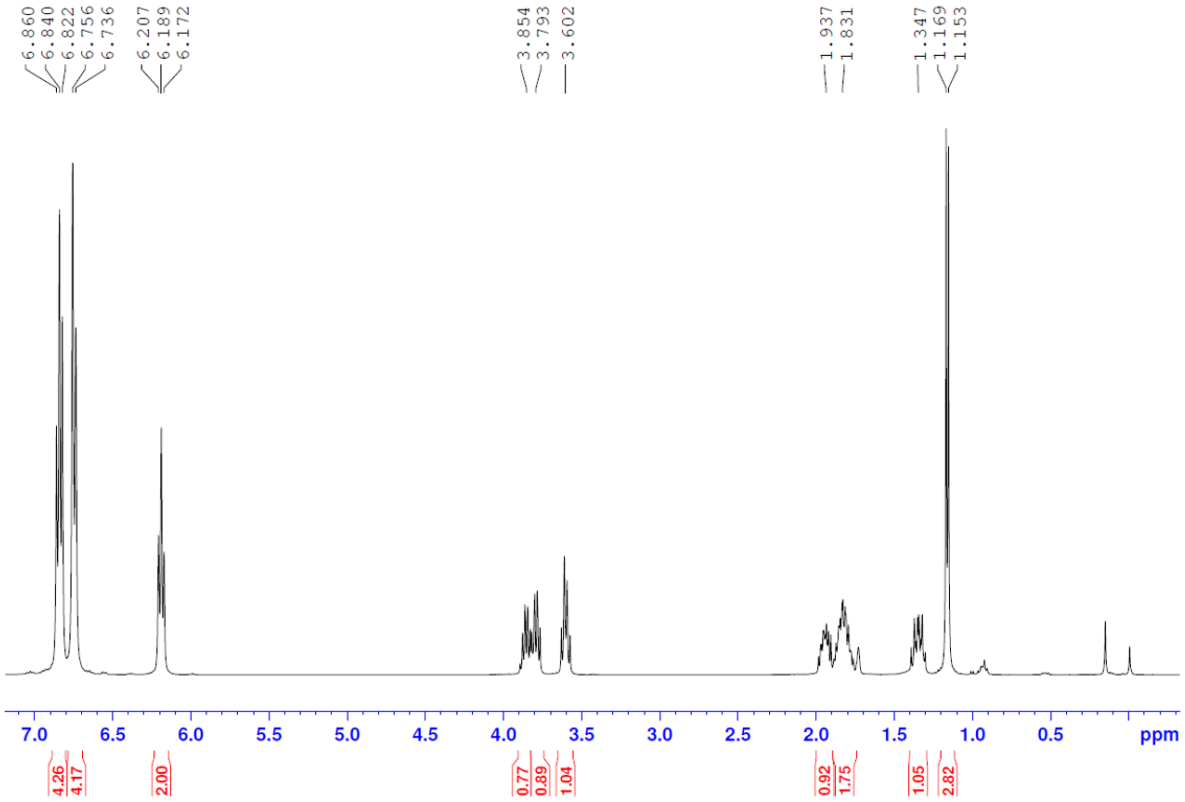

Figure 89 ^{1}H NMR spectrum of compound **2h-S_3** in D_8-THF

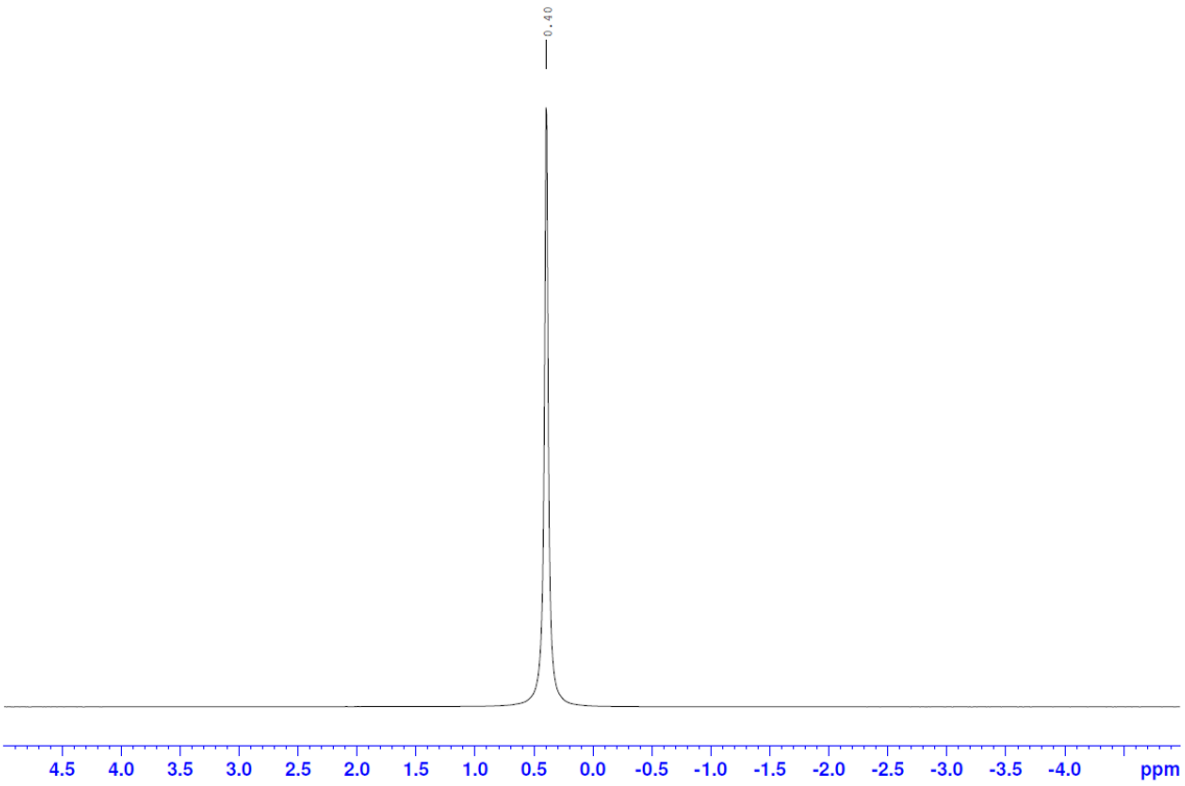

Figure 90 ^{7}Li NMR spectrum of compound **2h-*S*$_3$** in D_8-THF

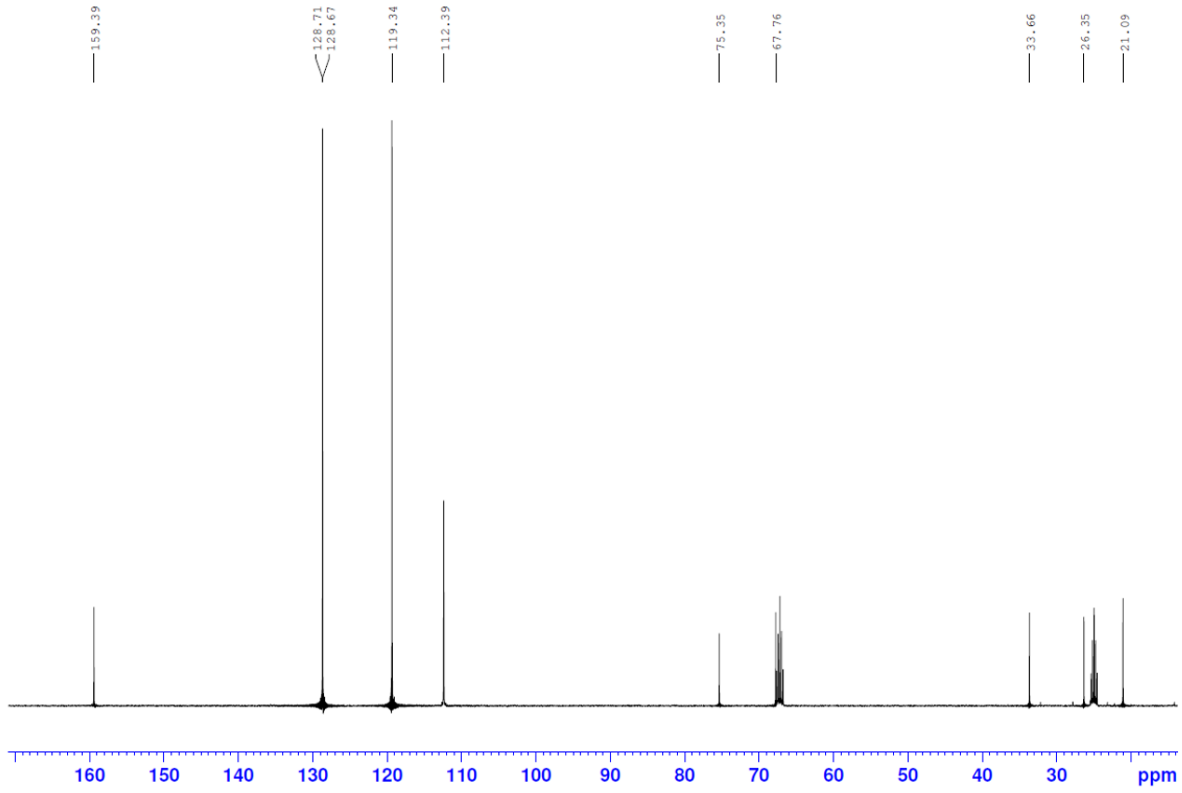

Figure 90 $^{13}C\{^{1}H\}$ NMR spectrum of compound **2h-*S*$_3$** in D_8-THF

Lithium bipyridylamide (**2i-*S*$_4$**)

To an argon-flushed Schlenk flask, 2 mmol (342 mg) of 2,2'-bipyridylamine was added to 5 mL of dry hexane. To this, an equimolar amount of *n*BuLi (0.63 mL, 1.6 M in hexane) was added affording a thick, white suspension. The suspension was stirred at room temperature for 1 hour and then solubilized with the addition of 10 mL of dry 2-MeTHF and gentle heating. Cooling the solution to -18°C over a period of 24 hours afforded a crop of colourless crystals in 66% yield. Due to limited solubility in D_8-THF, full spectroscopic characterisation was conducted in pyridine-D_5.

^{1}H-NMR (400.1 MHz, D_5-Py, 300 K): δ / ppm 8.22 (br. d, 1H, C_{Ar}-*H*), 7.50 (br. d, 1H, C_{Ar}-*H*), 7.41 (br. t, 1H, C_{Ar}-*H*), 6.45 (br. t, 1H, C_{Ar}-*H*), 3.87 (br. m, 2x H_α, 2-MeTHF), 3.62 (CH_3, 2-MeTHF), 1.82 (m, 1x H_β, 2-MeTHF), 1.70 (m, 1x H_β + 1x $H\gamma$, 2-MeTHF), 1.27 (m, 1x $H\gamma$ of 2-MeTHF), 1.18 (br. m, CH_3, 2-MeTHF).

^{7}Li-NMR (155.5 MHz, D_5-Py, 300 K): δ / ppm 3.85 (*Li*-NPy_2).

^{13}C{^{1}H}-NMR (100.6 MHz, D_5-Py, 300 K): δ / ppm 165.1 (C_q-Li), 147.7 (C_{Ar}-H), 137.1 (C_{Ar}-H), 118.1 (C_{Ar}-H), 110.6 (C_{Ar}-H), 75.6 (*C*(H)CH_3, 2-MeTHF), 66.1 (O*C*H_2, 2-MeTHF), 33.8 ($C\gamma$-H_2, 2-MeTHF), 26.6 (C_β-H_2, 2-MeTHF), 21.7 (CH_2, 2-MeTHF).

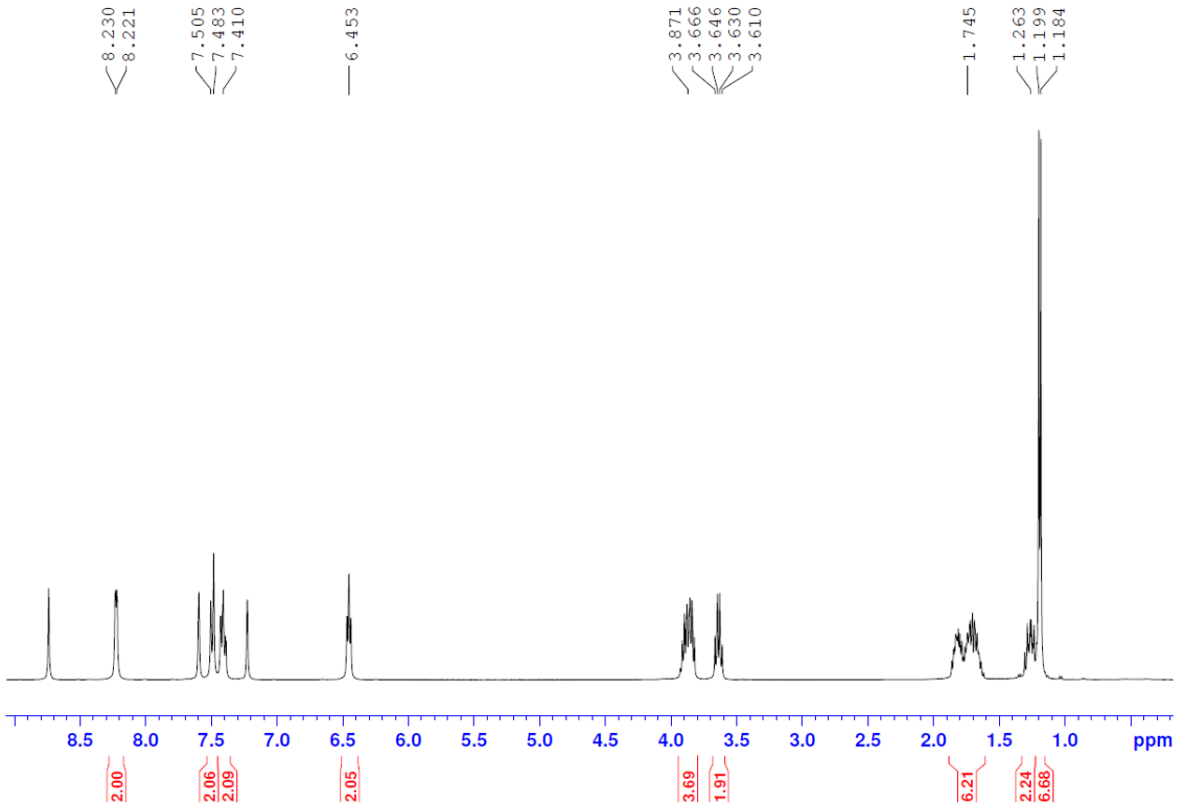

Figure 91 ^{1}H NMR spectrum of compound **2i-*S*$_4$** in D_5-Py

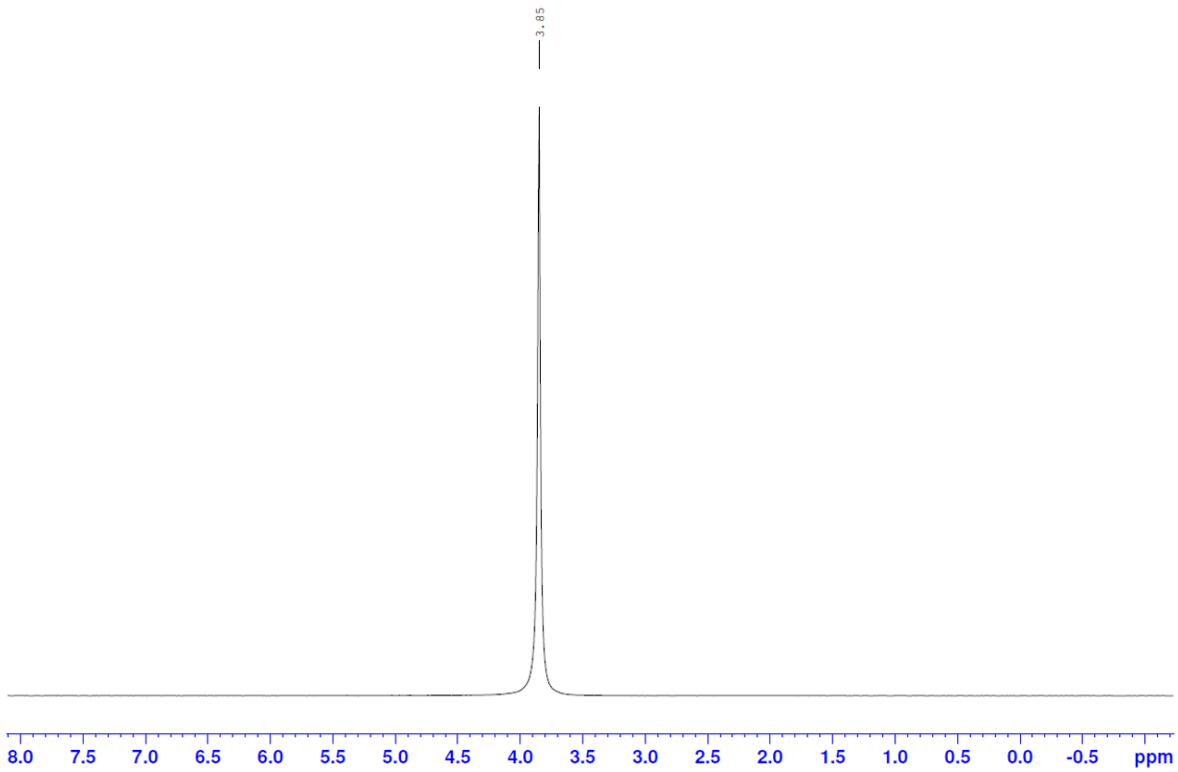

Figure 92 ^{7}Li NMR spectrum of compound **2i-*S4*** in D_5-Py

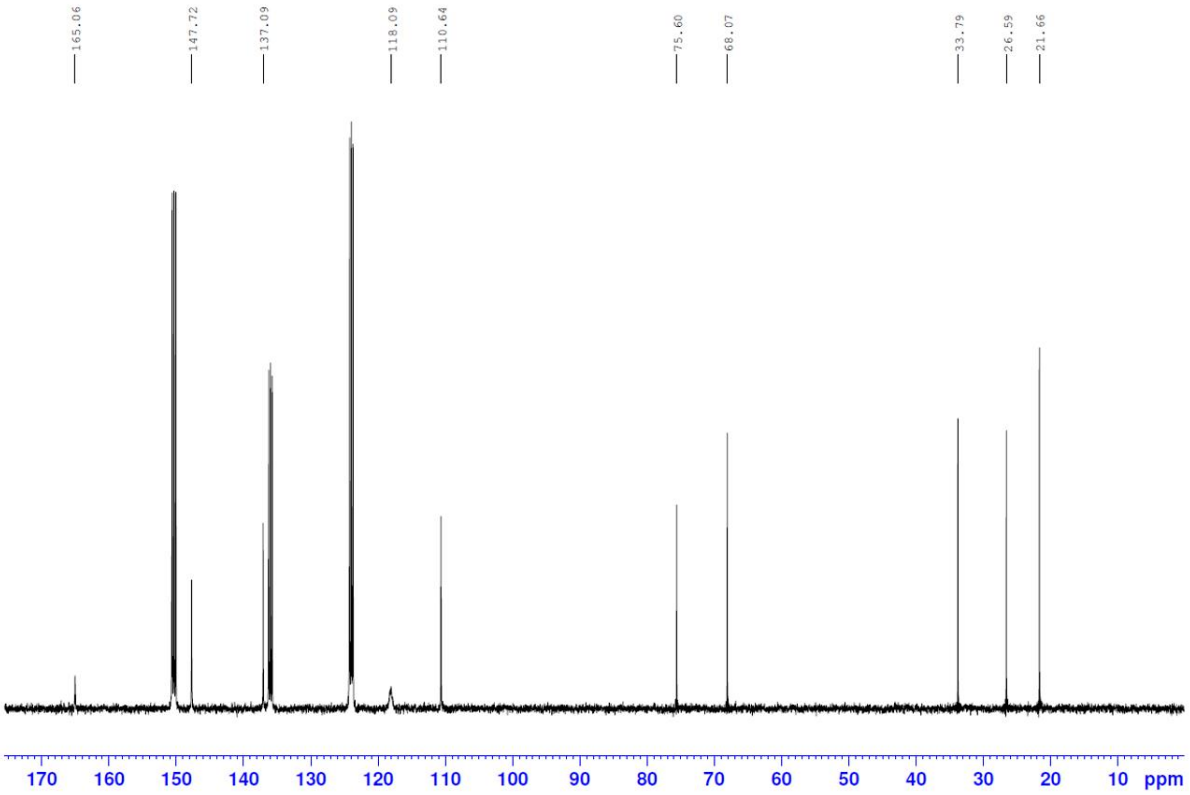

Figure 93 $^{13}C\{^{1}H\}$ NMR spectrum of compound **2i-*S2*** in D_5-Py

[{LiNPh$_2$}(O=CPh(NMe$_2$)]$_2$ (**8**)

In an argon-flushed Schlenk flask, 1 mmol (169 mg) of diphenylamine was dissolved 5 mL of dried toluene with subsequent addition of 1 mmol (0.63 mL, 1.6 M in hexane) of *n*BuLi at room temperature, affording a white suspension of LiNPh$_2$ (**2h**). After stirring the suspension for 1 hour at room temperature, 1 mmol (149 mg) of *N,N*-dimethylbenzamide was added giving a light-yellow suspension after addition, followed by precipitation of a yellow suspension. The mixture was stirred at room temperature for a further 10 minutes before gentle heating was applied to regain the light yellow solution. Slow cooling to room temperature produced a crop of colourless crystals which by X-ray diffraction analysis proved to be compound **8**. Yield: 260 mg, 40%.

^{1}H-NMR (300.1 MHz, D$_8$-Tol, 300 K): δ / ppm 7.15-7.05 (m, 5H, C$_{Ar}$-*H*, PhC(=O)NMe$_2$ + D$_8$-Tol), 7.03-6.92 (m, 2H, C-*H*$_{ortho}$, LiNPh$_2$ + D$_8$-Tol), 6.85 (m, 2H, C-*H*$_{meta}$, LiNPh$_2$), 6.68 (m, 1H, C-*H*$_{para}$, LiNPh$_2$), 2.32 (br. s, 3H, C*H*$_3$, PhC(=O)N*Me*$_2$), 2.02 (br. s, 3H, C*H*$_3$, PhC(=O)N*Me*$_2$).

^{7}Li-NMR (116.6 MHz, D$_8$-Tol, 300 K): δ / ppm 1.91 ([*Li*-NPh$_2$·PhC(=O)NMe$_2$]$_2$).

*Attempts to achieve ^{13}C{^{1}H} NMR spectrum in D$_8$-Tol were unsuccessful due to poor solubility in this solvent. Spectra recorded in D$_8$-THF reveals dissociation of PhC(=O)NMe$_2$ from LiNPh$_2$ – see **Figure 95**, **Figure 99** and **Table 2**.

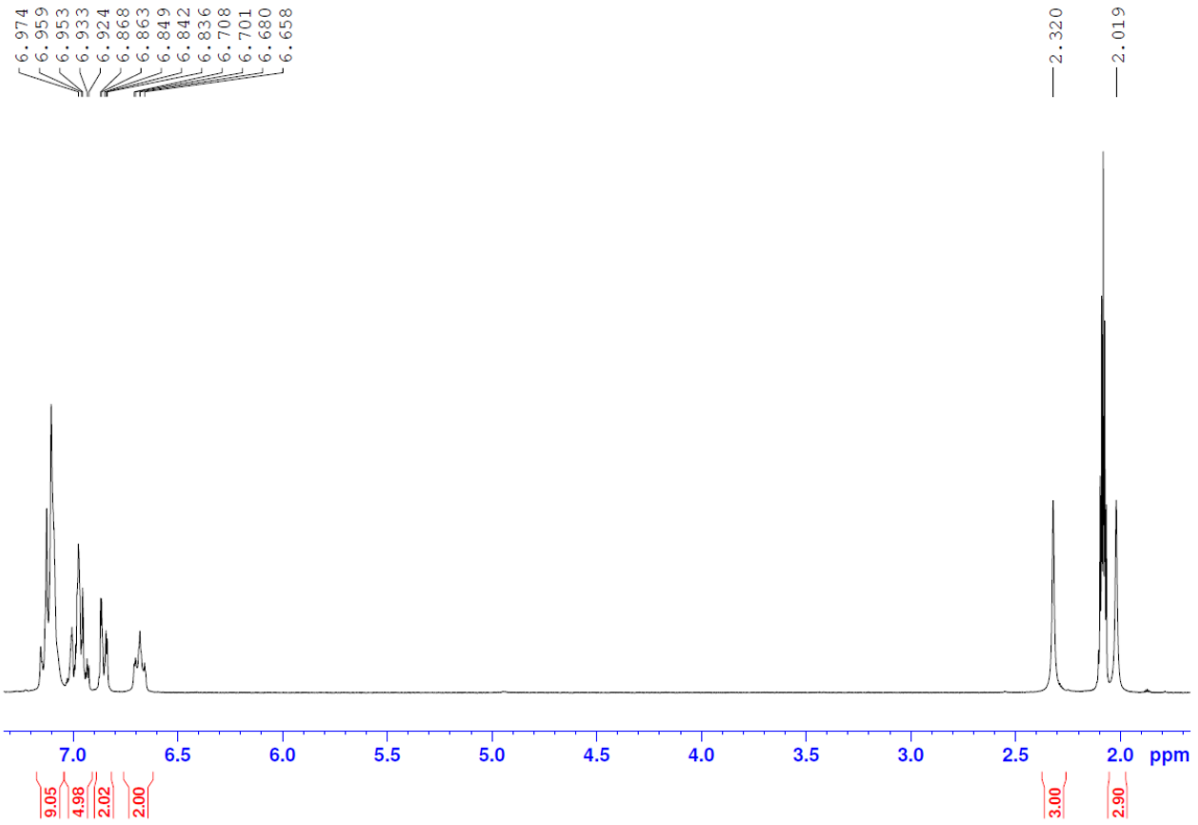

Figure 94 ^{1}H NMR spectrum of compound **8** in D$_8$-Tol

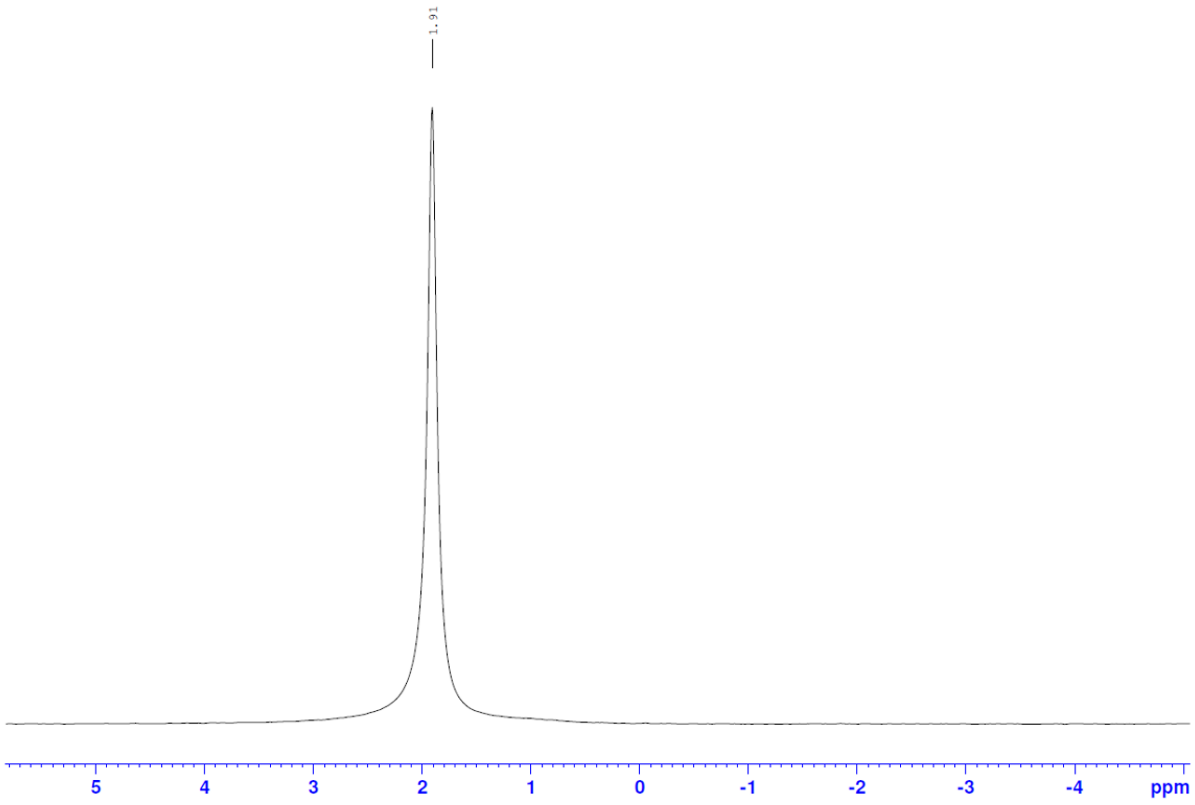

Figure 95 ^{7}Li NMR spectrum of compound **8** in D_8-Tol

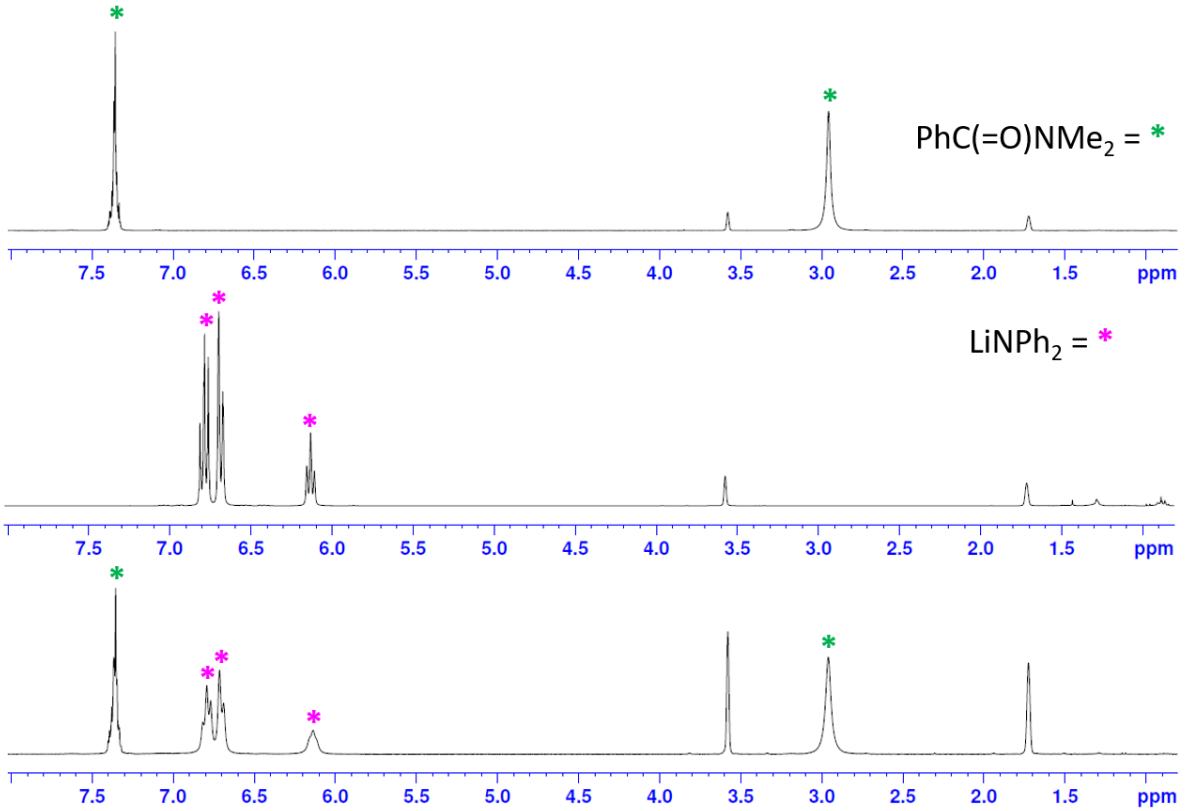

Figure 96 ^{1}H NMR spectrum of compound **8** in D_8-THF showing de-complexation into free LiNPh2 (**2h**) and PhC(=O)NMe2 (**7**) at room temperature

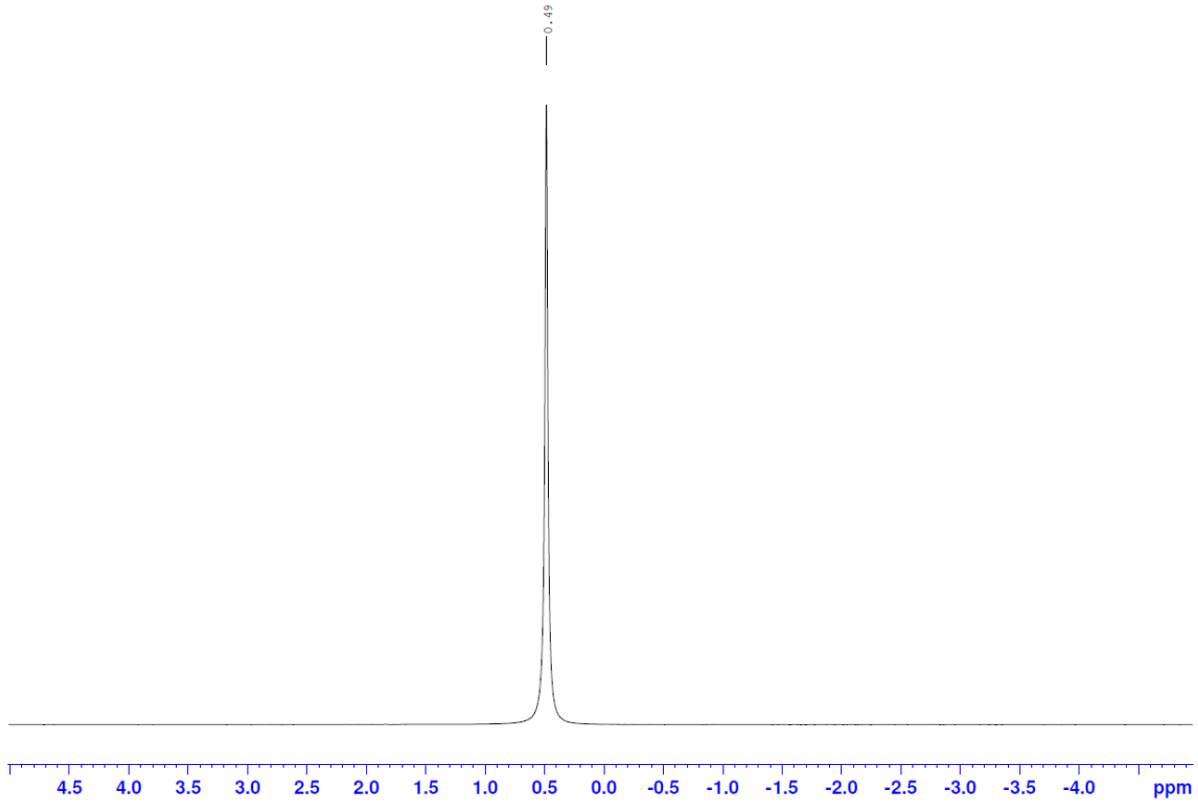

Figure 97 ^{7}Li NMR spectrum of compound **8** in D_8-THF

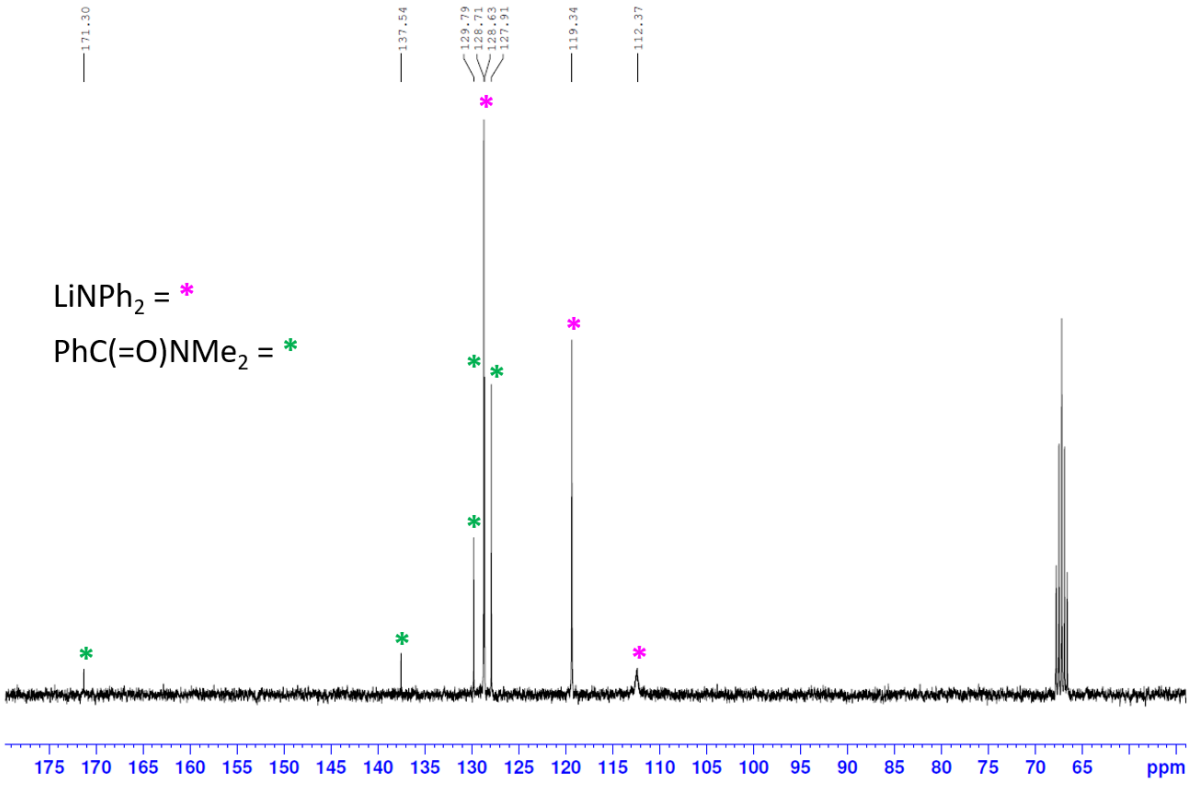

Figure 98 $^{13}C\{^{1}H\}$ NMR spectrum of compound **8** in D_8-THF

X-Ray Crystallographic Details

Crystallographic data for [{LiN(H)Ph}$_2$(2-MeTHF)$_4$] (**2b-*S*$_4$**) (CCDC 1973293), [{LiNPh$_2$}$_2$(2-MeTHF)$_3$] (**2h-*S*$_3$**) (CCDC 1973294), [{LiNPy$_2$}$_2$(2-MeTHF)$_2$] (**2i-*S*$_2$**) (CCDC 1973295) and [{LiNPh$_2$}(O=CPh(NMe$_2$)]$_2$ (**8**) (CCDC 1987696) were measured at 123 K for with an Oxford Diffraction Gemini S instrument and with graphite-monochromated Cu (λ=1.54180 Å) radiation. The structures were refined to convergence on F 2 using all unique reflections and programs from the SHELX family.[17] Selected crystallographic parameters are displayed in **Table 1**

*Due to significant disorder within the 2-MeTHF molecules, the crystallographic data for [{LiN(H)Ph}$_2$(2-MeTHF)$_4$] (**2b-*S*$_4$**) is used purely for connectivity purposes.

Table 1 Table of selected crystallographic parameters of compounds **2b-*S*$_4$, 2h-*S*$_3$, 2i-*S*$_2$** and **8**.

	[{LiN(H)Ph}$_2$(2-MeTHF)$_4$] (**2b-*S*$_4$**)	[{LiNPh$_2$}$_2$(2-MeTHF)$_3$] (**2h-*S*$_3$**)	[{LiNPy$_2$}$_2$(2-MeTHF)$_2$] (**2i-*S*$_2$**)	[{LiNPh$_2$}(O=CPh(NMe$_2$)]$_2$ (**8**)
CCDC Number	1973293	1973294	1973295	1987696
Empirical formula	$Li_2O_4N_2C_{32}H_{52}$	$Li_2O_4N_2C_{44}H_{60}$	$Li_2O_2N_6C_{30}H_{36}$	$C_{42}H_{42}Li_2N_4O_2$
Mol. Mass	542.63	694.82	526.53	648.67
Crystal system	Monoclinic	Monoclinic	Monoclinic	Triclinic
a/Å	9.0773(3)	10.2268(4)	9.7406(4)	9.5878(2)
b/Å	20.9604(6)	19.0435(7)	10.9189(4)	9.9347(2)
c/Å	9.2929(4)	10.7658(5)	14.1465(7)	9.9435(2)
α/°	90	90	90	105.659(2)
β/°	112.088(4)	102.453(4)	107.012(5)	94.8850(10)
γ/°	90	90	90	95.340(2)
V/Å^3	1638.34(11)	2047.35(15)	1438.74(11)	902.00(3)
Z	2	2	2	1
λ/Å	1.54184	1.54184	1.54184	1.54184
Measured reflections	7885	23108	10712	13772
Unique reflections	3103	7090	2857	3274
***R*int**	0.0313	0.0775	0.0786	0.03036
Observed rflns [I > 2σ(I)]	2523	6096	2274	3722
Goof	1.611	1.225	1.058	1.065
***R* [on *F*, obs rflns only]**	0.11252	0.0987	0.0591	0.0393
ω*R* [on *F*^{2}, all data]	0.3718	0.2948	0.1830	0.1120
Largest diff. peak/hole e/Å^{-3}	0.83/-0.61	0.72/-0.34	0.29/-0.26	0.18/-0.21

DOSY NMR Studies of $LiNPh_2$ (**2h**) with *N,N*-Dimethylbenzamide (**7**)

<u>D_8-Tol</u>

10 mg of compound **8** was added to 0.5 mL of D_8-Tol in a J. Young's NMR tube. Gentle heating was required for complete dissolution.

^{1}H DOSY NMR spectroscopic analysis reveals that $LiNPh_2$ and $PhC(=O)NMe_2$ remain as part of the same molecular entity in toluene solution with diffusion coefficients of $6.490x10^{-10}$ m^2/s and $6.554x10^{-10}$ m^2/s, respectively – **mean diffusion coefficient of $6.52x10^{-10}$ m^2/s.**

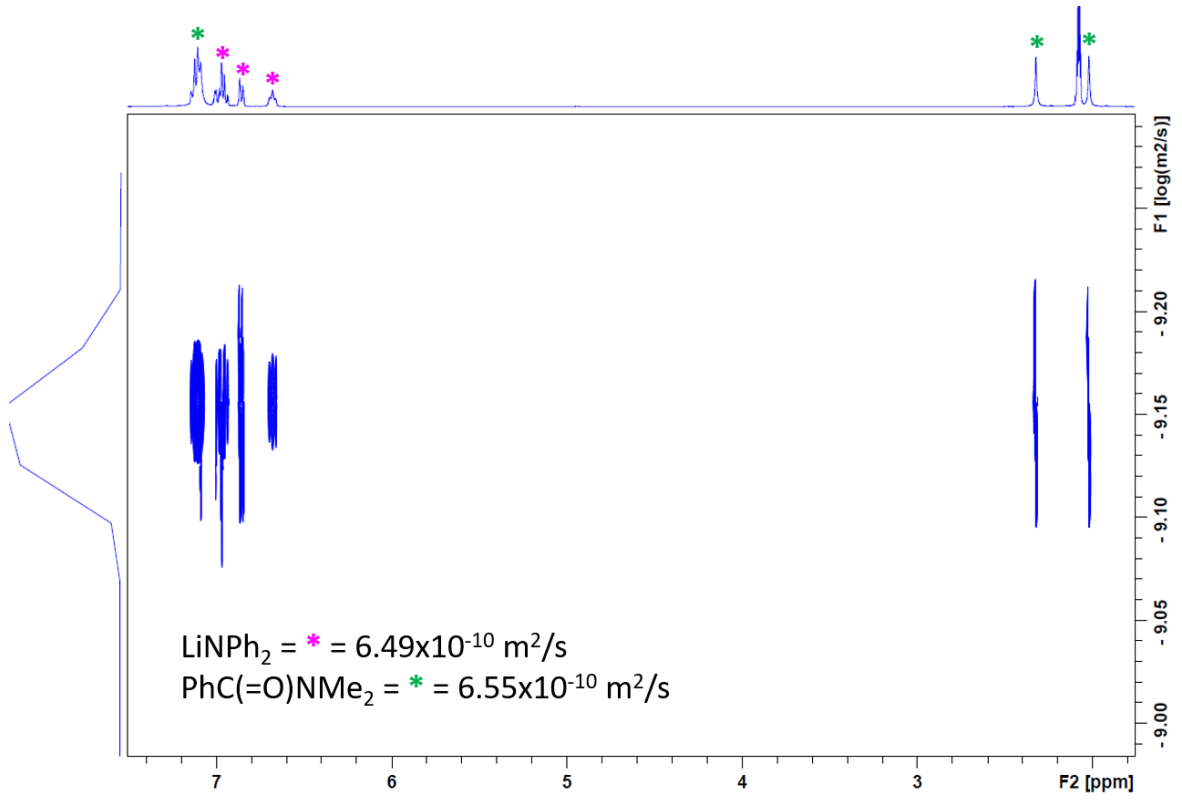

Figure 99 ^{1}H DOSY NMR spectrum of compound **8** in D_8-Tol

D_8-THF

In a J. Young's NMR tube, a 15 nM solution of $LiNPh_2$ (**2h**) and *N,N*-dimethylbenzamide in a 1:1 ratio was made in D_8-THF with tetramethylsilane (TMS) as a reference standard.[18]

^1H DOSY NMR spectroscopic analysis revealed that in bulk D_8-THF solution, $LiNPh_2$ and $PhC(=O)NMe_2$ do not remain part of the same molecular entity with independent diffusion coefficients of $7.638x10^{-10}$ m^2/s and $1.263x10^{-9}$ m^2/s. Measured and calculated against TMS ($1.627x10^{-9}$ m^2/s).

Table 2 Calculated molecular weights of $LiNPh_2$ and $PhC(=O)NMe_2$ from solution study in D_8-THF against TMS

	MW_{det} [g/mol]	MW_{calc} [g/mol]	MW_{diff} [%]
$LiNPh_2$ (*LiAS*$_3$) (**2h**)	363	391	8
Ph $C(=O)NMe_2$	153	149	-3

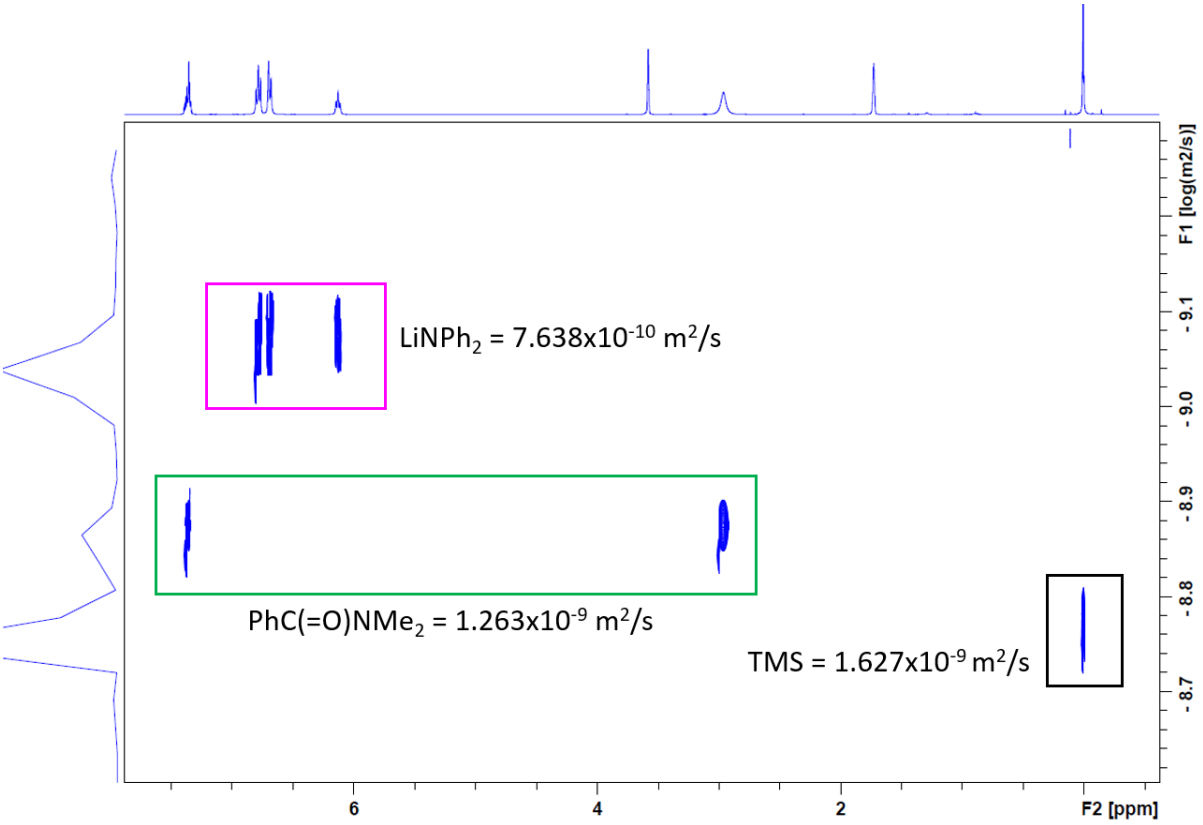

Figure 100 ^1H DOSY NMR spectrum of $LiNPh_2$ and $PhC(=O)NMe_2$ against TMS in D_8-THF

DOSY NMR Studies – 2-MeTHF

All DOSY NMR experiments in 2-MeTHF were conducted using the Internal Calibration Curve (ICC) method at 0.2 M concentration (0.5 mL 2-MeTHF) with 1,2,3,4-tetraphenylnapthalene (TPhN), 1-phenylnaphthalene (1-PhN) and tetramethylsilane (TMS) as inert, internal standards. A correlation between log D and log FW of the linear least-squares fit to the internal standards could be established in order to deduce the aggregation states of the lithium amides LiN(Me)Ph (**2a**), LiN(H)Ph (**2b**) and $LiNPh_2$ (**2h**) in 2-MeTHF. All lithium amide solids used for this study were prepared from hexane, in their non-solvated form.

LiN(Me)Ph (**2a**)

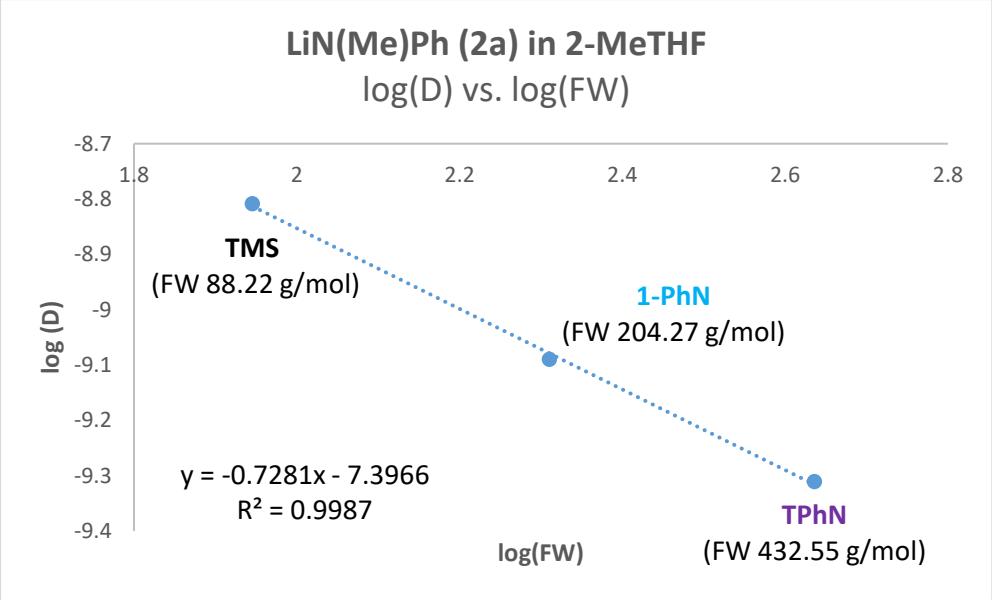

Figure 101 Graph of log(FW) vs. log(D) for solution-state study of LiN(Me)Ph (**2a**) in 2-MeTHF using ICC

Table 3 Formula weights and diffusion coefficients of 1-PhN, TPhN and TMS for ICC of LiN(Me)Ph (**2a**)

	FW [g/mol]	log(FW)	Diffusion Coefficient (D) [m^2/s]	log(D)
1-PhN	204.27	2.310205	$8.1447x10^{-10}$	-9.08912
TPhN	432.55	2.636036	$4.893x10^{-10}$	-9.31042
TMS	88.22	1.945567	$1.555x10^{-9}$	-8.80827
LiN(Me)Ph (**2a**)			$5.487x10^{-10}$	-9.2606

If y = -9.2606, then MW_{det} for LiN(Me)Ph = 363 g/mol.

MW_{calc} for $LiAS_3$ = 372 g/mol with error of 2%.

See **Table 6** for full details.

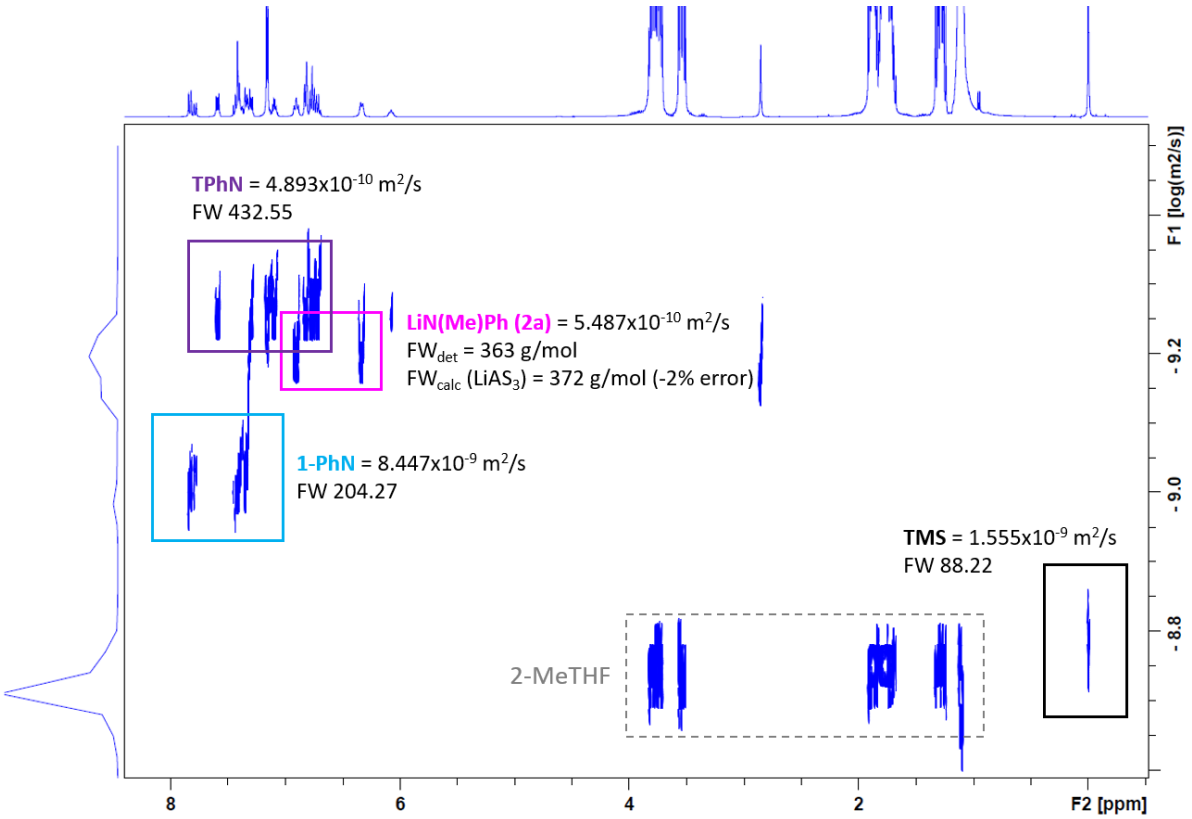

Figure 102 ^{1}H DOSY NMR spectrum of LiN(Me)Ph (**2a**) in 2-MeTHF against TMS, 1-PhN and TPhN

LiN(H)Ph (**2b**)

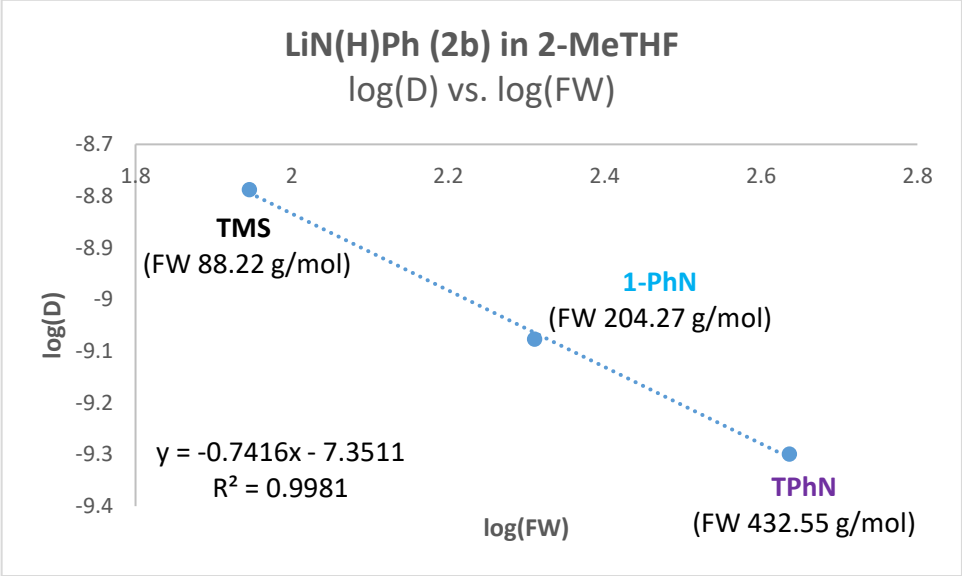

Figure 103 Graph of log(FW) vs. log(D) for solution-state study of LiN(H)Ph (**2b**) in 2-MeTHF using ICC

Table 4 Formula weights and diffusion coefficients of 1-PhN, TPhN and TMS for ICC of LiN(H)Ph (**2b**)

	FW [g/mol]	log(FW)	Diffusion Coefficient (D) [m^2/s]	log(D)
1-PhN	204.27	2.310205	$8.376x10^{-9}$	-9.07696
TPhN	432.55	2.636036	$5.022x10^{-10}$	-9.29912
TMS	88.22	1.945567	$1.63x10^{-9}$	-8.78781
LiN(H)Ph (**2b**)			$5.311x10^{-10}$	-9.2748

If y = -9.2748, then MW_{det} for LiN(H)Ph = 393 g/mol.

MW_{calc} for $LiAS_3$ = 357 g/mol with error of -9%.

See **Table 6** for full details.

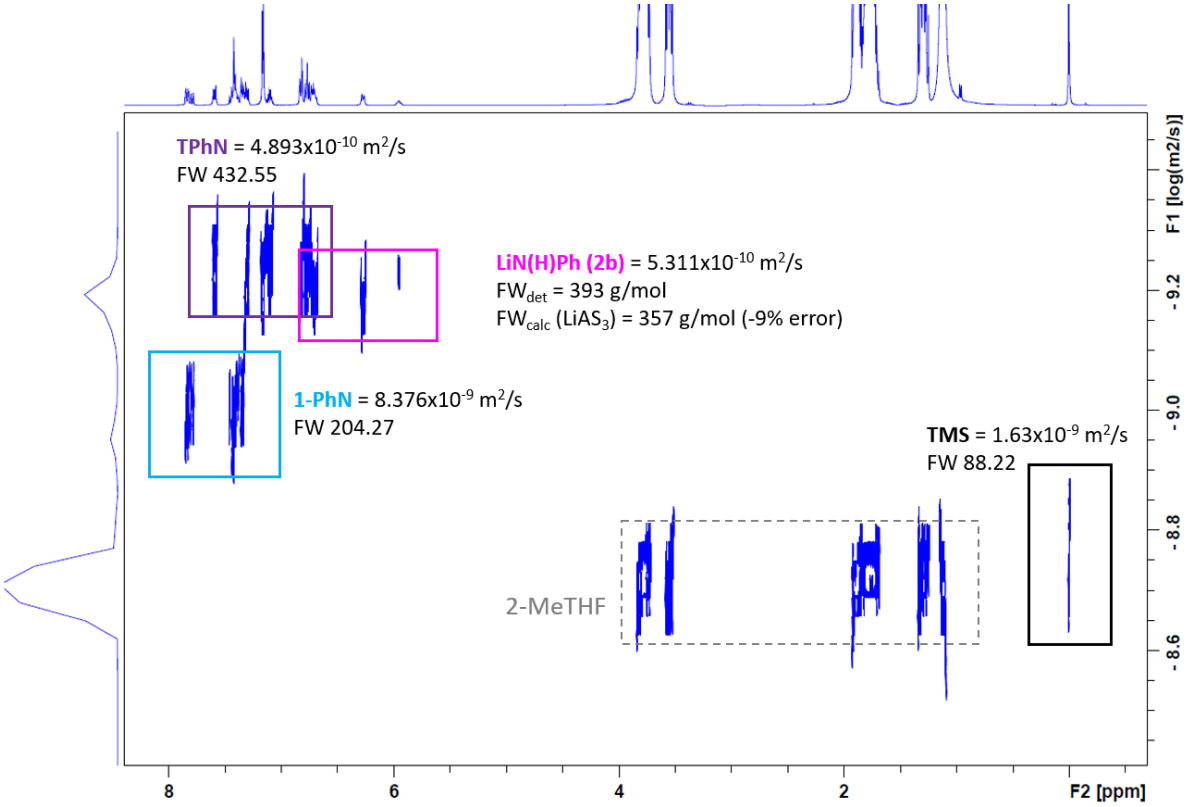

Figure 104 ^{1}H DOSY NMR spectrum of LiN(H)Ph (**2b**) in 2-MeTHF against TMS, 1-PhN and TPhN

LiNPh$_2$ (**2h**)

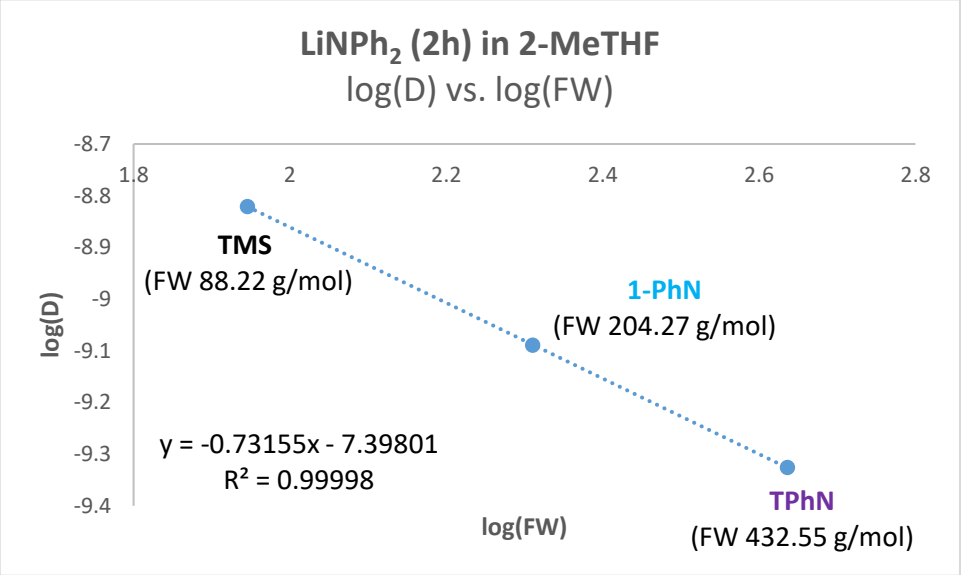

Figure 105 Graph of log(FW) vs. log(D) for solution-state study of LiNPh$_2$ (**2h**) in 2-MeTHF using ICC

Table 5 Formula weights and diffusion coefficients of 1-PhN, TPhN and TMS for ICC of LiNPh$_2$ (**2h**)

	FW [g/mol]	log(FW)	Diffusion Coefficient (D) [m^2/s]	log(D)
1-PhN	204.27	2.310205	8.143x10^{-9}	-9.08922
TPhN	432.55	2.636036	4.723x10^{-10}	-9.32578
TMS	88.22	1.945567	1.511x10^{-9}	-8.82074
LiNPh$_2$ (**2h**)			4.576x10^{-10}	-9.3395

If y = -9.3395, then MW$_{det}$ for LiNPh$_2$ = 451 g/mol.

MW$_{calc}$ for LiAS$_3$ = 434 g/mol with error of -4%.

See **Table 6** for full details.

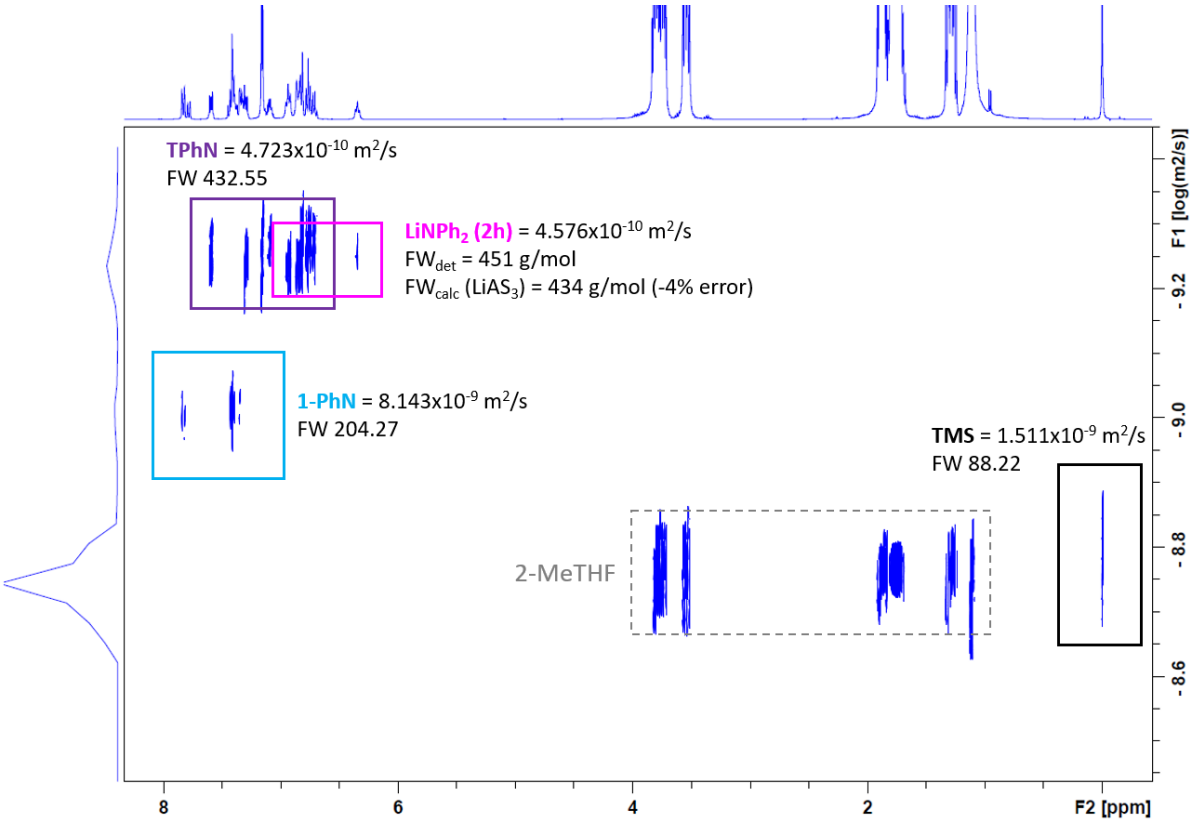

Figure 106 ^{1}H DOSY NMR spectrum of $LiNPh_2$ (**2h**) in 2-MeTHF against TMS, 1-PhN and TPhN

Table 6 Table of solution-state calculations for lithium amides **2a**, **2b** and **2h** in 2-MeTHF using Internal Calibration Curve (ICC)

Entry	Amide	Solvent	Diffusion coefficient Li-NR_2 [$x10^{-10}$ m^2/s]	Diffusion coefficient TMS [$x10^{-9}$ m^2/s]	Diffusion coefficient 1-PhN [$x10^{-9}$ m^2/s]	Diffusion coefficient TPhN [$x10^{-10}$ m^2/s]	MW_{det} [g/mol]	Structure	MW_{calc} [g/mol]	MW_{diff}
1	Li-N(Me)Ph (**2a**)	2-MeTHF	5.487	1.555	8.447	4.893	363	**$LiAS_3$**	**372**	**2%**
								$Li_2A_2S_2$	399	10%
								$LiAS_2$	285	-21%
								$Li_2A_2S_3$	486	33%
								$Li_2A_2S_4$	571	57%
2	Li-N(H)Ph (**2b**)	2-MeTHF	5.311	1.63	8.376	5.022	393	**$LiAS_3$**	**357**	**−9%**
								$Li_2A_2S_2$	370	-6%
								$LiAS_2$	271	−31%
								$Li_2A_2S_3$	457	16%
								$Li_2A_2S_4$	543	38%
3	Li-NPh_2 (**2h**)	2-MeTHF	4.576	1.511	8.143	4.723	451	**$LiAS_3$**	**434**	**-4%**
								$Li_2A_2S_2$	523	16%
								$LiAS_2$	347	-23%
								$Li_2A_2S_3$	609	35%
								$Li_2A_2S_4$	694	54%

DOSY NMR Studies – D_8-THF

All DOSY NMR experiments in D_8-THF were conducted using the External Calibration Curve (ECC) method at 15 nM (0.5 mL D_8-THF) as described by Stalke.[17] Using tetramethylsilane (TMS) as a reference standard, we have been able to approximate the aggregates of lithium amides LiN(Me)Ph (**2a**), LiN(H)Ph (**2b**) and $LiNPh_2$ (**2h**) as dissipated spheres and ellipsoids (DSE). All lithium amide solids used for this study were prepared from hexane, in their non-solvated form.

See **Table 7** for full details.

Jackman and Williard have studied the aggregation of lithium amides in solution and in the solid state, respectively.[19,20] Their studies support the feasibility of the found aggregates.

$$Li_2A_2S_2 \rightleftharpoons Li_2A_2S_3 \rightleftharpoons Li_2A_2S_4 \rightleftharpoons LiAS_2 \rightleftharpoons LiAS_3$$

Scheme 1 Aggregation of lithium amides in coordinating solvents according to Jackman and Williard[19,20]

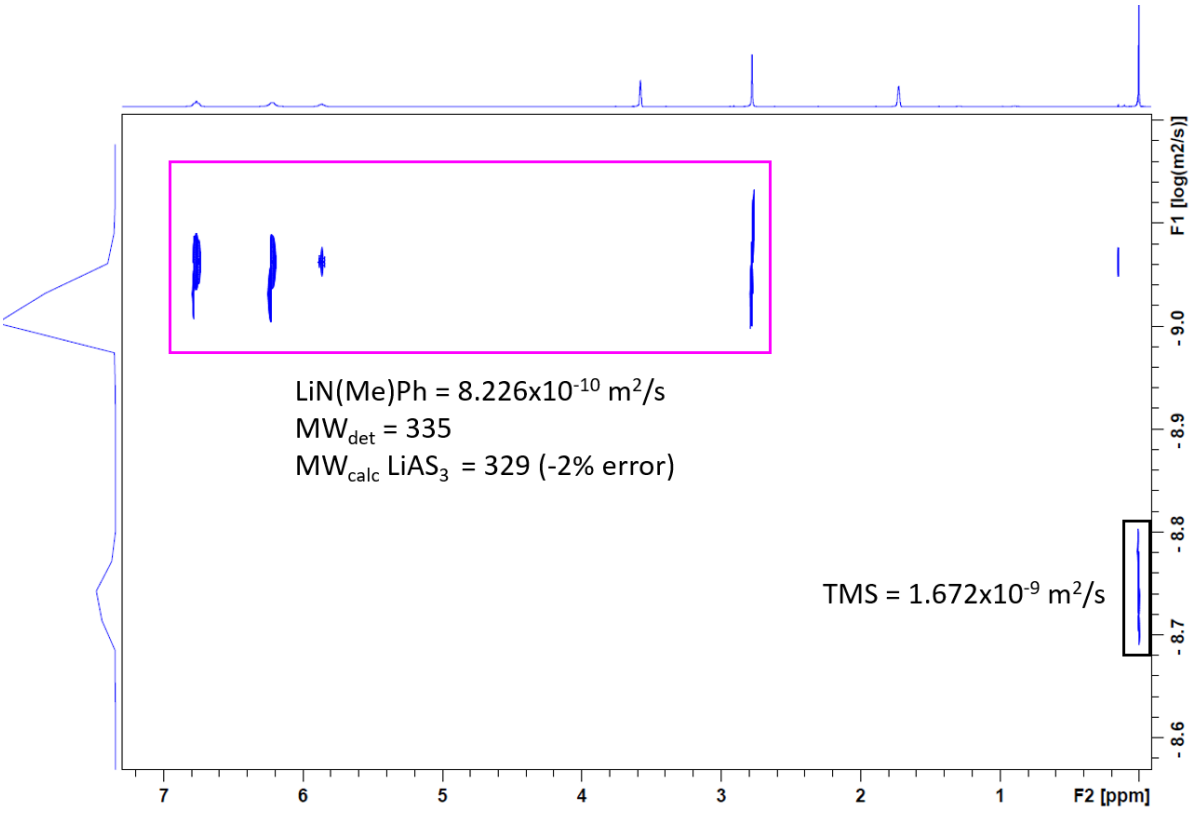

Figure 107 ^{1}H DOSY NMR spectrum of LiN(Me)Ph (**2a**) in D_8-THF against TMS

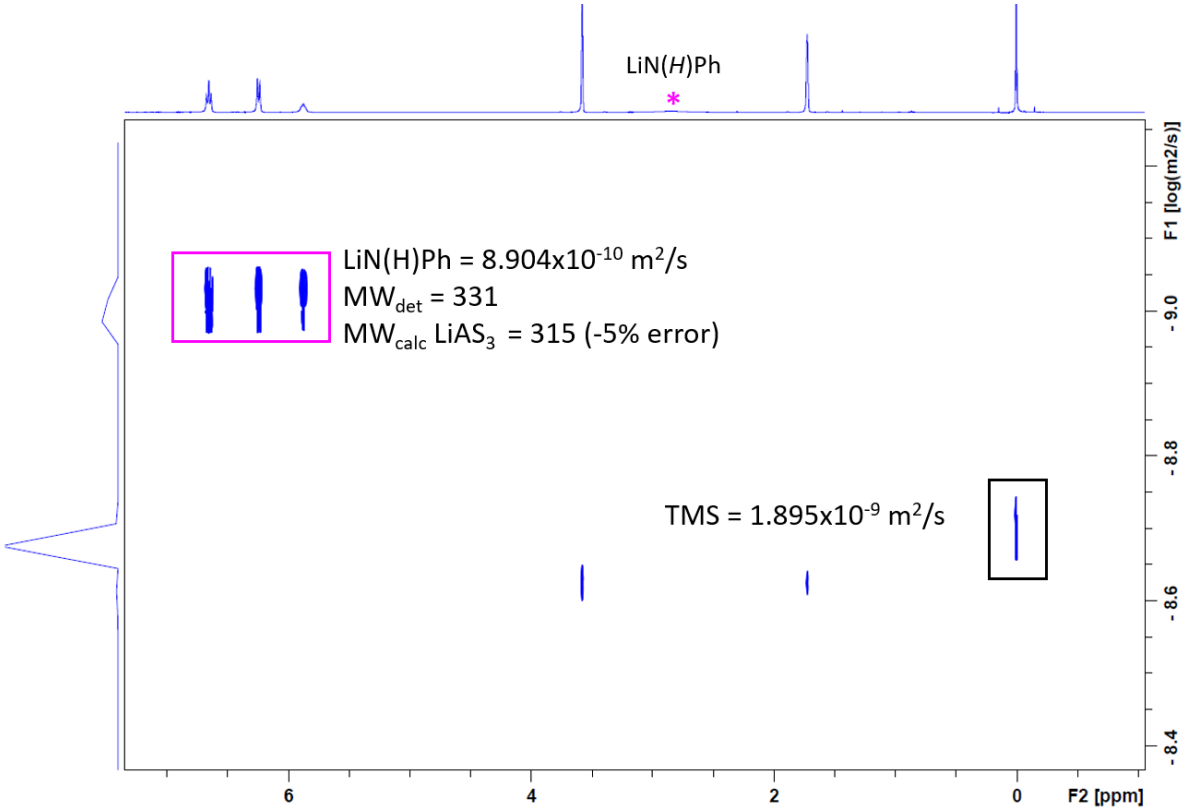

Figure 108 ^{1}H DOSY NMR spectrum of LiN(H)Ph (**2b**) in D_8-THF against TMS

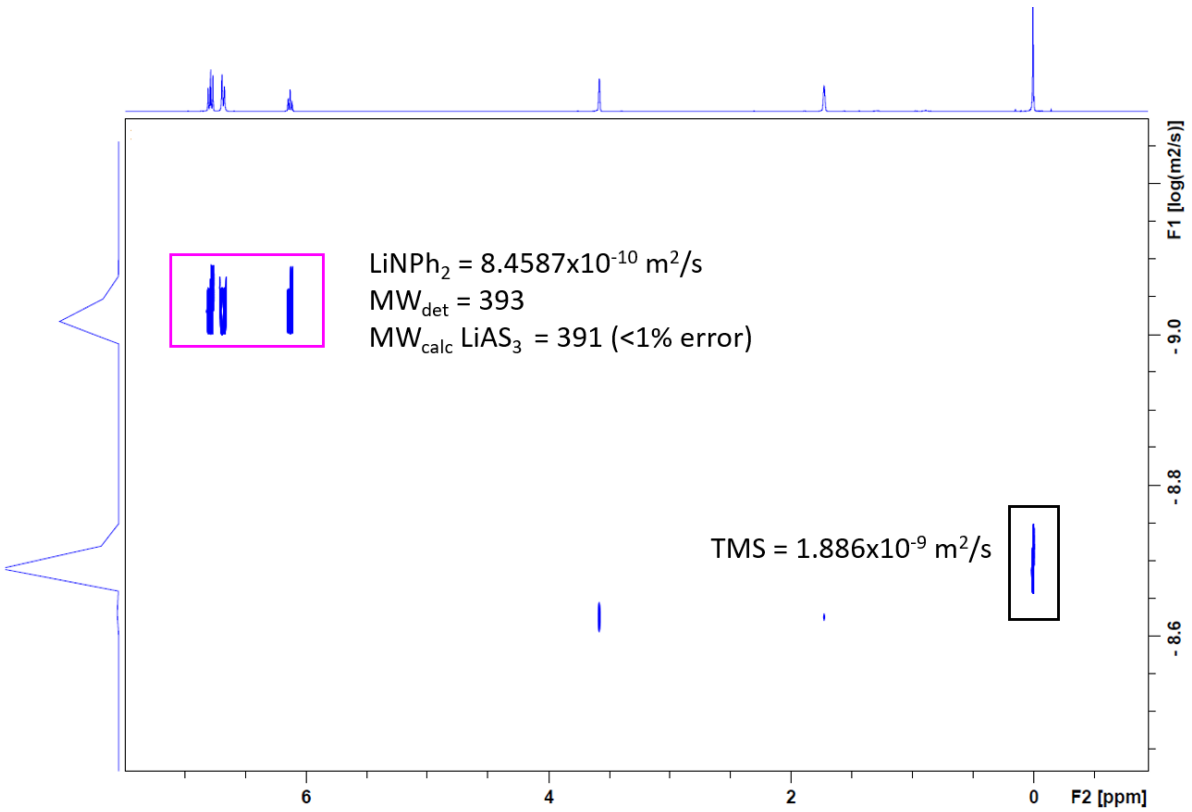

Figure 109 ^{1}H NMR spectrum of LiNPh$_2$ (**2h**) in D_8-THF against TMS

Table 7 Table of solution-state calculations for lithium amides **2a**, **2b** and **2h** in D_8-THF using External Calibration Curve

Entry	Amide	Solvent	Diffusion coefficient Li-NR_2 [x10^{-10} m^2/s]	Diffusion coefficient TMS [x10^{-9} m^2/s]	MW_{det} [g/mol]	Structure	MW_{calc} [g/mol]	MW_{diff}
1	Li-N(Me)Ph (**2a**)	D_8-THF	8.226	1.672	335	**$LiAS_3$**	**329**	**-2%**
						$Li_2A_2S_2$	370	11%
						$LiAS_2$	257	-23%
						$Li_2A_2S_3$	442	32%
						$Li_2A_2S_4$	515	54%
2	Li-N(H)Ph (**2b**)	D_8-THF	8.904	1.895	331	**$LiAS_3$**	**315**	**−5%**
						$Li_2A_2S_2$	342	3%
						$LiAS_2$	243	−27%
						$Li_2A_2S_3$	414	25%
						$Li_2A_2S_4$	487	47%
3	Li-NPh_2 (**2h**)	D_8-THF	8.4587	1.886	393	**$LiAS_3$**	**391**	**<1%**
						$Li_2A_2S_2$	494	26%
						$LiAS_2$	319	-19%
						$Li_2A_2S_3$	567	44%
						$Li_2A_2S_4$	639	87%

References

[1] a) A. P. Abbott, G. Capper, D. L. Davies, R. K. Rasheed, V. Tambyrajah, *Chem. Commun.* **2003**, 70; (b) H. Cruz, N. Jordão, L. C. Branco, *Green Chem.* 2017, **19**, 1653; (c) H. Wu, W. Guo, S. Daniel, Y. Li, C. Liu, Z. Zeng, *Chem. Eur. J.* 2018, **24**, 3444; (d) S. K. Davidsen, P. D. May, J. B. Summers, *J. Org. Chem.* 1991, **56**, 5482.

[2] (a) S. C. Watson, J. F. Eastham, *J. Organomet. Chem.* 1967, **9**, 165; (b) H. S. Lin, L. A. Paquette, *Synth. Commun.* 1994, **24**, 2503

[3] G. Li, M. Szostak, *Nat. Commun.* 2018, **9**, 4165.

[4] Z. Yin, Z. Wang, X. F. Wu, *Eur. J. Org. Chem.* 2017, 3992.

[5] L. Ran, Z. H. Ren, Y. Y. Wang, Z. H. Guan, *Chem. Asian J.* 2014, **9**, 577.

[6] S. Wang, J. Wang, R. Guo, G. Wang, S. Y. Chen, X. Q. Yu, *Tetrahedron Lett.*, 2013, **54**, 6233.

[7] F. Bruyneel, J. Marchand-Brynaert, *Synlett*., 2010, 1974.

[8] L. Hie, N. F. Fine Nathel, T. K. Shah, E. L. Baker, X. Hong, Y.F. Yang, P. Liu, K. N. Houk, N. K. Garg, *Nature*, 2015, **524**, 79.

[9] J.M. Gaudin, T. Lander, O. Nikolaenko, *Chemistry & Biodiversity*, 2008, **5**, 617.

[10] J. J. Eisch, J. U. Sohn, E. J. Rabinouitz, *Eur. J. Org. Chem.*, 2010, 2971.

[11] Y.L. Zheng, S. G. Newman, *ACS Catal.*, 2019, **9**, 4426.

[12] Y. Rao, X. Li, S. J. Danishefsky, *J. Am. Chem. Soc.*, 2009, **131**, 12924.

[13] (a) B. R. Kim, H.G. Lee, S.B. Kang, G. H. Sung, J.J. Kim, J. K. Park, S.G. Lee, Y.J. Yoon, *Synthesis*, 2012, **44**, 42; (b) T. Ohshima, T. Iwasaki, Y. Maegawa, A. Yoshiyama, K. Mashima, *J. Am. Chem. Soc.*, 2008, **130**, 2944.

[14] L. Lunazzi, D. Macciantelli, D. Tassi, A. Dondoni, *J. Chem. Soc., Perkin Trans. 2*, 1980, 717.

[15] S. Zhou, K. Junge, D. Addis, S. Das, M. Beller, *Angew. Chem. Int. Ed.*, 2009, **48**, 9507; *Angew. Chem.*, 2009, **121***,* 9671.

[16] P. J. Harford, A. J. Peel, J. P. Taylor, S. Komagawa, P. R. Raithby, T. P. Robinson, M. Uchiyama, A. E. H. Wheatley, *Chem. Eur. J.*, 2014, **20**, 3908.

[17] O.V. Dolomanov, L. J. Bourhis, R. J. Gildea, J. A. K. Howard, H. Puschmann*, J. Appl. Cryst.*, 2009, **42**, 339.

[18] R. Neufeld, D. Stalke, *Chem. Sci.*, 2015, **6**, 3354–3364.

[19] C. Su, J. Guang, P. G. Williard, *J. Org. Chem.*, 2014, **79**, 1032.

[20] L. M. Jackman, L. M. Scarmoutzos, *J. Am. Chem. Soc.*, 1987, **109**, 5348.